ENGINEERING BACTERIAL MAGNETIC NANOPARTICLES

By

Walter Nevondo

A thesis submitted in partial fulfillment of the requirements

for the degree of

Magister Scientiae (M.Sc.)

Department of Biotechnology

University of the Western Cape

Bellville

Supervisor: Professor D.A. Cowan

January 2013

TABLE OF CONTENTS

ABSTRACT

Magnetosomes, produced by magnetotactic bacteria (MTB), are the most attractive alternative source of non-toxic biocompatible magnetic nanoparticles (MNPs). A magnetosome contains Fe_2O_4 magnetite with properties superior to MNPs synthesized by the traditional chemical route. However, synthesis of magnetosomes on large scale has not been achieved yet because magnetotactic bacteria are fastidious to grow. In addition, magnetosomes are generally "soft" magnetic materials which can only be used for some applications, while other applications require "hard" magnetic materials. Here at the Institute of Microbial Biotechnology and Metagenomic (IMBM), a study is being conducted on cloning and expression of the magnetosome gene island (MIA), the genetic machinery for magnetosome formation, in an easy to culture *E. coli* strain. The magnetic properties of the magnetosome can be manipulated by doping with divalent metals such as Ni^{2+} or Co^{2+} for a variety of applications.
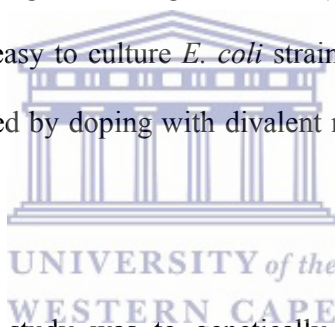
The specific objective of this study was to genetically engineer *E. coli* strains which accumulate intracellular Ni^{2+} or Co^{2+} in order to manipulate the magnetic properties of the magnetosomes. Three *E. coli* mutants and a wild type strain were transformed with high affinity Ni^{2+} or Co^{2+} uptake genes and evaluated for intracellular accumulation at different medium concentrations of $NiCl_2$ or $CoCl_2$. Cellular iron and magnesium were also evaluated because iron is the major component of the magnetosome and magnesium is important for cell growth. The wild type strain, EPI 300 habouring Ni^{2+} uptake permease the *hoxN* gene or Co^{2+} uptake ABC type transporter *cbiKMQO* operon was found to accumulate the most intracellular Ni^{2+} or Co^{2+} in medium conditions most likely to induce magnetosome formation and magnetite manipulation. This strain can be used to co-express the MIA and

Ni^{2+} or Co^{2+} uptake gene for mass production of magnetosome with altered magnetic properties.

Declaration

I declare that "*Engineering bacterial magnetic nanoparticles*" is my own work, that it has not been submitted for any degree or examination in any other university, and that all the sources I have used or quoted have been indicated and acknowledged by complete references.

Mr. Walter Nevondo   January 2013

....

UNIVERSITY *of the*
WESTERN CAPE

µ	Micro
Δ	Delta
Oe	Oersteds
ADP	Adenosine diphosphate
Amp	Ampicilin
ATP	Adenosine triphosphate
A/m	Ampere per meter
APS	Ammonium persulphate
BLAST	Basic local alignment search tool
bp	Base pare
Cam	Chloramphenecol
CPG	Casamino peptone glucose
dH$_2$O	Demineralised water
dATP	Deoxy-adenosine 5'- triphosphate
DNA	Deoxyribonucleic acid
dNTPs	Deoxyribonucleiotides
et al.	*et alia* (and others)
EDTA	Ethylenediamine tetra-acetic acid
ICP	Inducible couple plasma
IPTG	Isopropyl-b-D-thiogalactopyranoside
kDA	Kilo Dalton
LB	Luria Bertani
MIA	Magnetosome gene island
MIC	Minimum inhibitory concentration
MIT	Metal inorganic transporter
MNP	Magnetic nanoparticle
MTB	Magnetotactic bacteria

OD	Optical density
OES	Optical emmision spectroscopy
PAGE	Polyacrylamide gel electrophoresis
PCR	Polymarase chain reaction
rpm	Revolution per minute
SBD	Substrate binding domain
SDS	Sodium dodecyl sulphate
TAE	Tris acetic acid EDTA
TBDP	TonB Dependent protein
TEMED	N,N,N'N'-Tetramethylethylenediamine
TE	Tris EDTE
TMD	Transmembrane domain
Tris	Tris hydroymethyl-aminomethane
U	Units
v/v	Volume per volume
v/w	Volume per weight

1.   INTRODUCTION

1.1.   Magnetic nanoparticles (MNPs)

Nanotechnology is one of the fastest growing fields of science. The electronic evolution of the 1970s resulted in an increased demand for smaller devices. Since then, researchers have developed numerous methods of producing materials as small as 5 nm in diameter with electrochemical properties completely different from those of bulk material. Scanning electron microscopy (SEM) and atomic force microscopy (AFM) not only have allowed nano-scale materials to be visualized, but also made manipulation of particles at the atomic level possible, resulting in an increased understanding of electrical and physiochemical properties of nanoparticles.
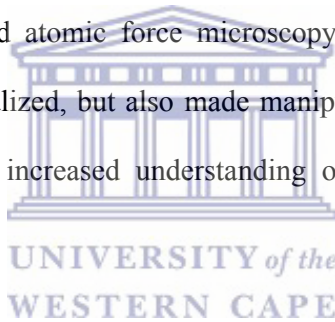
Magnetic nanoparticles (MNPs) are a class of nanoparticles which has been receiving increased research interest over the past years. The most common MNPs are those consisting of divalent metals such as iron, Ni^{2+}, chromium, Co^{2+} and their oxides (Yamamoto *et al.* 2011). These particles are used in a variety of applications, including magnetic resonance imaging (MRI) (Frimpong and Hilt, 2010), targeted drug delivery, hyperthermia treatment (de Souza *et al.* 2011), gene delivery (Kami *et al.* 2011) and biological separation. MNPs are also used in information media as components of storage materials such as magnetic stripes, compact discs and in current flow control materials such as transformers and generators (Buhler *et al.* 2000).

The applications of MNPs are mainly determined by their chemical composition, size and shape (Artus *et al.* 2011). Based on their magnetic behaviours, MNPs are classified in three groups: ferromagnetic, paramagnetic and superparamagnetic (Kirchmayr, 1996). Paramagnetic materials are those that lose magnetisation immediately after the removal of the external magnetic field (Mahmoudi *et al.* 2011). As the paramagnetic materials decrease in size, their magnetic saturation increases and they become superparamagnetic, but can still be easily demagnetised to their zero magnetic state. Magnetic materials which retain magnetisation even independent of external magnetic field are ferromagnetic materials. These materials can be completely demagnetised to their zero state by the use of negative magnetic force called magnetic coercive force (Figure 1), measured in ampere per meter (kA/m) or Oesteds (Oe) (Mahmoudi *et al.* 2011).
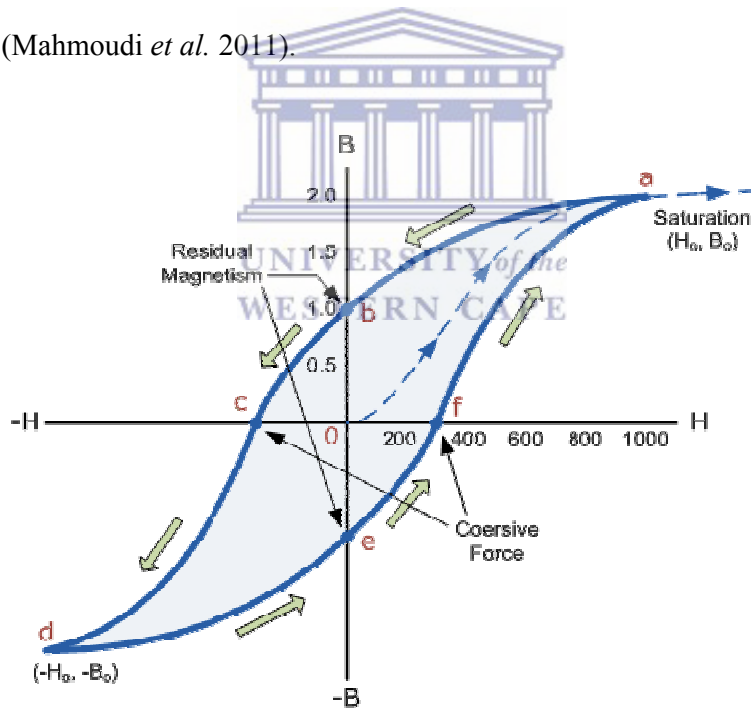
Figure 1: General representation of ferromagnetism of magnetic materials using hysteresis loop. Point "a" represents a point of magnetic saturation when magnetic force **H** is applied. When magnetic force **H** is reduced to zero, the curve will move from point "a" to point "b". At this point, it can be seen that some magnetisation remains in the material even though magnetic force **H** is zero. In order to completely demagnetise this material, reverse magnetic force (Coercive force) is required (Jiles and Atherton, 1986).

Ferromagnetic materials which require little coercive force to completely demagnetise are called soft magnetic materials (Chakraverty and Bondyopadhyay, 2007). These materials are easily magnetised by exposure to electrical current and can also be completely demagnetised by little coercive force (Figure 2). Soft magnets are used to control the flow of current in countless electronic devices such as MP3 players, computers, tape decks, transformers or as the magnetic cores of relays and inductors where current alternates frequently (Mchenry and Laughlin, 2000).

Magnetic materials which require higher coercive force to completely demagnetise are termed hard magnets (Chakraverty and Bondyopadhyay, 2007). Unlike soft magnetic materials, hard magnetic materials have low permeability (they are difficult to magnetise) and are mostly naturally magnetised, although they can also be magnetised through an external magnetic field in the production or maintenance of magnetic field (Chakraverty and Bondyopadhyay, 2007). They are generally used to create magnetic fields in devices such as generators and motors of automobiles (Mchenry and Laughlin, 2000).

MNPs are found in nature. They are produced by birds (Hanzlik *et al.* 2000), fish (Lohmann *et al.* 2008), ants (Acosta-Avalos *et al.* 1999), honeybees (Hsu *et al.* 2007) and bacteria (Blakemore, 1975). Interest in MNPs from biological sources has recently been increasing to replace complex and expensive chemical synthetic routes with more environmentally friendly and cost effective ones (Van Belle *et al.* 2007). In addition, chemically synthesised metal ferrite nanoparticles have been shown to be toxic and biologically incompatible (Berry and Curtis, 2003).
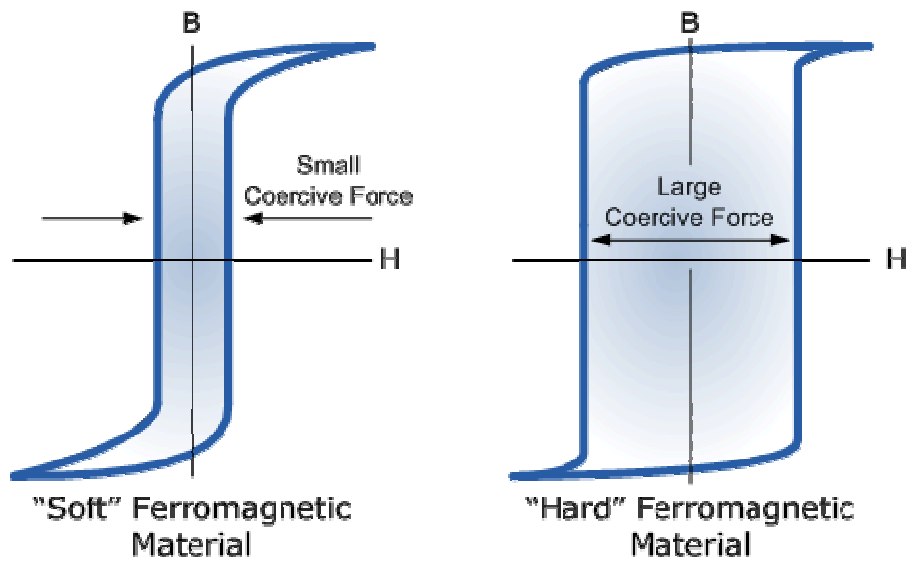
Figure 2: General representation of soft ferromagnetic material and hard ferromagnetic material. The loop of soft material is thin and held close to the central point while the loop of hard material is wide and away from the central point (Jiles and Atherton, 1986). More reverse magnetic energy is reguired to bring the loop of hard ferromagnetic material to zero than the energy required for soft ferromagnetic material
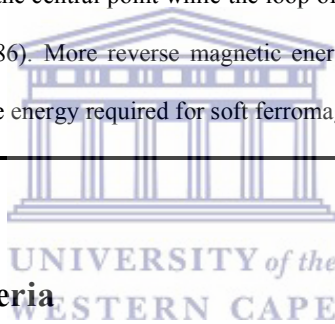
1.2. Magnetotactic bacteria

Magnetotactic bacteria (MTB) are Gram negative, motile, microaerophilic and aquatic microorganisms, which synthesize magnetic nanoparticles (MNPs) within a membrane bound organelle called the magnetosome (Blakemore, 1975). These bacteria were first described by Bellini, (1965) and were later rediscovered and characterized by Blakemore1975 who named them Magnetotactic bacteria (MTB). The 16S rRNA analysis revealed that most known cultured and uncultured MTB belong to the Proteobacteria; Alphaproteobacteria, Gammaproteobacteria and Deltaproteobacteria (Amann *et al.* 2006), although some uncultured species have been shown to belong to the *Nitrospira* (Vali *et al.* 1987) (Figure 3).
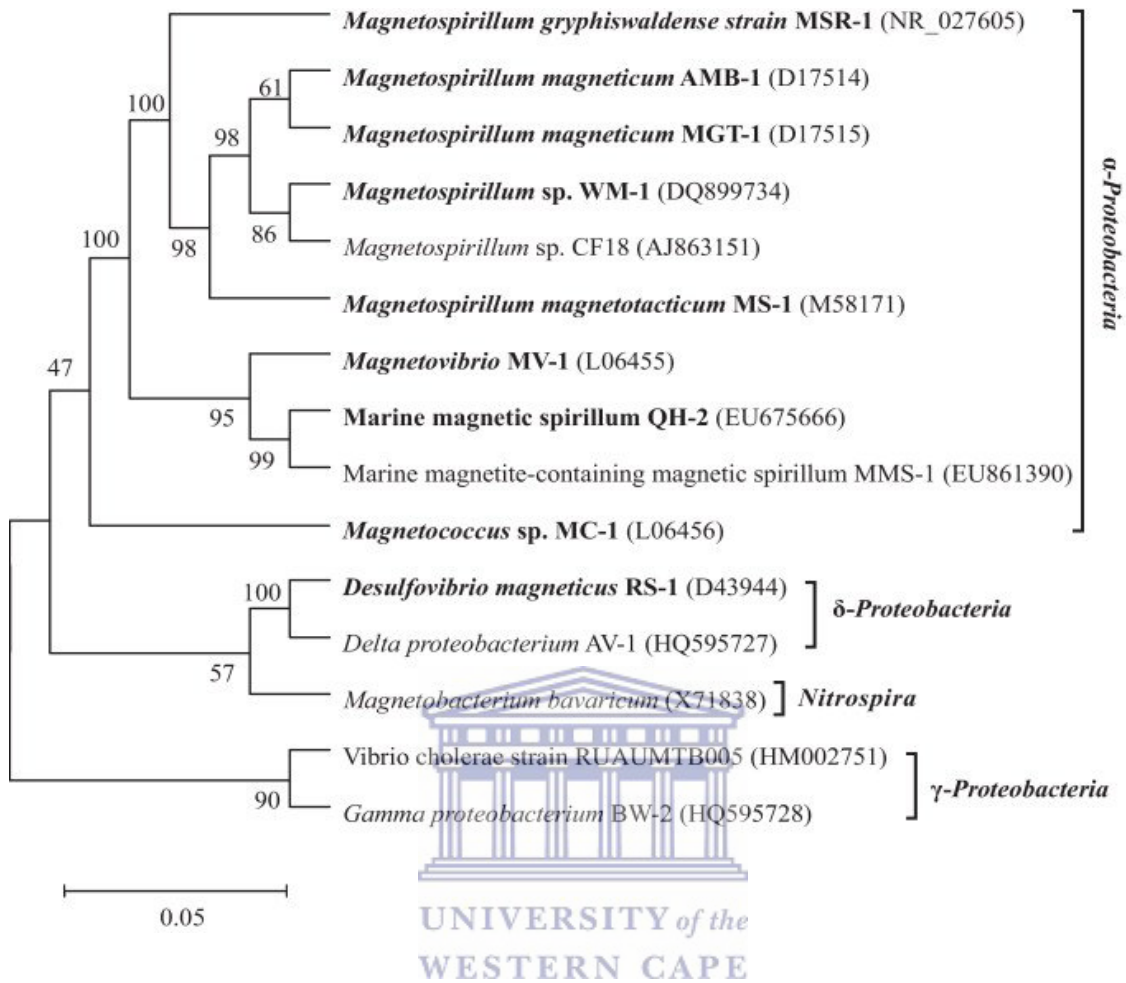
Figure 3: Phylogenetic relationships of the cultured and uncultured MTB. Most cultured MTB (shown in bold) belongs to alphaproteobacteria and only one (*Desulfovibro magneticus* RS-1) belongs to gammaproteobacteria (Yan *et al.* 2012)

MTB are found mainly in the anoxic-oxic interface (AOI) of water or sediments (Blakemore, 1975). They have been reported to inhabit diverse environmental conditions, including higher pH (pH~9) and temperature (63ºC) (Lefevre *et al.* 2011). Different studies have also reported diverse metabolic activities in MTBs. Most *Magnetospirillum* species have been shown to use organic acid as carbon and electron source (Schleifer *et al.* 1991) while others are capable of nitrogen fixation (Bazylinski *et al.* 2000). *Magnetococcus marinus* has been reported to use reduced sulphur compounds as an electron source (Bazylinski *et al.* 2004). MTB produce

membrane bound organelles called magnetosomes (Ragsdale and Kumar, 1996). Magnetosomes are intracellular vesicle like structures which contain iron oxide magnetite (Fe_3O_4) or iron sulphide greigite (Fe_3S_4) (Blakemore, 1982). This structure is a signature feature of MTB and helps them align to earth's magnetic field (Vali *et al.* 1987). Magnetites of the magnetosome have been shown to be of species-specific sizes ranging from 35 nm to 120 nm (de Souza *et al.* 2011). Magnetosome particles show three defined morphologies, roughly cuboidal (Mann *et al.* 1994); elongated-prismatic (Bazyliski *et al,* 2004) and bullet shaped (Lefevre *et al.* 2011).

Magnetosome formation is still not well understood, however significant progress has been made over the past few years. Membrane proteins of magnetosomes were reported to be similar to cytoplasmic membrane proteins (Tanaka *et al.* 2006). A study by Bazylinski and Schubbe (2007) suggests that magnetosome membranes are derived from the cytoplasmic membrane. This is because the magnetosome membrane of *Magnetospirillum magneticum* AMB-1 was found attached to the cytoplasmic membrane. Magnetosomes were also observed located adjacent to the cytoplasmic membrane (Bazylinski and Schubbe, 2007) (Figure 4).
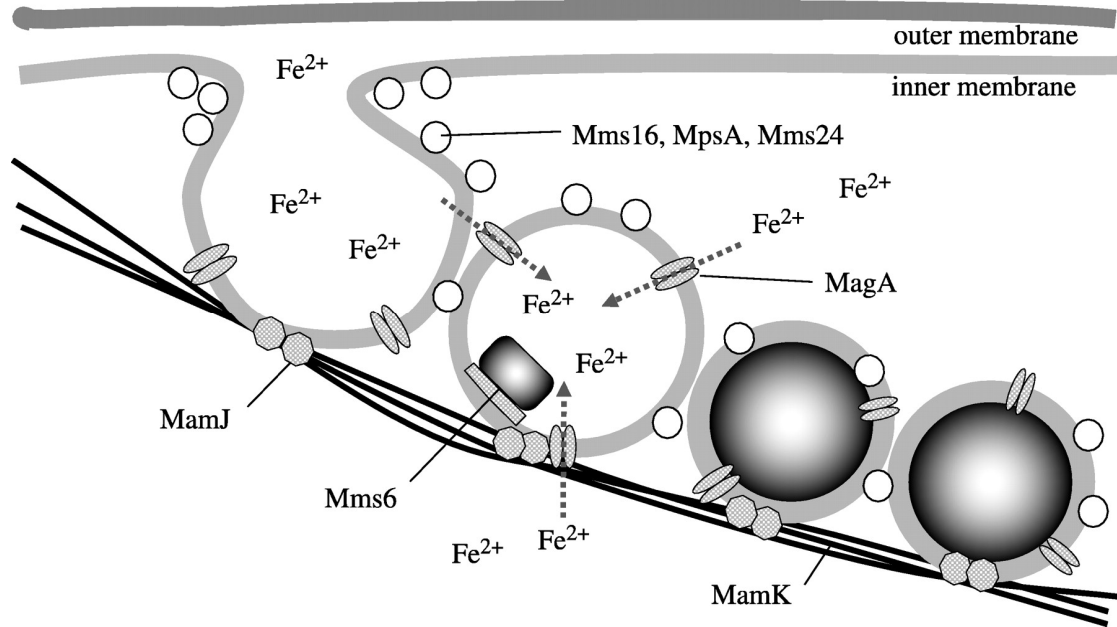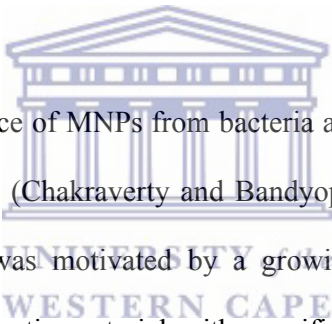
Figure 4: Model of magnetosome membrane and magnetite formation. During the initial stage of cytoplasmic membrane invagination to form magnetosome membrane, periplasmic iron flows freely into the new magnetosome vesicle. When the mature magnetosome detaches from the cytoplasmic membrane, MagA is required to transport iron across the magnetosome membrane. Mms 16, MpsA and Mms24 are some of the proteins suggested to facilitate magnetosome formation (Yan *et al.* 2012).

Genetic studies of *Magnetospirillum magneticum* AMB-1 revealed that about nineteen genes are essential in the formation of magnetosomes (Murat *et al.* 2010). Of these genes, *mamI*, *mamL*, *mamQ* and *mamB* were reported to be unique to MTB and are located in a 105 kb DNA fragment called the magnetosome gene island (Nahvi *et al.* 2004). Deletion of *mamI* and *mamL* showed no magnetosome formation in the cytoplasm (Murat *et al.* 2010). Analysis of the *mamB* sequence revealed that MamB has high homology to heavy metal transporter proteins, implying that this protein is involved in the transportation of iron into the magnetosome (Murat *et al.* 2010). Another protein, MagA has been implicated in iron

transport across the magnetosome membrane (Tanaka *et al.* 2006). However no additional studies have been done to confirm the involvement of these proteins in iron transport.

Bacterial magnetosomes are an ideal alternative for a biological source of MNP with properties superior to MNPs produced by the traditional chemical route. However magnetosomes are generally soft magnetite which require low magnetic coercive force to demagnetise (Bazyliski and Schubbe, 2007) making them suitable for some applications while other applications require hard magnetic materials (Buhler *et al.* 2000).

1.3. Improving MNPs

Manipulation of the coercive force of MNPs from bacteria and chemical synthetic routes has been the focus of most research (Chakraverty and Bandyopadhyay, 2007, Hsu *et al.* 2007; Van Belle *et al.* 2007). This was motivated by a growing discovery of more potential applications which require magnetic material with specific magnetic properties mainly in biomedicine and biotechnology (Wu and Zeng, 2010).

Numerous methods of synthesising MNPs with specific coercive force have been developed in the chemical synthetic route (Hyeon, 2002; Van Belle *et al.* 2007). These methods generally involve doping of pure ferrite MNPs with divalent metal. The most common divalent metal used to increase magnetic coercive force of ferromagnetic material is Co^{2+}, although other metals such as Ni^{2+}, copper, zinc and manganese are also used (Chakraverty and Bandyopadhyay, 2007). Co^{2+} is the metal of choice because it has the highest Curie temperature known (1121ºC) (Bruno, 1991) and highest coercive force (1.5 kA/m) compared to other divalent metals (Friedberg and Paul, 1975), making it a difficult metal to

demagnetise. Doped MNPs include Co^{2+} ferrite ($CoFe_2O_4$) (Maaz *et al.* 2007) and Ni^{2+} ferrite magnetic nanoparticles ($NiFe_2O_4$) (Maaz *et al.* 2010) which have coercive force of up to 95. 9 kA/m and 23.0 kA/m respectively.

In bacteria, different studies have reported manipulated coercive force of the magnetosome. Magnetosomes of three cultured MTB have been doped with up to 20 µM Co^{2+} resulting in Co^{2+} ferrite oxide nanoparticles ($CoFe_2O_4$) with increased coercive force (Staniland *et al.* 2008). The coercive force of the *Magnetospirillum magnetotacticum* MS-1 magnetosome has been changed by doping with zinc and Ni^{2+} (Kundu *et al.* 2009). Work by Perez-Genzalez *et al.* (2010) reported the incorporation of 1.14 % of manganese into the magnetosome of *Magnetospirillum gryphiswaldense* MSR-1. Recently, Tanaka *et al.* (2012) reported the incorporation of 3.0 % Co^{2+}, 2.7 % manganese and 15.6% copper into the magnetosome of *M. magneticum* AMB-1. The Tanaka *et al.* (2012) study also revealed that doping with copper and manganese reduces the coercive force while Co^{2+} increases the coercive force (Tanaka *et al.* 2012).

Metal doping of the magnetosome has proved to be more challenging than synthesizing metal doped MNP in chemical reactors. This is generally because at elevated concentration metals are toxic to all forms of life. This toxicity presents a limitation when high concentrations of metals need to be incorporated inside the magnetosome. For example doped $CoFe_2O_4$ with magnetic coercive force of 95.9 kA/m at room temperature has been produced by the chemical route using 0.2 M $CoCl_2$ and 0.4 M $FeCl_2$ (Maaz *et al.* 2007). In bacteria, the amount of metals to be incorporated into the magnetosome is determined by bacterial metal tolerance, transportation of metals from the environment into the cell and regulation thereof. These activities are all controlled at the genetic level.

1.4. Metals and bacteria

Bacteria require metals for different metabolic activities (Cvetkovic *et al.* 2010). About 40 % of all cellular enzymes require metals as co-factors, of these 16 % require magnesium, 9 % require zinc, 8 % require iron, and about 1 % require Co^{2+} or Ni^{2+} (Waldron *et al.* 2009). Ni^{2+} enzymes include urease (Watt and Ludden, 1999), NiFe hydrogenase (Eitinger and Mandrand Berthelot, 2000), carbon monoxide dehydrogenase (Ragsdale and Kumar, 1996); and superoxide dismutase (Youn *et al.* 1996). Co^{2+} is required for the synthesis of methionine aminopeptidase (Chang *et al.* 1989), proline dipeptidase (Browne and O'Cuinn, 1983) and some nitrile hydratases (Komeda *et al.* 1997). Zn^{2+} is required for structural scaffolding of RNA polymerase and tRNA synthatase and is also a co-factor for more than three hundred other enzymes (Coleman, 1998). Magnesium functions as a co-factor of DNA polymerase and ATP. Manganese is an important component of chlorophyll and plays a role in photosynthesis (Waldron *et al.* 2009).
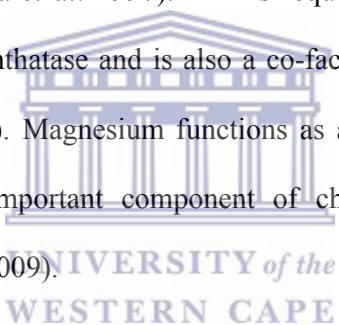
However, at elevated concentrations, metals are known to inhibit cell growth (Baek and An, 2011). High concentrations of transition metals affect the lactoperoxidase sensivity of *Escherichia coli* (Sermon *et al.* 2005). High Co^{2+} has been implicated in competitive binding to iron-sulphur proteins in *E. coli* resulting in the production of dysfunctional protein (Ranquet *et al.* 2007). Zinc accumulation was reported to affect the activity of dehydrogenases of *Bacillus*, *Salmonella* and *Arthrobacter* genera (Viret *et al.* 2006). Ni^{2+} accumulation was shown to inhibit DNA replication and translation by binding to proteins and nucleic acid (Macomber and Hausinger, 2011).

Bacteria acquire metals from the surrounding environment through metals uptake systems (Nies, 1999). Because metals are toxic to bacterial cells, these uptake systems are highly regulated through (Rowe *et al.* 2005). However, when metals are accumulated through non-specific uptake systems which are usually controlled by global regulatory systems (Papp and Maguire, 2004) metal toxicity is prevented through metal efflux systems (Silver and Phung, 2005). These metal efflux systems transport metals back to the extracellular environment.

1.4.1. Metals uptake in bacteria

Translocation of metals across bacterial membranes has been well studied (Silver and Phung, 2005). Most metals cross the outer membrane through porins (Schauer *et al.* 2007), while siderophores (iron complexes) and Ni^{2+} complexes have been shown to cross the outer membranes through TonB dependent transport (TBDT) (Noinaj *et al.* 2010) (Figure 5). In the periplasm, metals are transported across the cytoplasmic membrane by high affinity transporter proteins or low affinity transporter proteins (Agranoff and Krishna, 1998). Low affinity metal transporters usually have affinity to a variety of metals, although they show high affinity to one specific metal. These transporters are usually regulated by global regulatory systems such as the PhoPQ system (Newcombe *et al.* 2005).
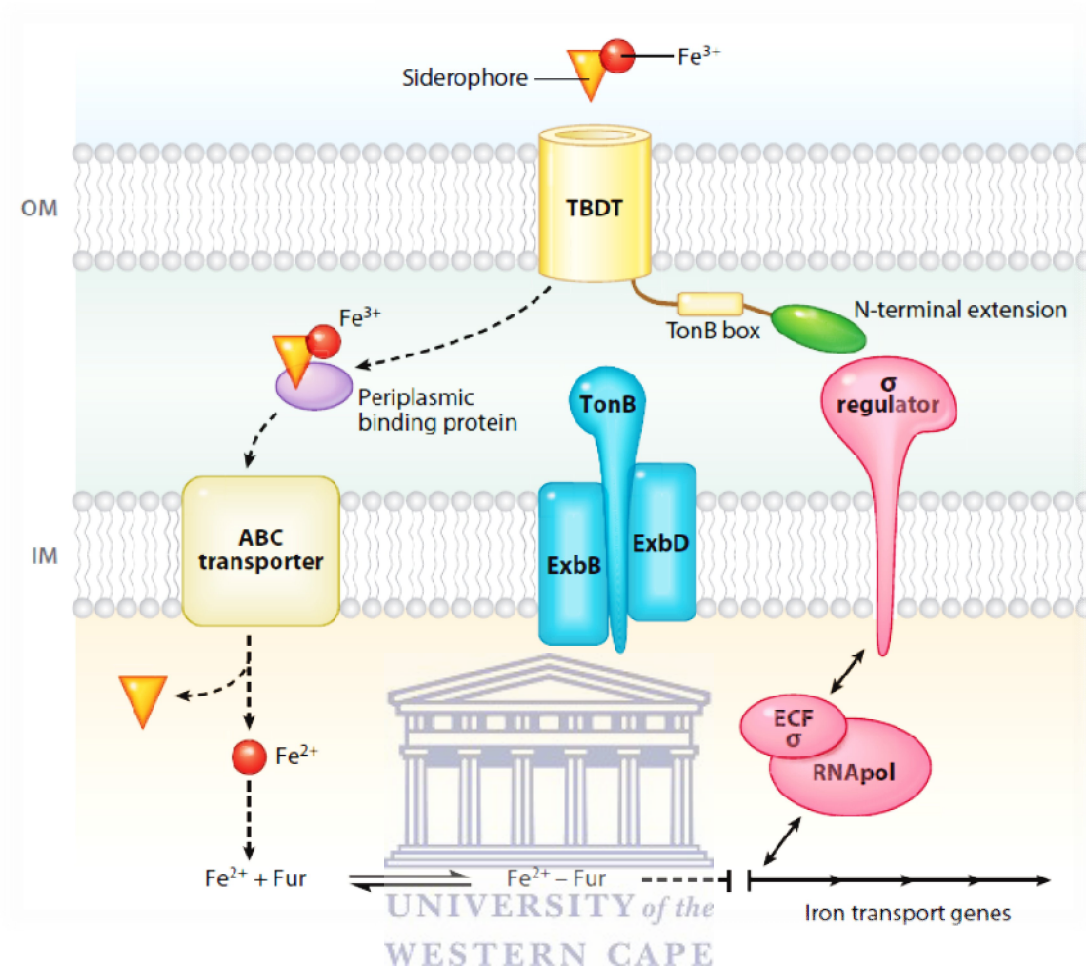
Figure 5: Illustration of iron transport across bacterial membrane. Iron in the environment forms complexes with siderophores which cross the outer membrane through TBDT (Noinaj *et al.* 2010).

High affinity metal transporters are either multi component systems which consist of multiple proteins, or single component permeases which transverse the membrane several times (Mulrooney and Hausinger, 2003). The multi component systems are ATP binding cassettes (ABC) which generally consist of two transmembrane domains (TMD) that form pores for metal passage, and two nucleotide binding domains (NBD) that hydrolyse ATP (Figure 6). The NBD is believed to bind and hydrolyse ATP, thereby generating conformational changes that lead to metal translocation (Tomii and Kanehisa, 1998). This system may also consist of

a periplasmic substrate binding domain (SBD) which serves as an initial metal sensor (Eitinger and Mandrand-Berthelot, 2000).

A
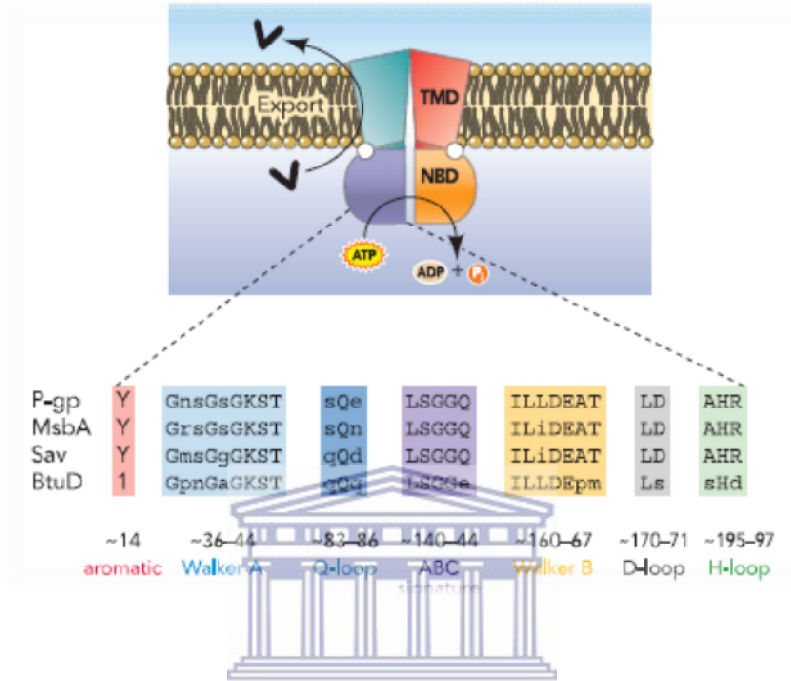
B
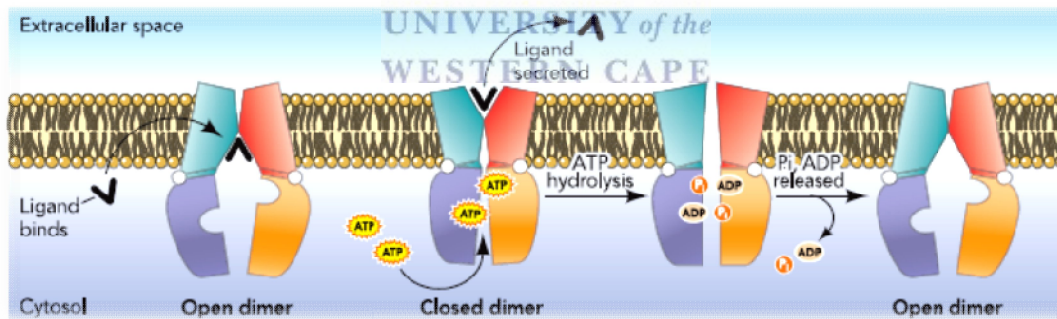
FIGURE 6 A: Illustration of a general ABC type transporter. The transporter consists of two major domains, the transmembrane domains (TMD) and the nucleotide binding domain (NBD). The signature motif and different characteristic features of the NBDs of these transporters are also shown. The signature motifs consist of the aromatic amino acids, the walker A and B sequence, the Q-loop, the ABC signature siguence, the D and H loop. **B:** Illustration of the ABC type transporter mechanism. Two ATP molecules bind to the NBD and cause conformational changes which result in the release of substrate from the SBP to the TMD. ATP is hydrolysed, resulting in the release of substrate into the cytoplasm together with two ADP molecules (Linton and Higgins, 2007).

Permeases are widely distributed in bacteria and are also found in Archaea and fungi (Wolfram and Eitinger, 1995). They include metal-specific as well as permeases with mixed specificity. Permeases have been observed to have affinities higher than those of ABC transporters, suggesting that they are adapted to supply minerals at lowest environmental levels (Mobley *et al.* 1995).

The work presented in this study pertains to Ni^{2+} and Co^{2+} accumulation in *E. coli*. Therefore the details regarding these metals will be presented, with little reference to mechanisms involved in the transportation and regulation of other divalent metals.

1.4.1.1. Non-specific Ni^{2+} and Co^{2+} uptake in bacteria

CorA is the best studied magnesium transporter. This transporter was initially reported to be a primary importer of Mg^{2+} in *E. coli* and *Salmonella typhimurium* (Papp and Maguire, 2004) but was later also shown to import Ni^{2+} and Co^{2+} with low affinity and specificity (Nelson and Kennedy, 1971). The CorA protein belongs to the fast non-specific metals inorganic family of transporters (MIT) and is constitutively expressed (Niegowski and Eshaghi, 2007). This protein accumulates Ni^{2+} and Co^{2+} in the cell even when the cytoplasmic concentration is high, resulting in intracellular metal build-up and toxicity (Nies, 1999). The *E. coli* CorA was shown to bind magnesium, Co^{2+} and Ni^{2+} with an affinity of 10-15 μM, 20-40 μM and 200-400 μM respectively (Niegowski and Eshaghi, 2007). The *corA* mutant has been shown to grow in 200 μM Co^{2+} concentration while a wild type with functional *corA* showed drastically reduced growth (Ranquet *et al.* 2007). In a metals tolerance bacterium *Cupriavidus metallidurans* CH34, mutation of the *corA* gene increased the minimum inhibitory concentration (MIC) of Co^{2+} from 55 mM to 70 mM (Kirsten *et al.* 2011).

1.4.1.2. Ni²⁺ ABC type transporters

Ni^{2+} ABC transporters have been reported in a number of different organisms, including *E. coli* (Navarro *et al.* 1993) and *Helicobacter pylori* (Hendricks and Mobley, 1997). In *E. coli* (Figure 7), this transporter consists of five proteins: A soluble periplasmic Ni^{2+} binding protein NikA; two transmembrane proteins NikB and NikC; and two ATP hydrolysis proteins NikD and NikE (Mulrooney and Hausinger, 2003). The genes coding these proteins constitute the *nik* operon and have been reported to be expressed under anaerobic growth conditions to provide Ni^{2+} for the three hydrogenases involved in anaerobic metabolism (Rowe *et al.* 2005).
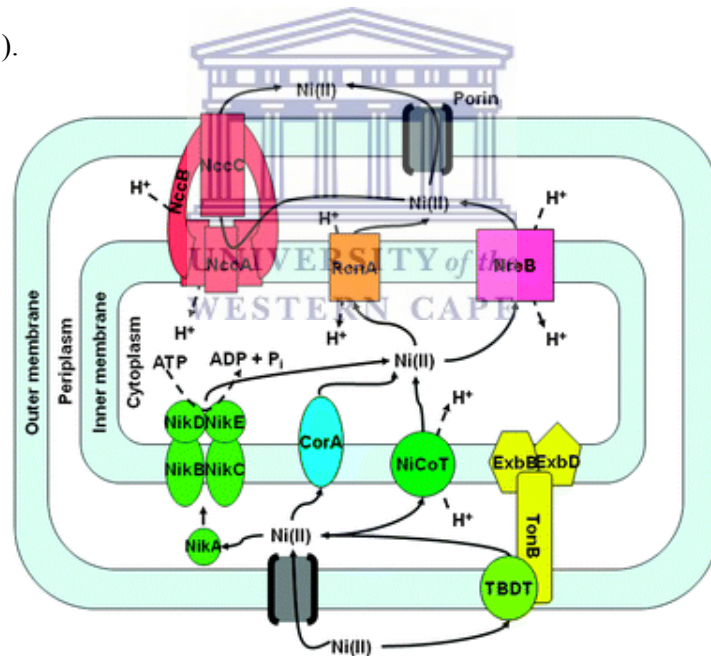
Figure 7: Schematic representation of nickel transporters in *E. coli*. Nickel crosses the outer membrane through porins and TBDP. Once inside the periplasm, nickel is accumulated into the cytoplasm through NikABCDE and CorA system. Low level of nickel inside the cytoplasm is mainly maintained through RcnA (Lee and Hausinger, 2011).

NikA is the initial Ni^{2+} sensor and is also responsible for a negative chemotaxic response to high levels of Ni^{2+} (de Pina *et al.* 1995). The *nikA* gene was shown to be down regulated by high Co^{2+} concentrations, suggesting that NikA might also have some affinity to Co^{2+} (Fantino *et al.* 2010). Fluorescence studies of NikA reveal that this protein binds Ni^{2+} with a K_d value >0.1 µM (de Pina *et al.* 1995). A study by Addy *et al.* (2007) reported a much higher NikA Ni^{2+} binding affinity, a K_d value of about 10 µM. Although both studies reported different values, these values are much lower than that reported for the non-specific CorA transporter (Niegowski and Eshaghi, 2007).

An *E. coli nikA* mutant was shown to have a drastically decreased Ni^{2+} uptake rate under low Ni^{2+} concentration compared to the wild type (Navarro *et al.* 1993). No significant Ni^{2+} uptake difference was detected between the *nikA* mutant and the wild type grown in high Ni^{2+} concentrations (Navarro *et al.* 1993), confirming that Ni^{2+} is also taken up by other low affinity transporters such as CorA at elevated media concentration (Nelson and Kennedy, 1971). The Ni^{2+} ABC importer of *E. coli* was reported to be positively controlled by a fumarate nitrate regulatory protein (FNR) and negatively controlled by NikR (Rowe *et al.* 2005). This regulation occurs through protein-DNA interactions at the *nikABCDE* promoter in response to intracellular Ni^{2+} concentration and oxygen tension (Chivers and Sauer, 2002). A decrease in oxygen tension was shown to activate FNR and up regulate *nikABCDE* expression, while the presence of excess Ni^{2+} activates NikR, which overrides the action of FNR and results in repression of *nikABCDE* transcription (Rowe *et al.* 2005).

Ni^{2+} ABC transporters have been reported in other microorganisms (Figure 8), including the *nik(MN)QO* system of *R. capsulatus* (Rodionov *et al.* 2006), *yntABCDE* of a Gram-negative

ureolytic bacterium *Yersinia pseudotuberculosis* (Sebbane *et al.* 2002), and the *abcABCD* of Gram-negative human pathogen *H. pylori* (Hendricks and Mobley, 1997).
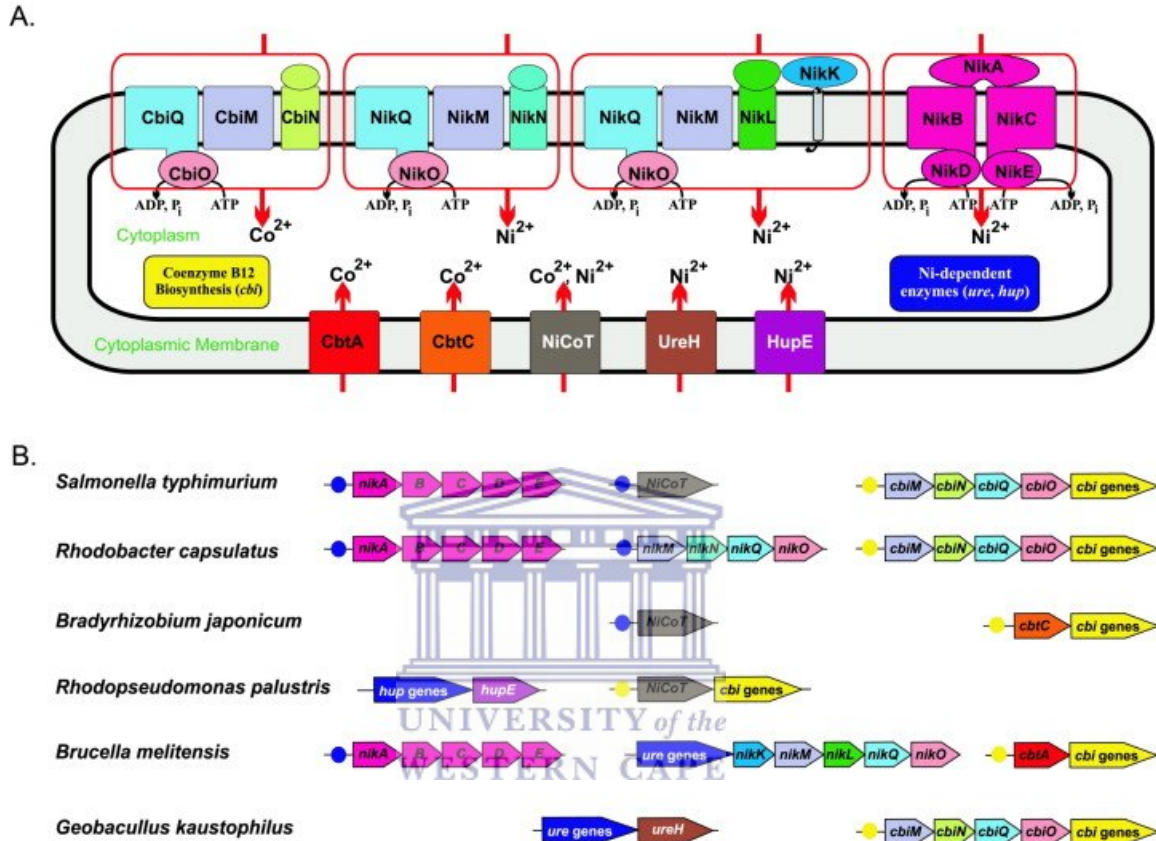
Figure 8: A: Summary of Ni^{2+} and Co^{2+} transporters in bacteria**.** Ni^{2+} operon (*nikABCDE*) and Co^{2+} operon (*cbiMNQO*) represented here are from *S. typhimurium*, *R. capsulatus* and *Brucella melitensis*. **B:** The diversity of Ni^{2+} and Co^{2+} ABC type transporters in prokaryotes (Gelfand and Rodionov, 2008).

1.4.1.3.   Ni^{2+} uptake permeases

In the Gram-negative aquatic and soil bacterium *C. metallidurans* H16, a 33.1 kDa permease called HoxN has been reported to import Ni^{2+} in extremely low Ni^{2+} concentrations (Wolfram and Eitinger, 1995). *C. metallidurans* H16 produces two types of Ni^{2+}-containing

17

hydrogenases which mediate the hydrogenesis of H_2 under anaerobic conditions. The synthesis of these enzymes requires the presence of Ni^{2+} which is transported into the cell through HoxN (Wolfram and Eitinger, 1995). HoxN is a transmembrane protein which transverses the membrane eight times (Figure 9). Expression of *hox*N in *E. coli* lead to 15 fold increase in Ni^{2+} accumulation compared to a wild type strain without *hox*N. The binding affinity of HoxN to Ni^{2+} was reported to be K_d of 20 nM, showing a much higher affinity than ABC type transporters (0.1-10 µM) (de Pina *et al.* 1995, Addy *et al.* 2007).

In *H. pylori*, another single component Ni^{2+} permease called NixA has been reported (Bauerfeind *et al.* 1996). Insertion inactivation of the *nix*A gene reduces urease (a Ni^{2+} containing enzyme) activity by about 42 %, with the remaining activity suggested to be arising from another ABC type Ni^{2+} transport system (Bauerfeind *et al.* 1996). The *E. coli* strain containing a functional *H. pylori nix*A has been shown to transport about 1250 pmol of Ni^{2+} per minute per 10^8 cells, whereas the control strain lacking *nix*A only transported an equivalent of 140 pmol Ni^{2+}, showing an 8.9 fold increase. A transport constant of 11 nM of Ni^{2+} has been reported for NixA confirming that it is a high affinity transporter (Mobley *et al.* 1995).

Ni^{2+} permeases have also been reported in *Bradyrhizobium japonicum* (Fu *et al.* 1994), *Mycobacterium tuberculosis* (Cole *et al.* 1998), *Yersinia pestis* (Eitinger *et al.* 2000) *Sulfolobus sulfataricus* P2 (She *et al.* 2001), and *Yersinia pseudotuberculosis* (Sebbane *et al.* 2002).
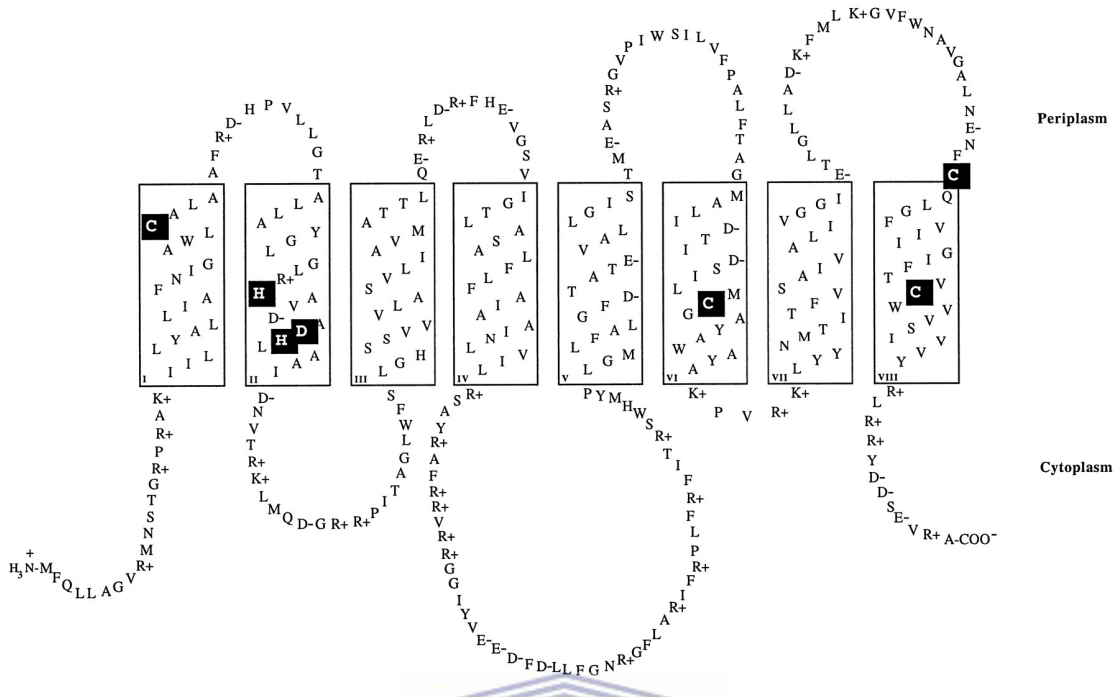
Figure 9: Topological representation of the *C. metallidurans* H16 Ni^{2+} permease (HoxN). This protein transverses the membrane eight times, with five loops in the periplasm and three loops in the cytoplasm. Both the N- terminus and C- terminus of this protein are in the cytoplasm (Wolfram and Eitinger, 1995).
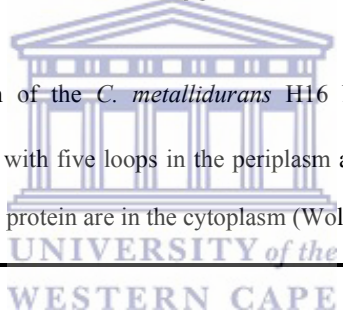
1.4.1.4. Co^{2+} ABC type transporters

Co^{2+} ABC type transporters have been reported for a number of different organisms (Figure 8). A gene cluster designated *cbiMNQO* was reported in *Salmonella enterica*, a Gram-negetive bacterium and *Rhodobacter capsulatus,* a purple non-sulfur photosynthetic bacterium capable of growing rapidly under non-photosynthetic conditions (Rodionov *et al.* 2006). Sequence alignment of the genes cluster show that it is the most widely distributed divalent metal uptake system in prokaryotes (Rodionov *et al.* 2006). The CbiMNQO system consists of transmembrane protein CbiQ and the ATP hydrolysis protein CbiO. The CbiN has

been proposed to be the substrate binding protein while the exact function of CbiM is still ellusive (Rodionov *et al.* 2006).

The CbiMNQO transport systems from *S. enterica* and *R. capsulatus* show different Co^{2+} import capacities when expressed in *E. coli* in the presence of 500 nM Co^{2+} (Rodionov *et al.* 2006). The *R. capsulatus* CbiMNQO was found to transport 8.8 fold more Co^{2+} than *S. enterica* CbiMNQO (Rodionov *et al.* 2006). Although these different capacities have been credited to different expression efficiency, the possibility of differences in the actual transport capacity has not yet been investigated fully. Regulation of the *cbiMNQO* gene cluster has been suggested to occur through the B_{12} riboswitch elements located within certain mRNA (Nahvi *et al.* 2004), which is not surprising since Co^{2+} is required in this organism mainly for the synthesis of vitamin B_{12} (Rodionov *et al.* 2003).
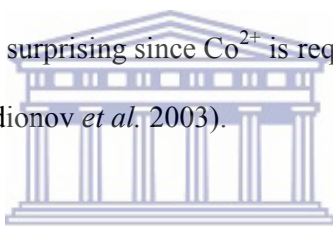
Other Co^{2+} ABC type transporters include Cbi(MN)QO of *Streptococcus salivarius* (Chen and Burne, 2003) and *Actinobacillus pleuropneumoniae* (Bosse´ *et al.* 2001), CbiKMQO of *Magnetospirillum magneticum* AMB-1 (Matsunaga *et al.* 2005), and CbiJKL of *Sinorhizobium meliloti* (Cheng *et al,* 2011).

1.4.1.5. Co^{2+} uptake permeases

A homologue of *A. eutrophus* H16 HoxN called NhlF was found in the gram-positive actinomycete *Rhodococcus rhodochrous* J1 which uses nitriles as both carbon and nitrogen source (Rodionov *et al.* 2006). NhlF is a product of a single component gene *nhl*F located in the nitrile hydrogenase (NHase) operon (Komeda *et al.* 1997). NHase (Co^{2+} containing protein) assay using benzonitrile as a substrate showed that the presence of *nhlF* yields

catalytically active NHase even at low Co^{2+} concentrations (1-5 µM). In particular NhlF increases the NHase activity 3.7 fold in the presence of 1 µM $CoCl_2$, showing a much higher affinity. Co^{2+} uptake by this protein was shown not to be affected by Mn^{2+}; Fe^{2+} or Cu^{2+}, but the presence of Ni^{2+} led to a marked decrease in Co^{2+} uptake suggesting that NhlF might also transport Ni^{2+}, although giving more preference to Co^{2+} (Komeda *et al.* 1997). The amino acid sequence and the topology model reveal that NhlF is a markedly hydrophobic protein containing eight transmembrane helices with the N-terminus in the cytoplasm (Komeda *et al.* 1997). NhlF is the only single component high affinity Co^{2+} importer that has been demonstrated experimentally to import Co^{2+} so far, although permeases such as CbtA and CbtC have also been suggested to import Co^{2+} (Gelfand and Rodionov, 2008) (Figure 8).

1.4.2. Metals efflux in bacteria

Some bacteria have been shown to tolerate higher metals concentrations. The *E. coli* isolated from sewage water was shown to tolerate up to 4 mM Ni^{2+} (Rubikas *et al.*1997), four times higher than what *E. coli* K12 has been reported to tolerate (Nies, 1999). A bacterial strain of *Bradyrhizobium* isolated from nodules of a legume plant was reported to grow in a medium containing 15 mM Ni^{2+} chloride (Chaintreuil *et al.* 2007).

Bacterial mechanisms for metals resistance have been the subject of most research (Silver and Phung, 2005). These resistance mechanisms involve metals efflux proteins which detoxify the cell by exporting metals to the external environment when cytoplasmic concentration increases above homeostasis limits (Nies and Silver, 1994). Efflux proteins have been reported for variety of metals, and include highly specific proteins and proteins which transport multiple metals. Most metals efflux genes are located in plasmids (Nies,

1999) although chromosomal metals efflux genes are also known. The most studied metals efflux proteins are the P-type ATPase and the Resistance Nodulation cell Division (RND) system (Nies and Silver, 1994). The P-type ATPase depends on the phosphorylation of ATP for energy while the RND systems are generally chemiosmotic systems which use proton motive force (Andrews *et al.* 2003).

1.4.2.1. P-type ATPase efflux systems

The P-type ATPases are integral membrane proteins which transverse the membrane eight to ten times (Nies and Silver, 1994). These proteins are ATP driven efflux with dual energy states (Odermatt *et al.* 1993). These proteins have been identified in archaea, prokaryotes and eukaryotes (Nies and Silver, 1994). Although these proteins differ between species, the general metal transport mechanism is common. The increase in cytoplasmic metals concentration results in the metal-protein interaction which is coupled with ATP dependent phosphorylation of the protein. This phosphorylation induces conformational changes which cause translocation of metal across the membrane (Nies and Silver, 1994). The binding of metals on the periplasmic domain is also believed to result in the pumping of secondary metals in to the cytoplasm (Nies and Silver, 1994).

Ni^{2+} and Co^{2+} P-type ATPases have not yet been reported. However, they have been reported for other metals, including the copper pump CopB of *H. pylori* (Odermatt *et al.* 1993); the cadmium pump CadA of *Bacillus subtilis* (Silver *et al.* 1993); the zinc efflux pump ZntA and the arsenic resistance pump ArsA of *E. coli* (Kaur and Rosen, 1993; Rensing *et al.,* 1997).

1.4.2.2. Ni^{2+} and Co^{2+} specific RND driven efflux systems

Ni^{2+} and Co^{2+} resistance mechanisms through RND systems have been well studied in heavy metals resistance bacterium *C. metallidurans* (Nies *et al.* 1987; Liesegang *et al.* 1993). This bacterium has two megaplasmids with at least seven metals resistance determinants (Nies *et al.* 1987). Three of these determinants, *cnrABCHRY*; *nccABCHY* and *czcABCY* have been shown to be involved in Ni^{2+} and Co^{2+} homeostasis (Nies *et al.* 1987). Amino acid sequence identity shows that the Czc and Cnr systems share 48% and 28% identity on two transmembrane domains while the substrate binding domains have 30% identity (Figure 10), suggesting a common ancestral operon (Liesegang *et al.* 1993). The *cnrABCHRY* and *nccABCR* have been reported to share an average sequence identity of 66% in the regulatory loci and 79% in the structural loci (Tibazarwa *et al.* 1999).
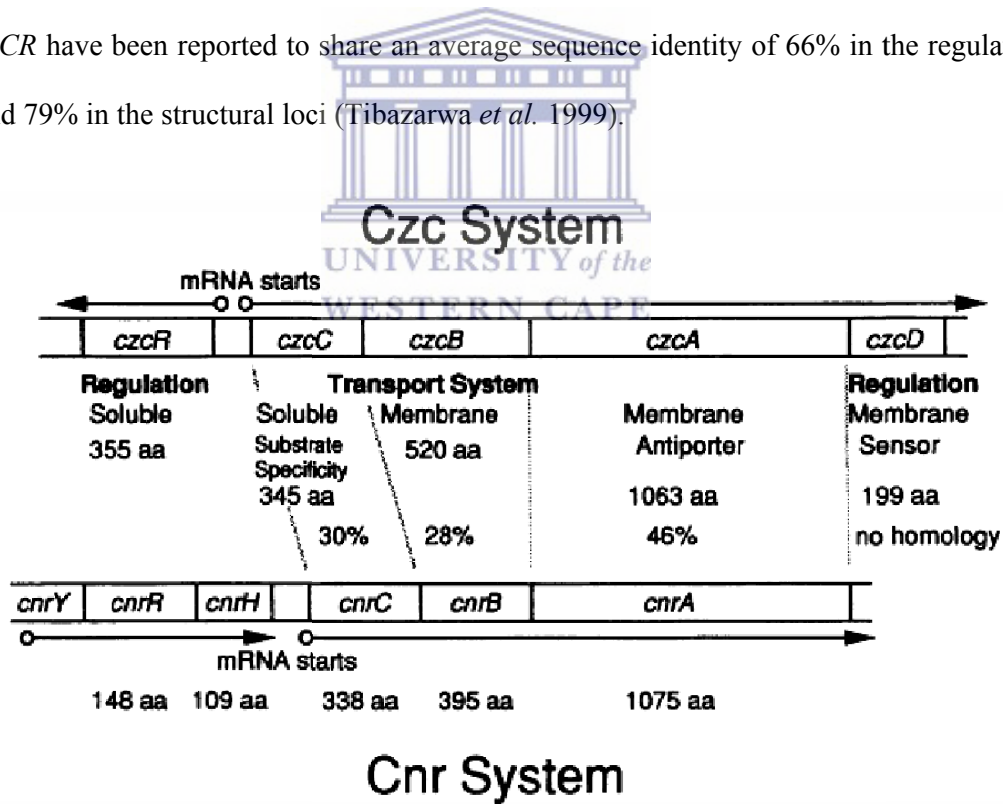
Figure 10: Model for genes arrangement in the *czc* and *cnr* system of *C. metallidurans* CH34. The transmembrane components of these two systems show 46% and 28% homology while the substrate binding components show 30% homology (Liesegang et al. 1993).

The *cnrABCHRY* gene cluster encodes Ni^{2+} and Co^{2+} efflux proteins, CnrABCRY. The CnrAB has a transmembrane domain; CnrC has a substrate binding domain while the CnrHRY is involved in regulation of Cnr system (Liesegang *et al.* 1993). Liesegang *et al.* (1993) have also demonstrated that CnrABC of *C. metallidurans* CH34 is only expressed under higher Ni^{2+} concentration. Grass *et al.* (2000) have shown that *cnr*ABC expression follows a saturation curve with half- maximum activation occurring at 49 μM Ni^{2+}. The *cnr* system has been shown to enable *C. metallidurans* CH34 to grow in 3 mM Ni^{2+} and 5 mM Co^{2+} (Sensfuss and Schlegel, 1988).

The *nccABCR* gene cluster encodes the Ni^{2+}, Co^{2+} and cadmium efflux proteins, NccABCR (Schmidt and Schlegel, 1994). The *ncc* system enables *Achromobacter xylosoxidans* 31A to grow in the presence of 40 mM Ni^{2+}, 20 mM Co^{2+} and 1 mM cadmium (Schmidt and Schlegel, 1994).
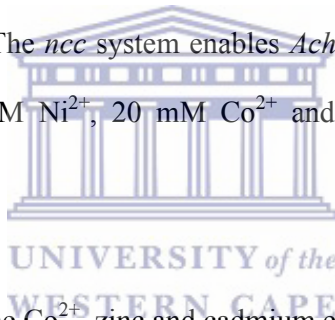
The *czcABCY* cluster encodes the Co^{2+}, zinc and cadmium efflux protein complex CzcABCY (Siddiqui and Schlegel, 1989). CzcAB was suggested to contain a potential transmembrane domain while CzcY has a regulatory domain (Liesegang *et al.* 1993). The CzcABC was shown to have an affinity of 22 μM to zinc, 140 μM to cadmium and 10 μM to Co^{2+} (Nies *et al.* 1987). Deletion of *czc*C resulted in a decrease of Co^{2+} and cadmium efflux. The deletion of *czc*A and *czc*B resulted in the complete loss of efflux activity of this system (Nies *et al.* 1989). The presence of *czcABC* in a recombinant *E. coli* strain has been shown to increase resistance to zinc and Co^{2+} 100 fold and 10 fold to cadmium (Nies *et al.* 1987).

In *E. coli*, a protein called RcnA (Figure 11) has been reported to export Ni^{2+} and Co^{2+} back to the periplasm when their intracellular concentrations increase above homeostasis limits

(Iwig *et al.* 2006). Transcription of *rcn*A was reported to occur at high intracellular Ni^{2+} and Co^{2+} concentrations and is repressed by a transcriptional repressor RcnR. Deletion of *rcn*R resulted in constitutive expression of *rcn*A and decreased intracellular amount of Ni^{2+} and Co^{2+}. Interestingly, increased intracellular Ni^{2+} concentration was shown to decrease the activity of Ni^{2+} uptake regulatory protein NikR, suggesting that NikR might be the first level of maintaining Ni^{2+} homeostasis in *E. coli* and *rcn*A is activated as the amount of Ni^{2+} continues to increase (Iwig *et al.* 2006). The *rcn*A mutation was shown to increase intracellular amount of Ni^{2+} in a medium containing 5 µM and 50 µM of Co^{2+} and Ni^{2+} respectively (Rodrigue *et al.* 2005).

UNIVERSITY *of the*
WESTERN CAPE
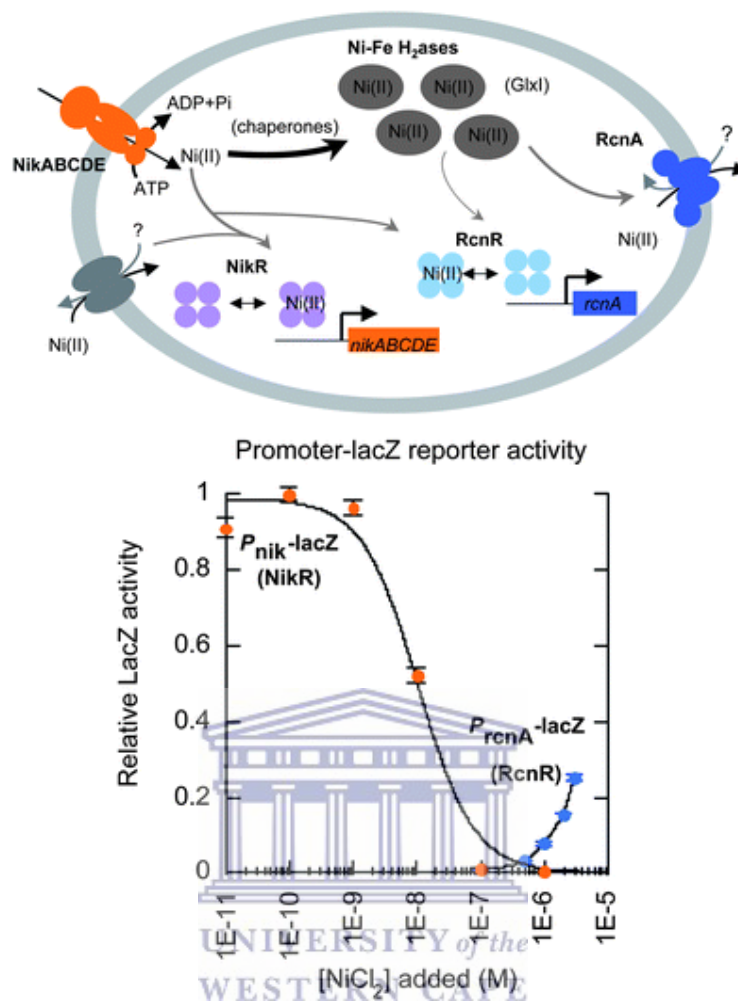
Figure 11: Nickel homeostasis mechanism through NikR-RcnR system. In a natural environment, nickel is accumulated into the cytoplasm through NikABCDE. As the concentration of nickel increases inside the cytoplasm, NikR binds to the promoter of *nikABCDE* preventing transcription of the operon. However, when the concentration of nickel continues to increase due to non-specific importers, *rcn*R is expressed. RcnR promotes the expression of *rcn*A which encodes RcnA, a transmembrane permease which exports nickel and cobalt back to the periplasm, thereby maintaining low levels of nickel in the cytoplasm (Hyeon, 2002).

1.5. Study rationale and aim

Bacterial magnetosomes are the most attractive source of magnetic nanoparticles. However, magnetosomes are chemically "soft" magnetic materials and can only be used for some

applications while other applications require "hard" magnetic materials. In addition, magnetotactic bacteria (MTBs) which synthesise the magnetosome are fastidious growers, making the synthesis of magnetosomes on an industrial scale difficult. Studies elsewhere (Qi *et al.* 2012), and here at Institute for Microbial Biotechnology and Metagenomics (IMBM) are being done to clone the genetic machinery for magnetosome synthesis, the magnetosome gene island (MIA) in *E. coli* in order to synthesise magnetosomes in an easy to culture organism.

The aim of this study was to genetically engineer *E. coli* strains which accumulate high intracellular Ni^{2+} or Co^{2+}. These strains will be used to express MIAs for the synthesis of chemically altered magnetosomes which can be used for a variety of applications.

1.5.1. The specific objectives are to:

- Clone different Ni^{2+} and Co^{2+} uptake genes in three mutants and a wild type strain

- Express the uptake genes in the presence or Ni^{2+} of Co^{2+}

- Study the cellular accumulation of Ni^{2+} and Co^{2+}

- Evaluate cellular iron and magnesium at different concentrations of Ni^{2+} and Co^{2+} in relation to iron
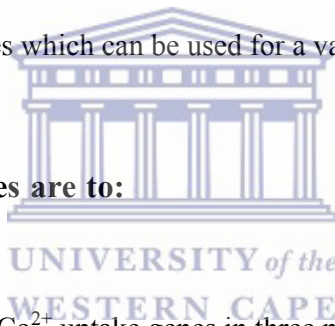
2. MATERIALS AND METHODS

2.1. Chemicals and reagents

Chemicals used in this study were supplied by Merck Chemicals and Sigma-Aldrich. All chemicals were of analytical grade. Culture media were supplied by Oxoid and Biolabs. Enzymes, cloning kits and DNA size markers were supplied by Fermentas. Oligonucleotide primers for polymerase chain reaction (PCR) were supplied by Inqaba laboratories. dNTPs were supplied by Life Technologies.
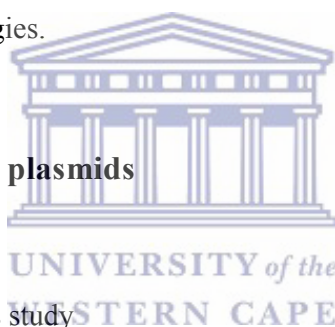
2.2. Bacterial strains and plasmids

TABLE 1: Plasmids used in this study

Plasmid	Relevant genotype/ characteristic	Source
pBAD (28)	F- ΔlacX74 (*Pvu* II) Δara714 *leu*::Tn*10 (CAM^R)*	Invitrogen
pJET 1.2 blunt	rep (pMB1) bla (Ap^R) *eco47IR* PlacUV5	Fermentas
pBAD*hox*N	pBAD (28) harboring *hox*N from *C. metallidurans* CH34	This study
pBAD*nhl*F	pBAD (28) harboring *nhl*F from *R. rhodochrous* J1	This study
pBAD*cbi*KMQO	pBAD (28) harboring *cbi*KMQO from *M. magneticum* AMB-1	This study

TABLE 2: Bacterial strains used in this study

E. coli strains	Relevant genotype	Reference	Source
JW 3789-1 (*ΔcorA*)	*λ rph-1 ΔcorA761::kan ΔcorA761::kan hsdR514*	Rowe *et al.* (2005)	CGSC (USA)
JW 3441-1 (*ΔnikA*)	*λ ΔnikA730::kan rph-1 Δ(rhaD-rhaB)568 hsdR514*	Wu *et al.* (1994)	CGSC (USA)
JW 2093-1 (*ΔrcnA*)	*λ ΔrcnA731::kan rph-1 Δ(rhaD-rhaB)568 hsdR514*	Koch *et al.* (2006)	CGSC (USA)
EPI-300	D(*ara, leu*)7697 *gal*U *gal*K 1- *rps*L *nup*G *trf*A *ton*A *dhfr*		University of the Western Cape, IMBM culture collection (SA)
Other strains			
Capriavidus metallidurans CH34			University of the Western Cape, IMBM culture collection (SA)
Rhodococcus rhodochrous J1			University of Stellenbosch culture collection (SA)

UNIVERSITY *of the*
WESTERN CAPE

2.3. Growth media

All *E. coli* strains were grown in Luria Bertani (LB) medium or M9 medium. LB broth was prepared by dissolving 10 g Tryptone; 5 g yeast extract and 10 g $NaCl_2$ in 1 litre of distilled deionised water (ddH$_2$O). LB agar was prepared by adding 15 g bacteriological agar in LB broth. M9 broth was prepared by dissolving 6 g Na_2HPO_4; 3 g KH_2PO_4; 0.5 g $NaCl_2$ and 1 g NH_4Cl in 880 ml ddH$_2$O and supplemented with 20 ml of filter sterilized solution containing 2 g/L glucose; 0.5 g/L $MgSO_4.7H_2O$;0.0152 g/L $CaCl_2.2H_2O$; 0.01 g/L sodium thiamine; 0.01 g/L Leucine and 0.001 g/L $FeSO_4.7H_2O$. Where indicated, ampicillin (amp) and chloramphenicol (cam) were added to a concentration of 200 mg/l and 170 mg/l respectively. *C. metallidurans* CH34 was grown in Casamino peptone glucose (CPG) medium containing 1 g Casamino acid; 10 g peptone; 5 g glucose dissolved in 1 litre ddH$_2$O. *Rhodococcus rhodochrous* J1 was grown in nutrient broth prepared by dissolving 10 g nutrient broth powder in 1 L ddH$_2$O. All media were sterilised by autoclave at 121ºC for 30 minutes.

2.4. Ni^{2+} and Co^{2+} tolerance

Tolerance of *E. coli* strains on Ni^{2+} and Co^{2+} was determined by growing cells at different concentrations of $NiCl_2$ or $CoCl_2$ and measuring absorbance at 600 nm. Glycerol stock culture was streaked on LB agar plate and grown overnight 37ºC. A single colony was inoculated in 5 ml M9 broth which was also grown overnight at 37ºC. A 50 μl of overnight culture was inoculated in 50 ml of M9 broth in 250 ml flasks supplemented with 0; 20; 40; 80; 160; 320; 640; 1280; 2580; or 5120 μM of $NiCl_2$ or $CoCl_2$. The flasks were incubated at 37ºC with shaking at 150 rpm until stationary phase. Cell density was measured using UV visible spectrophotometer at the wavelength of 600 nm.

2.5.   Chemically competent cells

The *E. coli* strain from glycerol stock was streaked on LB plates and incubated overnight at 37ºC. A single colony from an overnight culture was transferred to 5 ml LB broth in 50 ml falcon tubes and incubated overnight at 37ºC with shaking at 150 rpm. This culture was used to inoculate pre-warmed 100 ml LB broth in a 250 ml flask. The flask was incubated at 37ºC with shaking at 150 rpm until optical absorbance at 600 nm reached 0.4-0.6. The cells were transferred to a 500 ml centrifuge tube, incubated on ice for 15 minutes and harvested by centrifugation at 4500 x g (Backman J-26 XP, USA) for 5 minutes. The pellet was gently re-suspended in 10 ml of ice cold 0.1 M $CaCl_2$, incubated on ice for 30 minutes and harvested by centrifugation as above. The pellet was again gently re-suspended in 5 ml of ice cold solution of 0.1 M $CaCl_2$ containing 15 % glycerol. Aliquots of 100 μl were transferred into 1.5 ml tubes and stored at -80ºC.
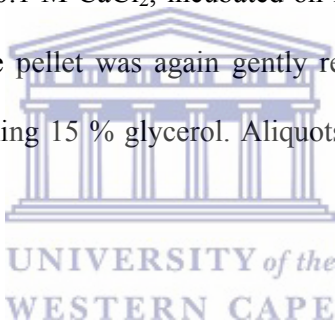
2.6.   Genomic DNA of source organisms

Genomic DNA of *Magnetospirillum magneticum* AMB-1 was kindly provided by Dr. Sarah Staniland from University of Leeds, England. Isolation of *C. metallidurans* CH34 and *R. rhodochrous* J1 genomic DNA was done using phenol/chloroform method. A single colony from overnight culture was inoculated in 2 ml CPG broth or nutrient broth and incubated for 16 hours at 30ºC with shaking at 150 rpm in a 10 ml tube. Cells were harvested by centrifugation at 10000 x g for 5 minutes, supernatant was discarded and the pellet was re-suspended in 500 μl TE buffer (0.005 M Tris base and 0.002 M EDTA, pH 8.0) . An amount of 30 μl of 10% SDS and 5 μl of proteinase K (20 mg/ml) were added to the cells followed by incubation at 37ºC for 1 hour. A 100 μl mixture of phenol/chloroform solution (50:50) was

added followed by centrifugation at 10000 x g for 5 minutes. The upper aqueous phase of the solution was transferred to a clean tube followed by addition of another 100 μl of phenol/chloroform solution. This was centrifugated at 10000 x g for 10 minutes. A 50 μl volume of sodium acetate (5 M sodium acetate and 5% acetic acid) and 100 μl of isopropanol were added to the extracted upper phase and mixed gently to precipitate the DNA. Using a clean sterile glass rod, a suspension of DNA was spooled out of the solution and washed by dipping the end of the rod into 1 ml of 70 % ethanol for 30 seconds. DNA was re suspended in 200 μl TE buffer and stored at -20ºC. DNA concentration was quantified using a Nanodrop ND-1000 spectrophotometer at 260 nm (Nanodrop, Delaware USA).

2.7. Plasmid DNA isolation
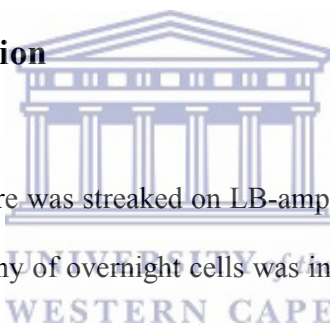
A glycerol stock of *E. coli* culture was streaked on LB-amp or LB-cam agar plate and grown overnight at 37ºC. A single colony of overnight cells was inoculated in 2 ml LB- amp or LB-cam broth in a 50 ml tube. The culture was incubated overnight at 37ºC with shaking at 150 rpm. Cells were transferred to a sterile tube followed by harvesting through centrifugation at 10000 x g for 5 minutes. The pellet was re- suspended in 200 μl GTE buffer (50 mM glucose; 25 mM Tris-Cl, pH 8.0 and 10 mM EDTA, pH 8.0). A 200 μl solution of NaOH/SDS (0.2 N NaOH and 1 % SDS) and 200 μM solution of potassium acetate solution (3 M potassium acetate and 11.5 % (v/v) acetic acid) were added. The tube was centrifuged at 10000 x g for 5 minutes and 500 μl of supernatant was transferred to a new 2 ml tube. A 100 μl of ice cold 100% ethanol was added followed by incubation at -20ºC for 30 minutes. The tube was centrifuged at 10000 x g for 15 minutes. The supernatant was discarded and 100 μl of 70% ethanol was added to the pellet. The tube was again centrifuged for 2 minutes at 10000 x g and ethanol was carefully removed. Ethanol was removed by leaving the tube open upside

down on a paper towel for two hours. A 50 μl volume of TE buffer was added to dissolve the pellet and plasmid DNA was stored at 4ºC. The concentration was quantified using Nanodrop ND-1000 spectrophotometer at 260 nm (Nanodrop, Delaware USA). Plasmid isolation for sequencing and cloning was done using a Qiagen miniprep kit according to manufacturer's recommendations.

2.8. PCR

The PCR was carried out in a 50 μl reaction using Dream Taq or Phusion polymerase according to manufacturer's recommendations. A typical reaction mixture contained 5 μl of 10 X Dream Taq buffer or 10 μl of 5 X Phusion buffer; 5 μl of 2 mM dNTP; 2 μl of 10 μM forward primer; 2 μl of 10 μM reverse primer; 1 μl of 100 ng/μl genomic DNA and 0.25 μl of Dream Taq polymerase or 0.5 μl of Phusion polymerase. Reaction mixture was adjusted to a final volume of 50 μl with sterile super quality (Milli Q) H_2O. Amplification was carried out in an automated thermal cycler under conditions in Table 3. All primers used in this study are listed in Table 4.

TABLE 3: PCR conditions used for amplifying 16S rRNA PCR

	Temperature (°C)	Time (min)	Cycles
Initial denaturation	95	5	1
Denaturation	95	0.45	35
Annealing	55	0.45	35
Extension	72	See table 5	35
Final extension	72	5	1

TABLE 4: Primers used in this study

Primers	Primer sequences	Extension time (min)	Tm (ºC)	%GC	Target gene	Reference
E9F	5' GAGTTTGATCCTGGCTCAG 3'	1	58	52.6	Bacterial 16S rRNA	Hansen *et al*, 1998
U1510R	5' GGTTACCTTGTTGTTACACTT 3'	1	58	38.1	Bacterial 16S rRNA	Baker *et al.* 2003
nCH34F	5' TCTAGAAGGAGGAGCGGAATGGAAG 3'	0.15	57.5	52	*hox*N	This study
nCH34R	5' AAGCTTCGCAGCTTAAACGCTACG 3'	0.15	55.4	50	*hox*N	This study
cRJ1F	5' GGTACCAAGGACAAGCGTTTGAC 3'	0.17	55.2	52.2	*nhl*F	This study
cRJ1R	5' AAGCTTCGTCAGCGTTATGGGTAT 3'	0.17	55.8	53.7	*nhl*F	This study
cAMB1F	5' GGTACCAGAACGAAGTCGCA 3'	0.57	52.5	55	*cbi*KMQO	This study
cAMB1R	5' AAGCTTTGCCTCCAGACCAC 3'	0.57	52.5	55	*cbi*KMQO	This study

2.9. Agarose gel electrophoresis

Visualisation of specific DNA fragments was done on 0.7% [w/v] of agarose gel prepared in 0.5 X TAE buffer (0.2 % [v/v] Tris base; 0.5 % [v/v] glacial acetic acid and 1% [v/v] 5 M EDTA, pH 8.0) and 10 μl/L of 0.5 μg/ml ethidium bromide.   DNA was mixed with a loading dye (60% [v/v] glycerol and 0.25% [w/v] Orange G) and loaded into the wells of cast gel. DNA molecular marker (lambda DNA restricted with *Pst*I) was used as standard. The samples were electrophoresed at 100 V in 0.5 X TAE buffer.

2.10. Cloning and transformation
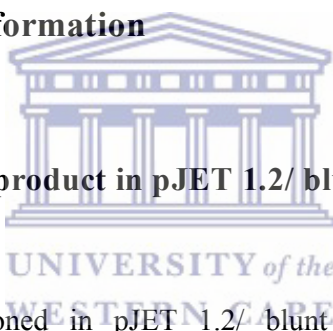
2.10.1.   Cloning of PCR product in pJET 1.2/ blunt

The PCR products were cloned in pJET 1.2/ blunt (Fermentas) according to the manufactures recommendations. The reaction mixture contained 10 μl of 2 X reaction buffer, 2 μl PCR product (55 ng/μl), 1 μl pJET vector, 5-10 U of T4 DNA ligase per μg of DNA and 6 μl ddH$_2$O. The mixture was incubated at room temperature for 20 minutes and then used to transform the host strains.

2.10.2.   Restriction digests

The pJET*cbi*MNQO, pJET*nhl*F and pBAD(cam) were double digested with *Hin*dIII and *Kpn*I. pJET*hox*N and pBAD(cam) were digested with *Hin*dIII and *Xba*I . Digestion was carried out in a sterile microfuge tubes in reaction volume of 20 μl. The reactions contained

2 μl of 10 X reaction buffer, 2 μl of plasmid DNA (100 ng/ μl), 5 units of enzyme per μg of DNA, and were made up to 20 μl with sterile ddH$_2$O. The digestion products were analysed by gel electrophoresis as indicated above.

2.10.3. Sub-cloning in pBAD

The amplified and restricted *hoxN*, *cbiKMQO* or *nhlF* were sliced out from agarose gel using sterile surgical blade on a 365 waveleangth UV transluminator and placed in a clean sterile microtube. The DNA fragment was extracted from agarose gel using the Nucleospin gel extraction kit (Macherey-Nagel) according to the manufactures recommendations. Directional cloning was done in a 20 μl reaction containing: 10 μl of 2 X reaction buffer, 2 μl of double digested gene of interest (55 ng/μl), 1 μl of double digested pBAD vector, 10 U of T4 DNA ligase per μg of DNA and made up to 20 μl with ddH$_2$O. The mixture was incubated at room temperature for 20 minutes and then used to transform host strains.

2.10.4. Sequencing

Sequencing was carried out using an automated DNA sequencer 373 at the University of Cape Town sequencing facility. Sequencing was performed with fluorescein labelled primers (Applied Biosystems, USA).

2.10.5. Transformation

An aliquot of 5 μl plasmid was placed in a 1.5 ml microtube followed by adding 100 μl of *E. coli* chemical competent cells. The mixture was incubated on ice for 30 minutes followed by

heat shock at 42ºC for 2 minutes. A 900 µl volume of LB broth was added on cells and incubated for 30 minutes at 37ºC. Fifty microliters of the expression mix was aseptically spread on LB plates containing antibiotic and incubated for 16 hours at 37ºC.

2.11. Expression and SDS-PAGE

2.11.1. Gene expression

Expressional analysis was carried out according to the modified method of Auer *et al.* (2001). The cells harboring pBAD-*hox*N from the glycerol stock were grown overnight at 37ºC on LB-cam plates. A single colony of overnight cells was inoculated in 2 ml LB-cam broth in a 50 ml tube. The tube was incubated overnight at 37ºC with shaking at 150 rpm. Cells were transferred to 10 ml LB-cam broth in a 50 ml flask and incubated as above until OD_{600}=0.5-0.6. L-arabinose was added to a final concentration of 0, 0.0002, 0.002, 0.02, 0.2, and 2% and cells were incubated at 15ºC for 2 hours with shaking. An aliquot of 2 ml was transferred to a microtube and cells were harvested by centrifugation at 10000 x *g* for 3 minutes.
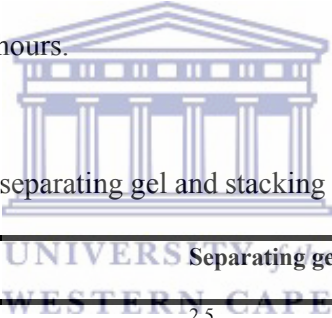
2.11.2. Cell lysis

The cell pellet was re-suspended in 100 µl of lysis buffer (50 mM Tris-HCl pH 8, 0.5 mM Phenylmethanesulfonyl floride (PMSF), and 400 mM $CaCl_2$), subjected to 3 cycles of sonication at 10% power for 10 second using a Sonoplus HD-070 sonicator (Bandelin, Germany) and stored at -20ºC.

2.11.3. **SDS-PAGE**

SDS-PAGE was carried out on a Mighty Small[TM] SE 280 vertical slab unit (Hoefer Inc, USA). Separating gel (10%) and stacking gel was prepared as indicated in Table 5. A sample of 10 μM SDS-PAGE sample buffer (50 mM Tris-HCl, pH 6.8; 2 % SDS; 1 % β-mercaptoethanol; 10 % glycerol; 12.5 mM EDTA and 0.02 % bromophenol blue) was added to 20 μl of sample and was loaded on a gel and run at 80 V for 2 hours. PageRuler[TM] pre-stained protein marker (Fermentas) was used to estimate the molecular weight of proteins in the sample. The gel was stained in Coomassie Brilliant Blue G-250 staining solution at room temperature for 16 hours and de-stained in a buffer containing 10% (v/v) acetic acid and 50% (v/v) methanol for 16 hours.

TABLE 5: Preparation of 10% separating gel and stacking gel
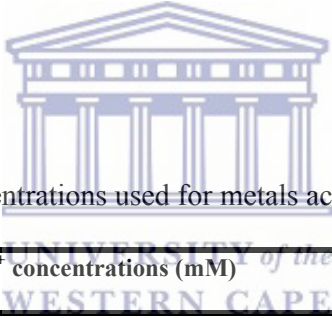
Reagent	Separating gel (ml)	Stacking gel (ml)
1.5 M Tris-HCl, pH 8.8	2.5	-
0.5 M Tris-HCl 6.8	-	1.250
20% (w/v) SDS	0.05	0.025
Acrylamide/Bis-acrylamide (30%/0.8% w/v)	3.3	0.67
10% (w/v) ammonium persulfate	0.05	0.025
TEMED	0.005	0.005
ddH$_2$O	4.1	3.075

2.12. Metal accumulation experiment

2.12.1. Accumulation at stationary phase

Bacterial cells from glycerol stock were grown overnight at 37°C in LB-cam plates. A single colony was inoculated into 300 ml of M9-cam broth in a 1 L flask and incubated at 37ºC with shaking at 150 rpm until OD_{600} reached 0.8 -1.0. L-arabinose was at a concentration of 0.2%. $NiCl_2$ or $CoCl_2$ (0-1 mM) was added as indicated in Table 6. Cells were incubated for two hours followed by harvesting by centrifugation at 10000 x g for 5 minutes at 4ºC. The pellet was washed twice with 1 mM EDTA and once with sterile ddH_2O.

TABLE 6: Ni^{2+} and Co^{2+} concentrations used for metals accumulation

E. coli strain	Ni^{2+}/ Co^{2+} concentrations (mM)		
EPI 300	0.005	0.05	0.1
JW 2093-1	0.001	0.01	0.02
JW 3789-1	0.1	0.5	1
JW 3441-1	0.005	0.1	0.5

2.12.2. Accumulation at exponential phase

Bacterial cells from glycerol stock were grown overnight at 37°C in LB-cam plates. A single colony was inoculated into 300 ml of M9-cam broth in a 1 L flask and incubated at 37ºC with shaking at 150 rpm until OD_{600} reached 0.1 - 0.2. L-arabinose was added at a concentration of 0.2%. $NiCl_2$ or $CoCl_2$ was added to the final concentration of 0.1 mM and $FeSO_4$ was added to a final concentration of 0.36 mM. Cells were grown up to OD_{600}

between 0.6-0.7 followed by harvesting by centrifugation at 10000 x g for 5 minutes at 4ºC. The pellet was washed twice with 1 mM EDTA and once with sterile ddH$_2$O.

2.13. Nitric acid digest and ICP-OES analysis

The washed pellet (section 2.12.2) was dried at 100ºC for 3 hours in an oven. Dry weight was measured and recorded. Dried cells were transferred into a clean 25 ml flask (cleaned by soaking overnight in 10 % nitric acid and washed with distilled deionised water). Cell digestion was carried out by heating dried cells in 5 ml of 70 % nitric acid at 180ºC for 1 hour. Metals analysis was done at the chemistry department of the University of the Western Cape by inductively coupled plasma optical emission spectroscopy (ICP-OES) using metal standard prepared in 2 % nitric acid.
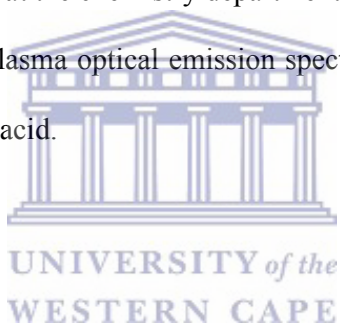
3. RESULTS AND DISCUSSIONS

3.1. Introduction

The objective of this study was to engineer *E. coli* strains which accumulate intracellular Ni^{2+} and Co^{2+}. These strains would be used to co-express the magnetosome gene island (MIA) and metal uptake genes for the synthesis of chemically altered magnetosomes. To achieve this objective, the following strategies were employed:

I.   High affinity Ni^{2+} or Co^{2+} uptake protein encoding genes were cloned and expressed in *E. coli* to improve intracellular accumulation as demonstrated by Wolfram *et al.* (2005). A Ni^{2+} uptake gene *hox*N from *C. metallidurans* CH34; a Co^{2+} uptake gene *nhl*F from *R. rhodochrous* J1 and a Co^{2+} ABC type gene cluster *cbi*KMQO from *M. magneticum* AMB-1 were used in this study.

HoxN was used in this study because it has been fairly well studied compared to other Ni^{2+} permeases (Wolfram *et al.* 1995) from a family of rare NiCoT permeases, which include NixA from *H. pylori*, HupH from *B. japonicum* and NhlF (Rodionov *et al.* 2006). NhlF is the only Co^{2+} uptake permease which has been experimentally investigated and shown to accumulate Co^{2+} (Rodionov *et al.* 2006). The CbiKMQO gene cluster from *M. magneticum* AMB-1 was included to compare its capacity with the Co^{2+} permease NhlF.

II. Ni^{2+} and Co^{2+} accumulation were studied in Ni^{2+} or Co^{2+} concentrations ranging from 0 to 1 mM. This was done to identify the lowest medium concentration which results in the most intracellular accumulation. A study by Deng *et al.* (2003) demonstrated that intracellular metal accumulation in bacteria increases as the medium concentration increased, until a point of bioaccumulation equilibrium is reached where increasing the medium concentration does not increase the intracellular accumulation (Figure 12). Equilibrium bioaccumulation occurs when the amount of metals being imported into the cell is in equilibrium with the amount of metals being exported out of the cell through a metal efflux mechanism (Deng *et al.* 2003).
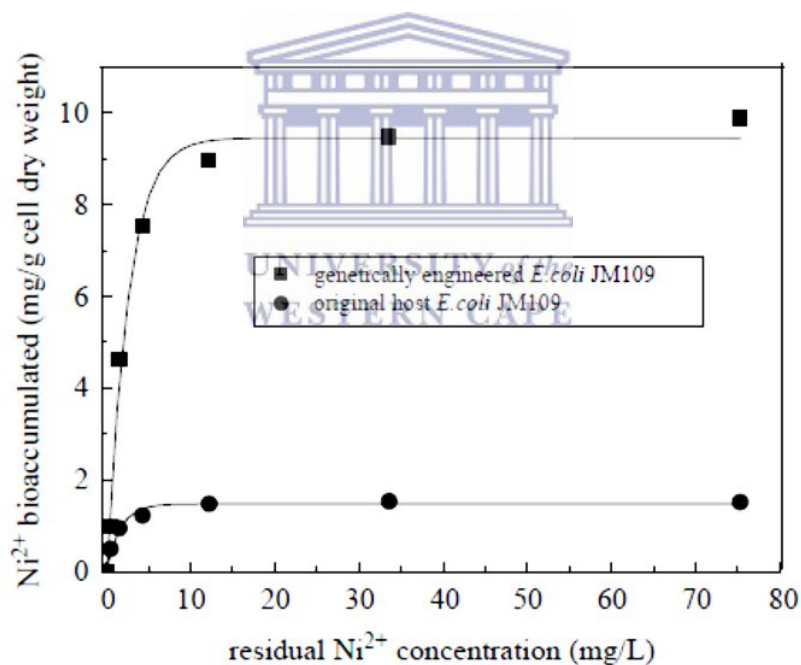
FIGURE 12: Diagrammatic representation of nickel equilibrium bioaccumulation in *E. coli* grown at increasing nickel concentrations (Deng *et al.* 2003).

III.	Ni^{2+} and Co^{2+} intracellular accumulation was also conducted in three Ni^{2+}/ Co^{2+} transport *E. coli* mutants. Three systems have been reported to transport Ni^{2+} and Co^{2+} in *E. coli*: The CorA transport systems of magnesium; Ni^{2+} and Co^{2+} (Nies, 1999); the NikABCDE high affinity ABC type Ni^{2+} transporter (Rodrigue *et al.* 2005) and the RcnA system which exports both Ni^{2+} and Co^{2+} from the cytoplasm (Rodrigue *et al.* 2005).

The *ΔcorA* mutant has been shown to grow at high Ni^{2+} and Co^{2+} concentrations (Nies, 1999). This mutant was selected for this study in order to determine Ni^{2+} and Co^{2+} intracellular accumulation through high affinity transporters in medium concentrations which inhibit the growth of the wild type strain. The *ΔnikA* mutant was used to study the Ni^{2+} uptake capacity of NikABCDE and HoxN permeases. This was done to identify the most efficient Ni^{2+} uptake system for intracellular accumulation. The *ΔnikA* mutant was transformed with *hox*N gene and compared for intracellular Ni^{2+} with the *ΔcorA* mutant. The *Δrcn*A mutant was used in order to determine whether higher intracellular accumulation could be achieved by preventing export. This strain does not export Ni^{2+} and Co^{2+} from the cell cytoplasm (Rodrigue *et al.* 2005); hence it is expected to contain high concentrations of these metals.

IV.	Intracellular accumulation studies were also conducted using metals concentrations which have been shown to result in magnetosome doping. In Co^{2+} doping, Staniland *et al.* (2008) demonstrated that the medium Fe:Co ratio of 1:4 resulted in 1.4% Co^{2+} inside the magnetosome. In Ni^{2+} doping, Kundu *et al.* (2009) used Fe: Ni ratio of 2:1 to incorporate Ni^{2+} in the magnetosome.

3.2. Ni^{2+} and Co^{2+} tolerance

The mutants selected for this study have been reported to have different phenotypes when grown in the presence of Ni^{2+} or Co^{2+}. The CorA mutant has been shown to be more tolerant to Ni^{2+} and Co^{2+} that the wild type (Rowe *et al.* 2005). The *ΔnikA* mutant confers high tolerance to Ni^{2+} (Wu *et al.* 1994) while the Δ*rcn*A mutant has been shown to be more sensitive to both Ni^{2+} and Co^{2+} (Koch *et al.* 2006).

In this study, we first verified this tolerance by conducting Ni^{2+} and Co^{2+} tolerance experiments. All strains were first transformed with pBAD(cam) as controls. Figure 13A-B shows tolerance curves of EPI 300 and the three mutants grown in M9 (cam) medium at increasing concentrations of NiCl$_2$ or CoCl$_2$. The Δ*corA* mutant was able to grow in up to 5.120 mM of both NiCl$_2$ and CoCl$_2$, the highest tolerance compared to the other strains. This is consistent with previous studies which reported high minimal inhibitory concentration (MIC) for a Δ*corA* mutant compared to wild type strain (Wu *et al.* 1994). The Δ*nikA* mutant grows in 2.560 mM NiCl$_2$ but was inhibited by 1.280 mM CoCl$_2$. This Co^{2+} tolerance is similar to that of EPI 300, but EPI 300 shows less tolerance to Ni^{2+}. As expected, the Δ*rcnA* mutant has the lowest tolerance for both Ni^{2+} and Co^{2+}. This mutant did not grow on 0.64 mM NiCl$_2$ and 0.31 mM CoCl$_2$.

These tolerance curves show that intracellular accumulation of Ni^{2+} and Co^{2+} in Δ*corA* can be conducted in higher medium concentrations of these metals than other strains without affecting toxicity.
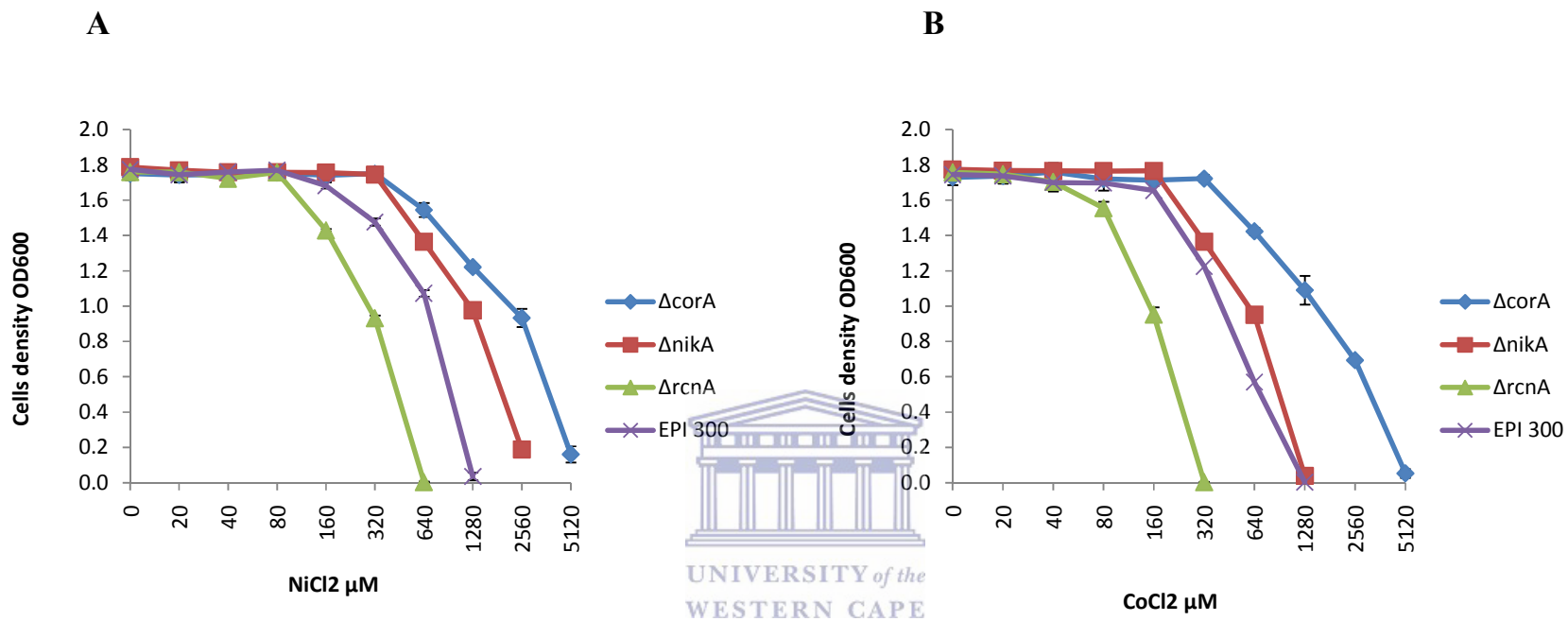
Figure 13A-B: Ni^{2+} and Co^{2+} tolerance curves of *E. coli* mutants and EPI 300 grown on M9-cam medium. **A** Nickel tolerance curves and **B** Cobalt tolerance curves. All strains reached cell density of over 1.75 in the absence of either nickel or cobalt. The results shown here are average of three independent experiments. Error bars represent the standard deviation of the three experiments.

3.3. Growth curves in the presence of Ni^{2+} or Co^{2+}

Longer lag time in the presence of Ni^{2+} or Co^{2+} was observed in EPI 300, the *ΔnikA* and the *Δrcn*A mutant when conducting tolerance curves. Lag time was directly linked to the amount of $NiCl_2$ or $CoCl_2$ in the medium. Mathematical models for metals concentrations against lag time have been proposed in studies elsewhere (Gikas *et al.* 2009). Delayed lag time has been reported in other studies such as Cabrera *et al.* (2005) who reported longer lag phase in *Desulfovibrio vulgaris* growth on minimal medium supplemented with different metals. The growth of *E. coli* V38 in medium supplemented with 4 mM Ni^{2+} was also delayed compared to strain grown without Ni^{2+} (Rubikas and Matulis, 1997). Although the dose response lag phase is not yet fully understood, it has been reported that when exposed to high metals concentrations, bacterial cells prioritise the use of energy on expressing metals efflux proteins at lag phase, hence the long lag time in the presence of metals (Ralfe *et al.* 2011).
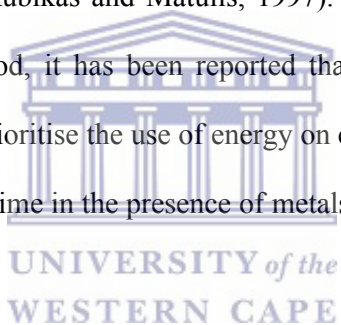
To investigate how Ni^{2+} or Co^{2+} will affect the growth of mutant strains used in this study, growth curves were conducted in M9 (cam) medium containing of 0.1 mM $NiCl_2$ or $CoCl_2$. Figure 14A-C and Table 7 show summaries of results obtained from growth profiles. *E. coli* strains, EPI 300; *ΔnikA* and *ΔrcnA* show a prolonged lag phase in the presence of 0.1 mM $NiCl_2$ or $CoCl_2$. This delayed growth was followed by slow log phase (Table 7). The growth of the *ΔnikA* mutant was not significantly affected at 0.1 mM $NiCl_2$ but was affected by 0.1 mM $CoCl_2$, confirming a previous report which shows that *nikA* mutation reduces cell sensitivity to Ni^{2+} (Eitinger and Mandrand-Berthelot, 2000).
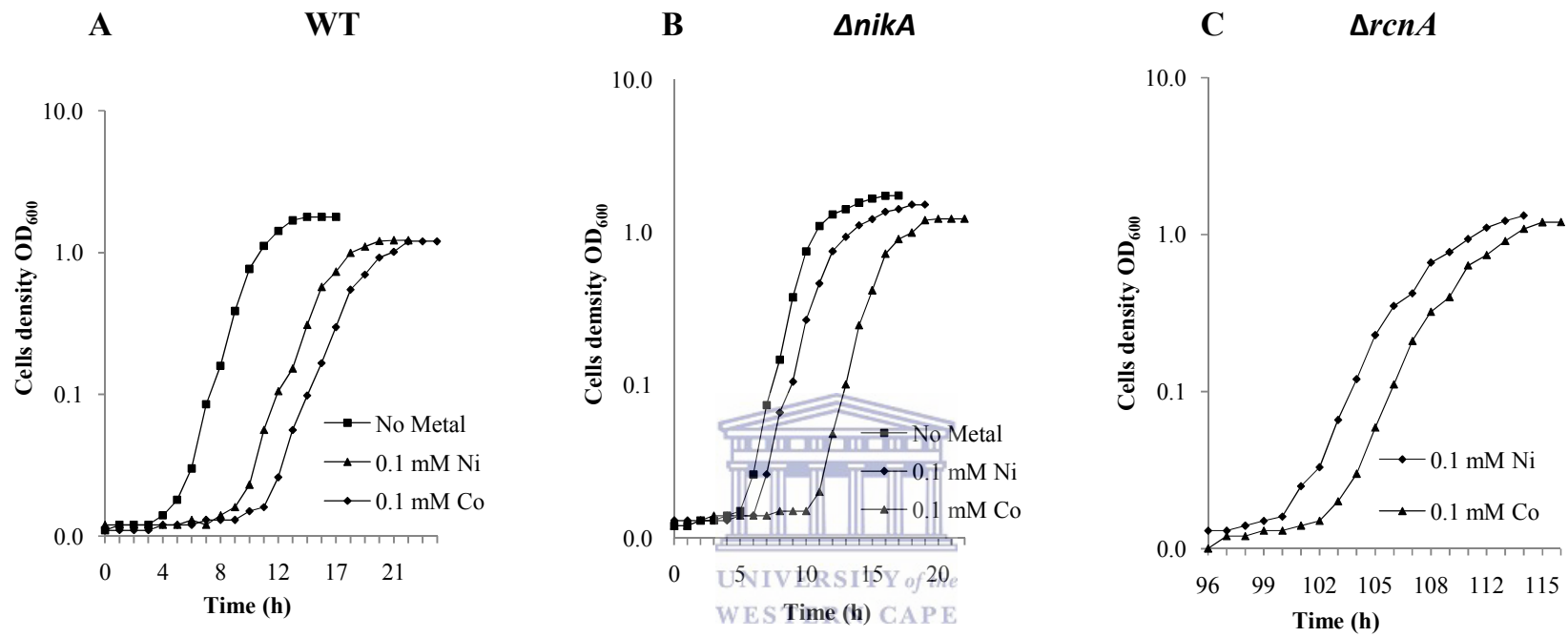
Figure 14 A-C: Growth curves of *E coli* strains: EPI 300 (A)*, ∆nik*A mutant (B) and *∆rcnA* mutant in M9-cam supplemented with 0.1 mM NiCl$_2$ or CoCl$_2$ and without NiCl$_2$.

Table 7: Lag and doubling time of *E. coli* strains used in this study

E. coli strains	No Ni^{2+} or Co^{2+}		0.1 mM NiCl$_2$		0.1 mM CoCl$_2$	
	Lag time (h)	Doubling time (min)	Lag time (h)	Doubling time (min)	Lag time (h)	Doubling time (min)
EPI 300	5 ± 0.14	55 ± 2.7	9 ± 0.51	73 ± 3.3	11 ± 0.04	75 ± 6.5
ΔcorA	5 ± 0.22	54 ± 5.3	5 ± 0.33	54 ± 3.9	5 ± 0.025	54 ± 6.1
ΔnikA	5 ± 0.09	52 ± 3.1	6 ± 0.14	58 ± 1.8	11 ± 0.52	72 ± 5.8
*Δrcn*A	7 ± 0.11	61 ± 2.9	96 ± 2.66	86 ± 3.8	96 ± 1.98	91 ± 8.6

Growth curves were conducted in M9 (cam) medium with or without 0.1 mM NiCl$_2$ or CoCl$_2$ supplimentation. The data presented here represents the mean ± standard deviation of three independent experiments.

3.4. 16S rRNA PCR Analysis

Before amplification of metals uptake genes, source organisms were first verified by amplification of the 16S rRNA gene. The amplicons were analysed in agarose gel (Figure 15) and were all found to be about 1.5 kb. These were cloned in pJET 1.2/ blunt and sequenced. Sequence alignment was done with sequences in the GenBank database using NCBI tool to confirm that the organisms were correct.
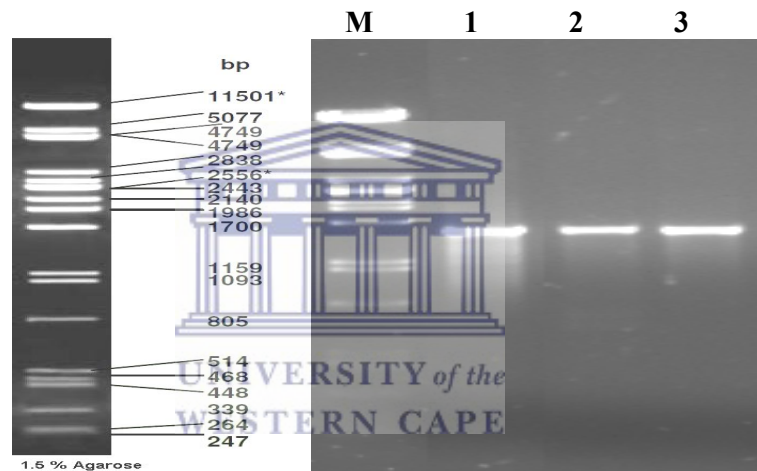
FIGURE 15: Agarose gel of 16S rRNA amplicon. Lane M is a phage λ DNA marker digested with *Pst*I, lane 1 to 3 is 1.5 kb 16S rRNA of *C. metallidurans* CH36, *R. rhodochrous* J1 and *M. magneticum* AMB-1.

3.5. Cloning of the metal uptake genes

The *hoxN, nhlF* and *cbiKMQO* genes were amplified (Figure 16) and cloned in pJET 1.2/ blunt to confirm the sequences before they were finally cloned in pBAD (Figure 17).
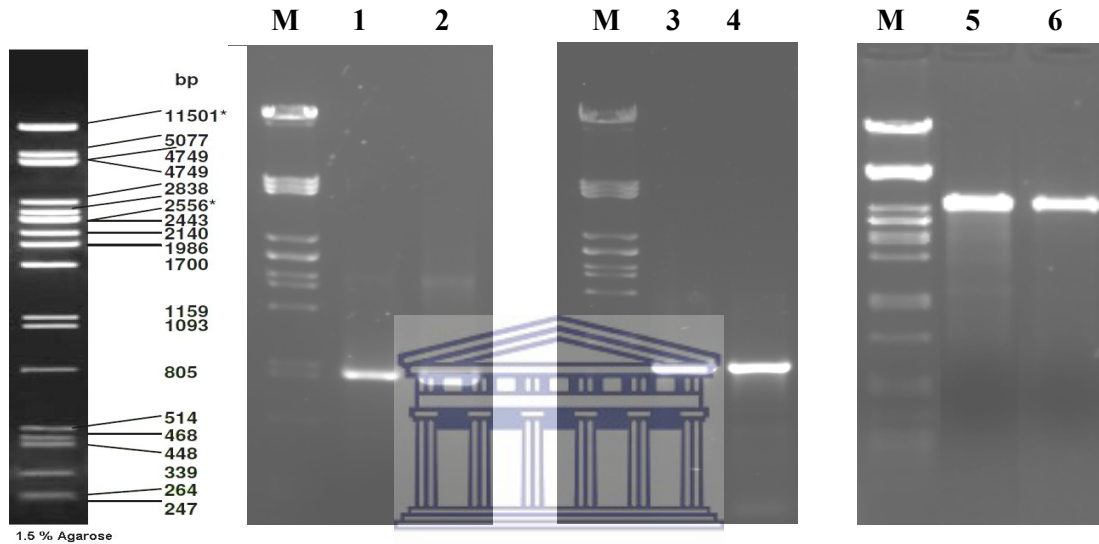
FIGURE 16: Agarose gel electrophoresis of PCR products of *hox*N, *nhl*F and *cbiKMQO* genes. Lane M shows a λ phage DNA marker digested with *Pst*I, lane 1and 2 shows a 1kb *nhl*F PCR product lane 3 and 4 shows a 834 bp *hoxN* PCR product , and lane 5 and 6 shows a 3kb *cbiKMQO* PCR product.
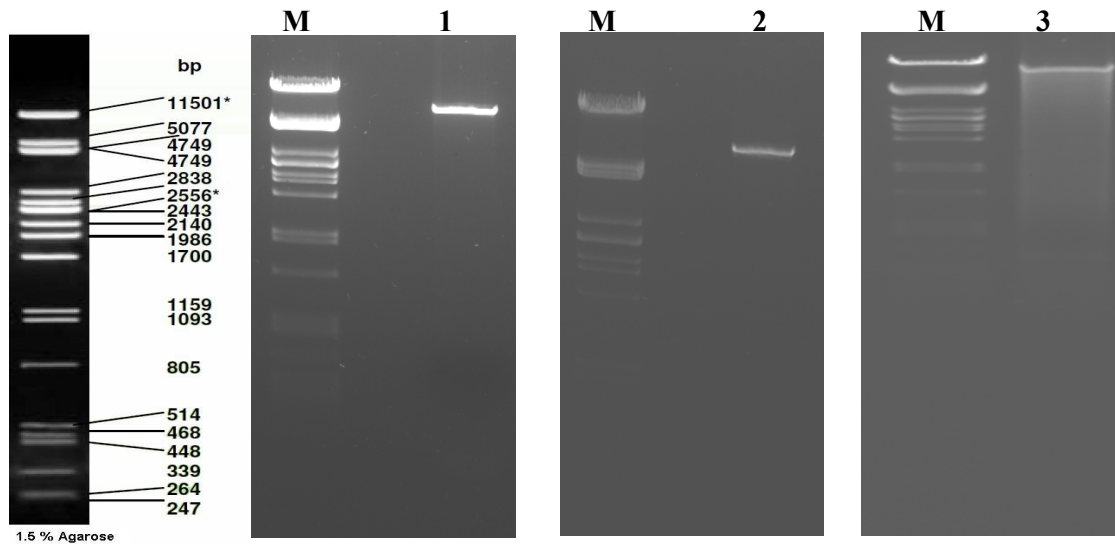
FIGURE 17: Agarose gel electrophoresis of pBAD carrying *hoxN*, *nhlF* or *cbiKMQO* genes. All plasmids were first linearised by digesting with *Hin*dIII. Lane M is a λ phage DNA marker digested with *PstI*, lane 1 shows a linear 6.6 kb pBAD*hoxN* DNA band, lane 2 shows a linear 6.8 kb pBAD*nhlF* DNA band and lane 3 shows a linear 9 kb pBAD*cbiKMQO* band.

3.6. Expression of metal uptake proteins

The pBAD expression system has been used for the expression of various membrane proteins under the control of the arabinose promoter (Wang *et al.* 2003). Expressional level under this promoter can be optimised by varying the concentration of arabinose, making this system suitable for expression of recombinant membrane proteins (Khlebnikov *et al.* 2001) which are known to be toxic to the cell at higher concentration (Wang *et al.* 2003).

Metals uptake proteins, like all membrane proteins are difficult to isolate from the cell due to a number of factors. This includes their high susceptibility to proteolytic degradation (Auer *et al.* 2001), and incorporation into the inclusion bodies, which reduces the amount of isolated protein (Wang *et al.* 2003) making them invisible in SDS-PAGE. Different methods have

been reported for expression and isolation of high concentration of membrane protein from *E. coli* (Wang *et al.* 2003). The efficiency of these methods depends on the size and nature of the membrane protein. Generally, different studies recommend that post induction time and incubation temperature be reduced to minimise proteolysis degradation and formation of inclusion bodies (Wang *et al.* 2003). Here, a modified method of Auer *et al.* (2001) was used to verify expression of metal uptake protein using a pBAD system. Figure 18 shows the SDS-PAGE analysis of the expression of *hox*N under the arabinose promoter at different concentrations of L- arabinose. The highest expression was achieved with 2% L-arabinose. At L-arabinose of 0.02 and 0.2% also give good expression.

FIGURE 18: SDS-PAGE analysis of *E. coli* EPI 300 cells harbouring pBAD*hox*N. Cells were induced with different concentrations of L-arabinose, harvested, disrupted in lysis buffer and loaded onto the gel. Lane M contains protein molecular weight ladder, lane 1 to 6 contains disrupted cells which were induced with 0; 0.0002; 0.002; 0.02; 0.2; and 2% L-arabinose respectively. The expected product is 30 kDa. The highlighted band indicates putative HoxN monomer.

3.7. Ni^{2+} and Co^{2+} accumulation

Different methods for metal bioaccumulation in recombinant *E. coli* expressing metal uptake genes have been previously reported. These methods differ depending on the general objective of the experiment. However in most of these methods the metal of interest is added during late logarithmic to stationary growth phase and the post-harvest time is commonly one to two hours. For example Krishnaswamy and Wilson (2000) induced expression of Ni^{2+} uptake gene, *nixA* in pGPMT3 plasmid vector when the cell density reached OD_{600} of 0.5-0.7, adding Ni^{2+} when OD_{600} was 1 and harvesting cells an hour later. The same method was used elsewhere (Deng *et al.* 2003). The idea of inducing expression at logarithmic growth is to get high amount of recombinant protein because at this stage cells are metabolically active. However, at logarithmic growth cells also express high amounts of proteases which degrade membrane proteins (Wang *et al.* 2003). Auer *et al.* (2001) induced the expression of membrane protein at OD_{600} of 1 to minimise this proteolytic degradation.

Addition of metals only when the cells approach stationary phase prevents long lag times and allows for the harvest of a high quantity of biomass. However, in magnetosome doping, metals were added to the growth medium prior to bacterial inoculation (Staniland *et al.* 2008; Perez-Gonzalez *et al.* 2010), allowing incorporation into the magnetosome throughout magnetosome formation.

According to a recent study by Ralfe *et al.* (2011), *E. coli* accumulates the most intracellular Ni^{2+} and Co^{2+} at stationary phase as shown by the up regulation of these specific uptake proteins during this time. The Ralfe *et al.* (2011) study also shows that unlike Ni^{2+} and Co^{2+},

iron is accumulated at lag phase. In this current study two approaches were employed to analyse intracellular Ni^{2+} and Co^{2+} accumulation:

i.   A modified method of Auer *et al.* (2001) where metal uptake was induced at late log phase (Figure 19A) was used. This was done to minimize proteolytic degradation and to obtain high biomass. High biomass was important because of the low detection limits of the ICP-OES technique. As indicated in the Ralfe *et al.* (2011) study, highest intracellular Ni^{2+} and Co^{2+} are accumulated during stationary phase, suggesting that a proper comparison of intracellular Ni^{2+} or Co^{2+} between the wild type strain and recombinant strain harboring Ni^{2+} or Co^{2+} uptake genes can be made at stationary phase.

ii.   Accumulation was also done in *E. coli* EPI 300 in conditions most likely to allow magnetosome formation and doping as demonstrated in previous studies (Staniland *et al.* 2008; Kundu *et al.* 2009). These conditions include a suitable ratio of Fe: Dopant (metal to be doped into the magnetosome) in the growth medium and adding the dopant prior to bacterial inoculation. Staniland *et al.* (2008) incoporated 1.4 % of Co^{2+} into the magnetosome using medium containing Fe: Co ratio of 1:4.   The M9 growth medium used in this study contains 0.036 mM iron concentration. Unlike MTB, *E. coli* has no known requirement for Co^{2+}. Therefore the Fe: Co ratio used by Staniland *et al.* (2008) was adjusted in this study to 1:3 by adding 0.1 mM $CoCl_2$ in the growth medium which contains 0.036 mM iron. Kundu *et al.* (2009) incorporated Ni^{2+} into the magnetosome using a medium containing Fe:Ni ratio of 2:1. The amount of iron was twofold higher than Ni^{2+} mainly because Ni^{2+} is a strong competitive inhibitor of iron uptake. In this study a Fe:Ni ratio of 4:1 was used. Kundu *et al.* (2009) used low Ni^{2+} concentration (14 μM) in the medium because MTB are poorly tolerant to metals. In this study, concentrations of up to 1 mM were used because *E. coli* tolerate metals better

that MTB. At these high medium concentrations, Ni^{2+} can inhibit iron uptakes, which can result in Ni^{2+} toxicity and inhibition of magnetosome formation. To avoid this, the concentration of iron was raised fourfold and not twofold. However here metals where added at initial exponential phase to avoid extended lag time (Figure 19B).
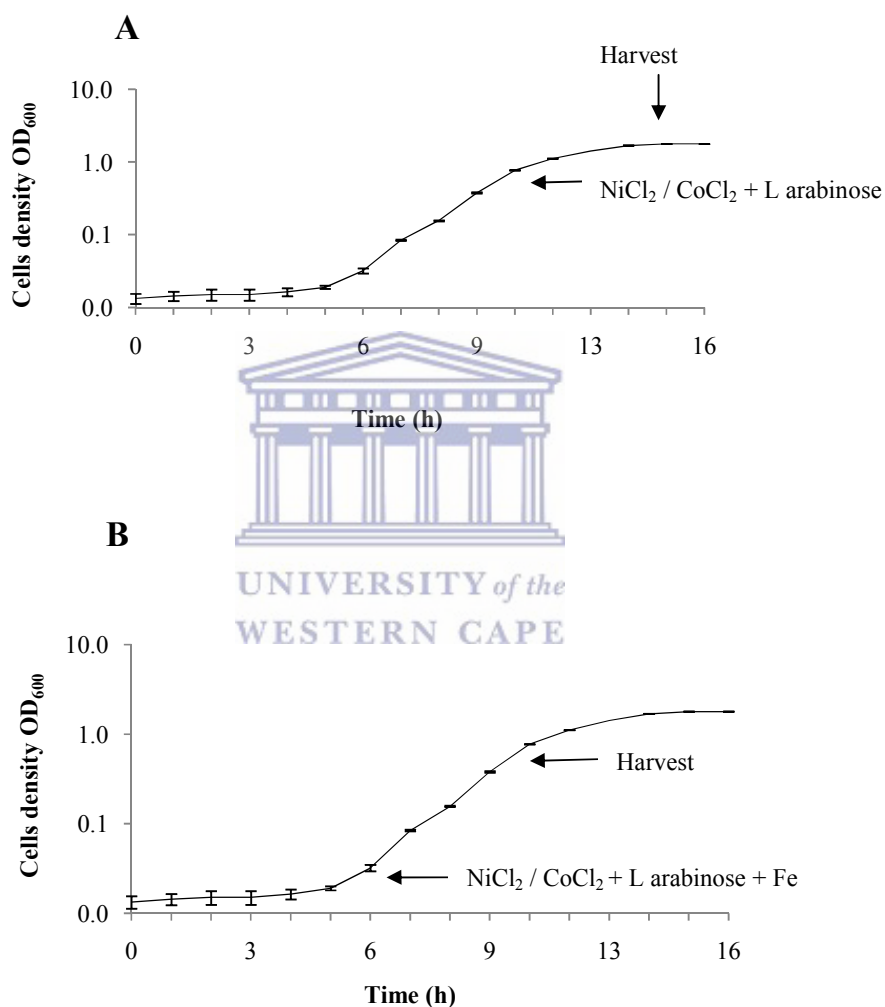
Figure 19 A-B: Representative growth curves of *E. coli* EPI 300 and its recombinant strains harbouring pBAD*hox*N, pBAD*nhl*F and pBAD*cbi*KMQO. The curves illustrate the point of induction, metals addition and harvest. A: Induction and metals addition were done at early stationary phase and cells were harvested at stationary phase, B: Induction and metals addition were done at early log phase and cells were harvested at late log phase.

3.7.1. Ni^{2+} accumulation

3.7.1.1. Ni^{2+} accumulation at stationary phase

Table 8 shows that the intracellular amount of Ni^{2+} in all strains increased as the amount of Ni^{2+} in the medium increased, consistent with previous reports (Pal and Paul, 2010; Bleriot *et al.* 2011). A point of highest intracellular accumulation, where an increase in medium concentration does not increase intracellular accumulation was expected as shown in the study of Deng *et al.* (2003). Deng *et al.* (2003) demonstrated that *E. coli* JM109 grown in increasing concentrations of Ni^{2+} reached a point of equilibrium bioaccumulation when the cellular amount is 1.52 mg/g cells dry weight. This value is within the same range with those obtained in this study for *ΔnikA* harboring *hoxN* at 0.5 mM NiCl$_2$ (1.289 ± 0.278 mg/g) and *ΔcorA* harboring *hoxN* at 1 mM NiCl$_2$ (1.109 ± 0.107 mg/g). It is most likely that *ΔnikA* reached equilibrium bioaccumulation at medium concentration between 0.5 mM and 1 mM NiCl$_2$ while *ΔcorA* habouring *hoxN* reached equilibrium bioaccumulation at just over 1 mM NiCl$_2$ in the medium. A further increase in medium concentration up to 2 mM in case of the *ΔcorA* mutant and up to 1 mM in case of the *ΔnikA* mutant would have provided a clear equilibrium bioaccumulation. However, because of limited time available to complete this work, this was not done.

The presence of *hoxN* increased intracellular Ni^{2+} by up to 31 fold (Table 8). However when the amount of NiCl$_2$ in the medium was increased the contribution of HoxN to intracellular Ni^{2+} was not as significant. The *E. coli* EPI 300 harboring *hoxN* accumulated 11 fold more Ni^{2+} than the wild type without *hoxN* in a medium containing 5 μM NiCl$_2$ (Table 8). This is consistent with a study by Wolfram *et al.* (1995) who showed that *E. coli* CC118 harboring

C. metallidurans CH34 *hox*N accumulates 15 fold increased cellular Ni^{2+} compared to the wild type at 5 μM Ni^{2+} concentration (Wolfram *et al.* 1995). Wolfram's finding and the results of this study also agree with a report by Eitinger and Mandrand-berthelot (2000) who showed that HoxN is a high affinity protein which scavenge Ni^{2+} at trace environmental concentrations.

The *ΔnikA* mutant does not show a significantly decrease in Ni^{2+} accumulation. This was demonstrated by comparable amount of intracellular Ni^{2+} in EPI 300 and the *ΔnikA* mutant (Table 8 and appendix 1). This was surprising because the tolerance study showed that *ΔnikA* mutant is more tolerant to $NiCl_2$ than EPI 300, suggesting that this mutant does not accumulate as much intracellular Ni^{2+} as EPI 300. However the growth curves of this two strains in the present of 0.1 mM $NiCl_2$ were quite similar (Figure 14A-B), suggesting that at 0.1 mM $NiCl_2$ mutation at *nikA* gene does not significantly decrease the intracellular accumulation. This is also in line with the finding of Navarro *et al*. (1993) as indicated in the previous chapter.

The *ΔcorA* mutant has a significantly reduces intracellular amount of Ni^{2+} compared to the wild type strain (EPI 300) and *ΔnikA* mutant (Table 8), confirming previous reports that *corA* also transports Ni^{2+} (Snavely *et al.* 1990). The *ΔrcnA* mutant accumulates the least cellular Ni^{2+} compared to the other strains, although its intracellular contant is comparable with that obtained in EPI 300 at 5 μM $NiCl_2$. This strain was expected to contain the most intracellular Ni^{2+} since it lacks Ni^{2+} and Co^{2+} specific efflux proteins. As shown in the growth profile done at 0.1 mM $NiCl_2$ and Ni^{2+} tolerance studies, this strain has difficulties growing on Ni^{2+}.

Under the conditions used in this study, the HoxN Ni^{2+} uptake system was shown to be more efficient than the NikABCDE system. This was demonstrated by almost 6 fold differences between the *ΔnikA* mutant harboring *hoxN* and the *ΔcorA* mutant with functional NikABCDE at 0.1 mM $NiCl_2$. When both the HoxN and the NikABCDE systems are present (EPI 300 + *hoxN*), there was no significant increase in intracellular Ni^{2+} compared to strain with only *hoxN* (*ΔnikA* + *hoxN*). This may be because the NikABCDE system is down regulated in the presence of Oxygen as reported by de Pina *et al.* (1995).

Table 8: Stationary phase intracellular Ni^{2+} in *E. coli* strains harboring *hox*N

	Cellular Ni mg/g dry weight											
NiCl$_2$ mM	EPI 300	EPI300+*hox*N	INC	*ΔnikA*	*ΔnikA* +*hox*N	INC	*ΔcorA*	*ΔcorA* +*hox*N	INC	*Δrcn*A	*Δrcn*A +*hox*N	INC
No metal	0.000 ± 0.000	0.000 ± 0.000	0	0.000 ± 0.000	0.000 ± 0.000	0	0.000 ± 0.000	0.000 ± 0.000	0	0.000 ± 0.000	0.000 ± 0.000	0
0.005	0.002 ± 22E-5	0.022 ± 82E-5	11	0.003± 6E-6	0.031 ± 41E-5	31				0.003 ± 3E-6	0.063 ± 0.002	21
0.01										0.005 ± 27E-5	0.089 ± 0.002	17.8
0.02										0.019 ± 0.009	0.091 ± 0.001	4.8
0.05	0.028 ± 21E-7	0.126 ± 0.007	4.5									
0.1	0.154 ± 0.035	0.394 ± 0.031	2.4	0.135 ± 0.084	0.366 ± 0.034	2.7	0.064 ± 0.002	0.265 ± 0.026	4.1			
0.5				1.087 ± 0.240	1.289 ± 0.278	1.2	0.132 ± 0.016	0.500 ± 0.034	3.8			
1							0.673 ± 0.093	1.109 ± 0.107	1.6			

Intracellular Ni^{2+} was measured in cells grown in M9 (cam) medium. The culture was grown until OD$_{600}$ reached 0.8-1, followed by addition of up to 0.2% L-arabinose and NiCl$_2$ and harvested at the end of stationary phase. INC represents the fold increase between control strain and strain harboring *hox*N .The results shown here represent the mean ± standard deviation of ICP-OES analysis of three independent experiments.

3.7.1.2. Intracellular iron and magnesium at different Ni^{2+} concentrations

Iron and magnesium are important trace metals required by most bacteria for various metabolic activities (Snavely *et al.* 1990). In magnetotactic bacteria (MTB), iron is the major component of the magnetosome (Blakemore, 1975). Outten and O' Halloran, (2001) reported that *E. coli* is able to maintain a cellular iron "quota" of 180 μM. In MTB intracellular iron concentration has been shown to be up to 21 mg per gram of cell dry mass in cells grown under micro-aerobic conditions and 10.8 mg/g when cells were grown under aerobic conditions (Heyen and Schuler, 2003).

The results in Table 9 and Appendix 2 show that the intracellular iron concentration was not reduced by the addition of up to 0.1 mM NiCl$_2$. However at 0.5 mM NiCl$_2$, intracellular iron was significantly reduced, suggesting higher Ni^{2+} concentrations inhibit iron uptake. This is consistent with the study of Bereswill *et al.* (2000) who demonstrated that high Ni^{2+} concentration inhibits iron uptake.

The *ΔcorA* mutant showed low intracellular iron, suggesting that CorA is important in iron transport. Hantke, (1987) also reported that CorA is involved in iron uptake in *E. coli* and *S. typhimurium*. However Papp and Maguire (2004) reported contrary findings, showing that CorA does not transport iron. Papp and Maguire conducted their study in a solution containing extremely low iron concentration (0.001 mM). It is unlikely in their case that the wild type strain and the *ΔcorA* mutant will have any significant difference in intracellular iron content because iron is not a specific substrate of CorA. As a result, magnesium and other divalent metals in the medium whose concentrations are higher will inhibit iron import through CorA. In this current study, M9 medium contained 0.036 mM iron, a significantly

higher concentration than in the Papp and Maguire study. This may be the reason for the different results.

The amount of cellular iron per gram of dry weight of bacterial cell has been previously studied. Barton *et al.* (2007) reported that bacterial cells contain 0.015g/ 100g of dry weight cellular iron. In *E. coli* W3110 grown in M9 medium supplemented with up to 16 µM iron citrate, the amount of iron was 0.18 mg/g at stationary phase and 0.2 mg/g at logarithmic growth (Abdul-Tehrani *et al.* 1999). As shown in Table 9, the amounts obtained in this current study are slightly higher, most likely due to the high iron concentration in the medium (0.036 mM). However, these amounts are still within the same range as those of previous studies.
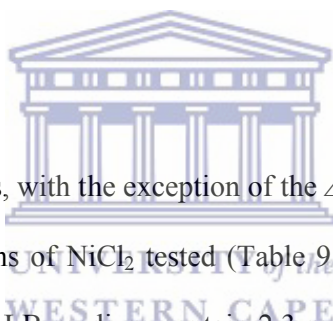
Cellular magnesium in all strains, with the exception of the *ΔcorA* mutant, was not reduced in the presence of all concentrations of $NiCl_2$ tested (Table 9 and Appendix 3). Previous data show that *E. coli* K12 grown in LB medium contain 2.3 mg of magnesium per gram of cell dry weight at early log phase, 1.3 mg/g at late log phase and 0.86 mg/g at stationary phase (de Medicis *et al.* 1986). *E. coli* DG336 grown in minimal salt medium containing 0.6 mM magnesium ion was reported to accumulate 2.8 mg of magnesium per gram of cells dry weight measured at late log phase (Kung *et al.* 1975). The results in Table 9 and Appendix 3 show different values from those reported above. Cellular magnesium content of between 2.835 ± 0.338 mg/g and 3.048 ± 0.144 mg/g dry weight was observed in EPI 300 and the Δ*rcn*A mutant at all concentrations of Ni^{2+} tested. These values are higher than those reported previously at stationary phase (0.86 mg/g). The differences can be attributed to two factors: LB medium contains chelating agents which reduce intracellular bioaccumulation of divalent metals, hence lower magnesium content in the Medicis *et al.* (1986) report. High

magnesium concentration in the medium is most likely to increase intracellular concentration. M9 medium used in this experiment contains 2 mM magnesium ion, three fold higher than the 0.6 mM used in the study by Kung *et al.* (1975).

The *ΔnikA* and Δ*rcnA* mutants show the same intracellular magnesium as the wild type, indicating that these genes do not import magnesium. Cellular magnesium was very low in the *ΔcorA* mutant compared to the other strains, which was not surprising since CorA is the main magnesium transporter (Rodrigue *et al.* 2005).

Table 9: Stationary phase intracellular iron and magnesium in *E. coli* strains harboring *hoxN*

	Cellular Fe and Mg mg/g dry weight							
NiCl$_2$ mM	EPI 300 + *hox*N		Δ*nikA* + *hox*N		Δ*corA* + *hox*N		Δ*rcn*A + *hox*N	
	Fe	Mg	Fe	Mg	Fe	Mg	Fe	Mg
0	0.329 ± 0.036	3.126 ± 0.341	0.369 ± 0.088	2.988 ± 0.158	0.084 ± 0.006	0.594 ± 0.008	0.340 ± 0.037	2.982 ± 0.093
0.005	0.373 ± 0.006	3.049 ± 0.183	0.336 ± 0.015	2.900 ± 0.172			0.351 ± 0.093	2.946 ± 0.129
0.01							0.300 ± 0.089	2.855 ± 0.245
0.02							0.282 ± 0.083	2.814 ± 0.110
0.05	0.372 ± 0.001	2.945 ± 0.003						
0.1	0.320 ± 0090	2.919 ± 0.043	0.332 ± 0.002	2.906 ± 0.138	0.074 ± 0.008	0.582 ± 0.088		
0.5			0.082 ± 0.002	2.953 ± 0.108	0.055 ± 0.003	0.551 ± 0.009		
1					0.033 ± 0.008	0.541 ± 0.046		

Intracellular Iron was measure in cells grown in M9-cam broth until OD$_{600}$ reached 0.8-1. L-arabinose and NiCl$_2$ were added and cells were harvested at stationary phase. The results shown here represent the mean ± standard deviation of ICP-OES analysis of three independent experiments.

3.7.1.3. Intracellular Ni^{2+}, iron and magnesium in conditions for magnetosome doping

Intracellular Ni^{2+} accumulation in EPI 300 and its recombinant strain harboring *hoxN* was also studied at conditions most likely to induce magnetosome formation. EPI 300 was used in this experiment because it accumulated the most cellular Ni^{2+} at 0.1 mM $NiCl_2$ without affecting cellular magnesium and iron (Table 8-9 and appendix 2) at stationary phase. The concentration of $FeSO_4$ in M9 (cam) medium was increased tenfold from 0.036 mM to 0.36 mM to simulate conditions for magnetosome formation and doping as shown by Kundu *et al.* (2009).
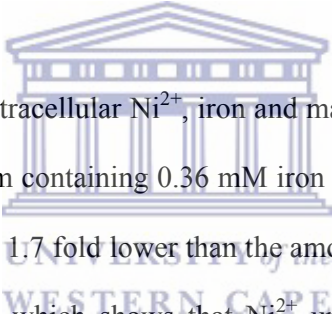
Table 10 shows the amount of intracellular Ni^{2+}, iron and magnesium in EPI 300 grown until mid-exponential phase in medium containing 0.36 mM iron and 0.1 mM Ni^{2+} concentrations. Intracellular Ni^{2+} in EPI 300 was 1.7 fold lower than the amount obtained at stationary phase, consistent with an earlier study which shows that Ni^{2+} uptake occurs at stationary phase (Rolfe *et al.* 2011). The same study also showed that the *rcn*A gene which encodes the Ni^{2+} efflux protein is upregulated at the later stage of lag phase (Rolfe *et al.* 2011), further explaining the lower intracellular Ni^{2+} at log phase. This intracellular Ni^{2+} was further reduced 10 fold in the presence of 0.36 mM $FeSO_4$. However, iron did not seem to interfere with Ni^{2+} accumulation through HoxN, suggesting that these metals only compete for low affinity and non-specific metal proteins. Intracellular Ni^{2+} was increased in the presence of HoxN, showing a 2.95 fold increase. This was also the case in the presence of 0.36 mM iron, further suggesting that HoxN does not import iron.

Intracellular iron was slightly higher than values obtained at stationary phase at 0.036 mM iron and more than 1.5 fold higher when iron in the medium was increased to 0.36 mM iron, consistent with previous study which reported that iron is accumulated at lag phase (Ralfe *et al.* 2011). In *E. coli* W3110, cellular iron content at logarithmic phase was reported to be 0.27 mg/g dry weight in cells grown in LB medium supplemented with 17 μM iron citrate. In M9 medium supplemented with 16 μM iron citrate, cellular iron was 0.2 mg/g dry weight (Abdul-Tehrani *et al.* 1999). The amount of iron in the medium in this study was significantly higher (0.36 mM), which is most likely to be the reason for higher values obtained intracellularly.

Intracellular magnesium was slightly higher at log phase, which also suggests that magnesium might be accumulated at lag phase of growth. Magnesium is required for growth hence a higher magnesium concentration would be expected at log phase than at stationary phase. The report by de Medics *et al.* (1989) shows that *E. coli* contains 2.3 mg/g dry weight at early log phase and 1.3 mg/g at late log phase, showing a decrease as the cells approach stationary phase. In this current study, a consistent average of 3.6 mg/g of dry weight was obtained. As indicated earlier, this higher amount is most probably due to high magnesium concentration in M9 medium.

Table 10: Intracellular Ni^{2+}, iron and magnesium of EPI 300 harboring *hox*N at higher iron concentration in the medium

Metals	Cellular Ni (mg/g dry weight)		Cellular Fe (mg/g dry weight)		Cellular Mg (mg/g dry weight)	
	EPI 300	EPI 300 + *hox*N	EPI 300	EPI 300 + *hox*N	EPI 300	EPI 300 + *hox*N
0 mM	0.000 ± 0.000	0.000 ± 0.000	0.390 ± 0.024	0.391 ± 0.043	3.661 ± 0.336	3.670 ± 0.451
0.1 mM Ni	0.087 ± 0.007	0.257 ± 0.015	0.397 ± 0.037	0.320 ± 0.096	3.606 ± 0.211	3.700 ± 0.495
0.1 mM Ni+ 0.36 mM Fe	0.008 ± 12E-9	0.255 ± 0.008	0.616 ± 0.042	0.610 ± 0.008	3.698 ± 0.083	3.602 ± 0.172

Intracellular Ni^{2+}, iron and magnesium were determined in cells grown until early log phase in M9 (cam) medium followed be addition of Ni^{2+} or Ni^{2+} and iron. The results shown here represent the mean ± standard deviation of ICP-OES analysis of three independent experiments

UNIVERSITY *of the* WESTERN CAPE

3.7.1.4. Suitable strain for Ni^{2+} doping of the magnetosome

The results presented in Table 8 shows that the *ΔnikA* mutant habouring *hoxN* accumulates the most intracellular Ni^{2+} at 0.5 mM $NiCl_2$ in the medium (1.289 ± 0.278 mg/g). This is significantly higher than 0.213 mg/g obtained by Koch *et al.* (2006). However, at this medium concentration, the amounts of cellular iron were decreased. Iron is important for magnetosome formation, suggesting that intracellular Ni^{2+} accumulation for magnetosome doping should be conducted at lower medium Ni^{2+} concentration. At 0.1 mM $NiCl_2$ in the medium, EPI 300 habouring *hoxN* accumulates the most intracellular Ni^{2+} (0.394 mg/g). This value was reduced to 0.255 mg/g in the presence of 0.36 mM iron in the medium when the cells were harvested at exponential phase. This decrease was coupled with an increase in intracellular iron, from 0.320 ± 0.096 mg/g to 0.610 ± 0.008 mg/g (Table 10).

Unfortunately Ni^{2+} accumulation experiments were conducted in strains without the MIA. As a result, it is difficult to indicate with certainty the amount of intracellular Ni^{2+} which will result in magnetosome doping. However, the amount obtained in EPI 300 harboring *hoxN* at 0.1 mM $NiCl_2$ in the medium is the highest obtained compared to all the other conditions tested. Of all the strains studied, this strain is the most suitable strain for Ni^{2+} doping in the magnetosomes.

3.7.2. Co^{2+} accumulation

3.7.2.1. Co^{2+} accumulation at stationary phase

Intracellular Co^{2+} accumulation was studied in *E. coli* strains harboring *cbiKMQO* or *nhlF*. The results in Table 11 show that the amount of intracellular Co^{2+} increases as the amount of $CoCl_2$ is increased in the medium, as was shown for Ni^{2+} accumulation and other studies (Pal and Paul, 2010; Bleriot *et al.* 2011). The comparable intracellular amount of Co^{2+} in the Δ*nikA* mutant habouring *cbiKMQO* or *nhl*F at 0.5 mM $CoCl_2$ and the Δ*corA* mutant harboring *nhl*F at 1 mM $CoCl_2$ (Table 11) suggest an equilibrium bioaccumulation. However, this cannot be stated with certainty since the medium concentration was raised only up to 1 mM. Most certainly equilibrium bioaccumulation would have been obtained if the medium Co^{2+} concentration was raised up to at least 2 mM.
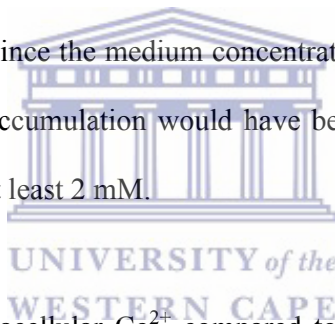
The *ΔcorA* mutant has low intracellular Co^{2+} compared to EPI 300 and the Δ*nikA* mutant (Table 11 and appendix 4-5), indicating that CorA is also important for Co^{2+} transport (Nies, 1999). The Δ*rcnA* mutant has the least cellular Co^{2+} compared to the other strains. This is because this strain grows poorly in the presence of metals.

The CbiKMQO protein cluster was more efficient than NhlF. This is clearly indicated by the folds increase as shown in Table 11. However, at higher medium concentration of $CoCl_2$, both CbiKMQO and NhlF did not make significant difference in intracellular accumulation, as was also seen for Ni^{2+} accumulation. This suggests that at high medium concentration, Co^{2+} is accumulated into the cells through other non-specific transporters (Nies, 1999).

Table 11: Stationary phase intracellular Co^{2+} in *E. coli* strains harboring *cbiKMQO* or *nhlF*

	Cellular Co mg/g dry weight																
Co mM	EPI 300+ *cbi*	INC	EPI 300+*nhl*F	INC	*ΔnikA* + *cbi*	INC	*ΔnikA*+*nhl*F	INC	*ΔcorA* + *cbi*	INC	*ΔcorA*+*nhl*F	INC	*Δrcn*A + *cbi*	INC	*Δrcn*A+*nhl*F	INC
0	0.000 ± 0.000	0	0.000 ± 0.000	0	0.000 ± 0.000	0	0.000 ± 0.00	0	0.000 ± 0.00	0	0.000 ± 0.00	0	0.00 ± 0.000	0	0.000±0.00	0
0.005	0.049 ± 3E-2	7	0.022 ± 31E-4	3.4	0.038 ± 0.001	9.5	0.020 ± 1E-4	5					0.088 ± 3E-1	22	0.052 ±5E-4	13
0.01													0.107 ± 3E-4	17	0.081 ± 3E-1	13.5
0.02													0.206 ± 0.02	15	0.133 ± 3E-2	10
0.05	0.216 ± 0.006	5.7	0.187 ± 0.003	4.9												
0.1	0.673 ± 0.011	5.3	0.425 ± 0.01	3.3	0.693 ± 0.093	5.4	0.477 ± 0.02	2.9	0.294 ± 0.02	5.5	0.191 ± 0.08	3.6				
0.5					1.492 ± 0.185	1.09	1.45± 0.185	1.05	0.866 ± 0.13	2.6	0.730 ± 0.14	2.2				
1									1.527 ± 0.09	2.3	1.197 ± 0.08	1.8				

Intracellular Co^{2+} was measured in cells grown in M9-cam medium. The cells were grown until OD_{600} reached 0.8-1, followed by addition of up to 0.2% L-arabinose and $CoCl_2$ and harvested at the end of stationary phase. INC represents the fold increase between control strain without recombinant Co^{2+} uptake gene and strain harboring *cbiKMQO* or *nhl*F. *cbi* represent *cbiKMQO*. The results shown here represent the mean ± standard deviation of ICP-OES analysis of three independent experiments.

3.7.2.2.   Intracellular iron and magnesium at stationary phase in the presence of Co^{2+}

Intracellular iron and magnesium have been studied in all strains grown at different concentration of $CoCl_2$ (Table 12 and appendices 6-9). Co^{2+} did not affect intracellular magnesium for all the medium concentrations tested. However, the *ΔcorA* mutant has significantly lower intracellular iron and magnesium, showing that CorA is important for both iron and magnesium import.   The *ΔnikA* and *ΔrcnA* mutants accumulated similar magnesium and iron as EPI 300 (appendix 6+8), showing that NikA and RcnA do not transport iron or magnesium. The *cbiKMQO* and *nhlF* genes did not result in transport of either iron or magnesium, confirming that these systems are Co^{2+} specific transporters (Rodionov *et al.* 2005). This was shown by similar amount of cellular iron and magnesium in strains harboring *nhl*F or *cbiKMQO* and the untransformed strains (Appendices 6-9).
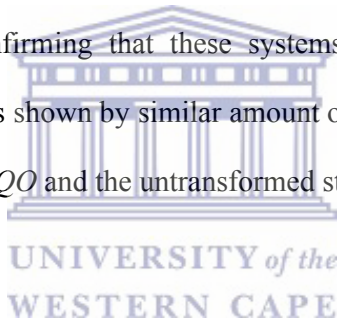
Table 12: Stationary phase intracellular iron and magnesium *in E. coli* strains harboring *cbiKMQO* or *nhlF*

	Cellular Fe and Mg (mg/g dry weight)							
CoCl$_2$ mM	*ΔnikA + cbi*KMQO		*ΔnikA + nhl*F		*ΔcorA + cbi*KMQO		*ΔcorA + nhl*F	
	Fe	Mg	Fe	Mg	Fe	Mg	Fe	Mg
0	0.307 ± 0.022	3.198 ± 0.207	0.323 ± 0.005	3.265 ± 0.125	0.051 ± 0.003	0.589 ± 0.019	0.056 ± 0.004	0.614 ± 0.069
0.005	0.381 ± 0.009	2.975 ± 0.109	0.379 ± 0.080	3.251 ± 0.265				
0.01								
0.02								
0.05								
0.1	0.349 ± 0.067	2.939 ± 0.195	0.320 ± 0.009	2.975 ± 0.170	0.058 ± 0.004	0.639 ± 0.043	0.052 ± 0.004	0.623 ± 0.137
0.5	0.068 ± 0.002	2.913 ± 0.137	0.080 ± 0.003	2.941 ± 0.246	0.055 ± 0.008	0.679 ± 0.141	0.031 ± 0.001	0.352 ± 0.067
1					0.050 ± 0.002	0.471 ± 0.103	0.022 ± 0.008	0.461± 0.206

Cellular Iron was measured in cells grown in M9-cam broth until OD$_{600}$ reached 0.8-1. L-arabinose and CoCl$_2$ were added and cells were harvested at stationary phase. The results shown here represent the mean ± standard deviation of ICP-OES analysis of three independent experiments.

3.7.2.3. Intracellular Co^{2+}, iron and magnesium at exponential phase

Table 13 is a summary of results of intracellular Co^{2+}, iron and magnesium obtained in cells grown until exponential phase in 0.1 mM $CoCl_2$ and 0.36 mM iron. The amount of cellular Co^{2+} in *E. coli* EPI 300 at 0.1 mM $CoCl_2$ was almost 3 fold lower compared to the value obtained at stationary phase. This may be due to the up regulation of the Co^{2+} efflux protein at log phase (Rolfe *et al.* 2011).

The amount of intracellular iron was slightly increased compared to values obtained at stationary phase, indicating that iron is accumulated at lag phase and exponential phase (Ralfe *et al.* 2011). Increasing iron concentration in the medium resulted in the increase in intracellular accumulation. However, unlike with Ni^{2+}, the amount of intracellular Co^{2+} was not decreased in the presence of 0.36 mM medium iron concentration, suggesting that this concentration of iron does not inhibit Co^{2+} uptake in EPI 300. Both NhlF and CbiKMQO do not seem to transport iron and magnesium. Magnesium slightly increased from 2.905 ± 0.103 mg/g at stationary phase to 3.656 ± 0.215 mg/g at exponential phase, indicating that most of this metal is accumulated at exponential phase.

TABLE 13: Exponential phase intracellular Co^{2+}, iron and magnesium in EPI 300 habouring *cbi*KMQO or *nhl*F
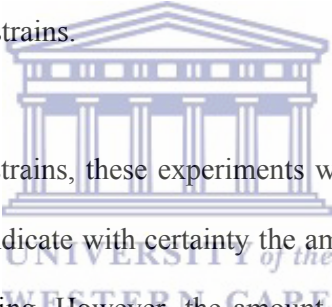
Metals	Cellular Co (mg/g dry weight)		Cellular Fe (mg/g dry weight)		Cellular Mg (mg/g dry weight)	
	EPI 300 + *nhl*F	EPI 300 + *cbi*KMQO	EPI 300 + *nhl*F	EPI 300 + *cbi*KMQ	EPI 300 + *nhl*F	EPI 300 + *cbi*KMQ
0 mM	0.000 ± 0.000	0.000 ± 0.000	0.410 ± 0.553	0.411 ± 0.023	3.711 ± 0.523	3.656 ± 0.321
0.1 mM Co	0.321 ± 0.185	0.239 ± 0.004	0.470 ± 0.050	0.406 ± 0.008	3.705 ± 0.608	3.642 ± 0.061
0.1 mM Co+ 0.361 mM Fe	0.399 ± 0.014	0.368 ± 0.039	0.577 ± 0.269	0.517 ± 0.022	3.575 ± 0.892	3.697 ± 0.100

Cellular Co^{2+}, iron and magnesium were determined in cells grown until early log phase in M9-cam medium followed by addition of Co^{2+} or Co^{2+} and iron. The results shown here represent the mean ± standard deviation of ICP-OES analysis of three independent experiments.

UNIVERSITY *of the*
WESTERN CAPE

3.7.2.4. Suitable strain for Co^{2+} doping of the magnetosomes

The most cellular Co^{2+} was accumulated by the *ΔcorA* mutant (1.527 ± 0.086 mg/g) harboring *cbi*KMQO at 1 mM CoCl$_2$, although no of the other mutants was tested at this Co^{2+} concentration. This amount is comparable with accumulation by the *ΔnikA* mutant harboring either *cbi*KMQO (1.492 ± 0.185 mg/g) or *nhl*F (1.450 ± 0.185 mg/g) at 0.5 mM CoCl$_2$. However, at 0.5 mM Co^{2+} concentration, the amount of intracellular iron was decreased in *ΔnikA*, suggesting that this concentration of Co^{2+} may not be suitable for magnetosome doping. At 0.1 mM CoCl$_2$, the *ΔnikA* (*cbiKMQO*) and EPI 300 (*cbiKMQO)* strains accumulates the most intracellular Co^{2+} (0.693 ± 0.093 mg/g and 0.673 ± 0.011 mg/g respectively) compared to other strains.

As with the Ni^{2+} accumulating strains, these experiments were conducted in strains without the MIA making it difficult to indicate with certainty the amount of intracellular Co^{2+} which will result in magnetosome doping. However, the amount obtained in EPI 300 and *Δnik*A mutant harboring *cbi*KMQO at 0.1 mM CoCl$_2$ is the best obtained and therefore the most suitable for magnetosome doping.

4. CONCLUSIONS

The magnetosomes, produced by MTBs, are the most attractive alternative source of non-toxic and biocompatible magnetic nanoparticles (MNPs). However, magnetosomes are generally "soft" magnetic materials which can be used for some applications while other applications require chemically altered magnetic nanoparticles (Li *et al.* 2009). Magnetotactic bacteria (MTB) are fastidious in growth (Blakemore, 1975), making the production of magnetosomes on a commercial scale difficult. Synthesis of the magnetosome in an easy to culture *E. coli* strain by expressing the magnetosome gene island (MIA) is one of the possibilities for commercial scale synthesis. The magnetic properties of this recombinant magnetosome may be altered by doping with divalent metals such as Ni^{2+} (Kundu *et al.* 2009) or Co^{2+} (Staniland *et al.* 2008).
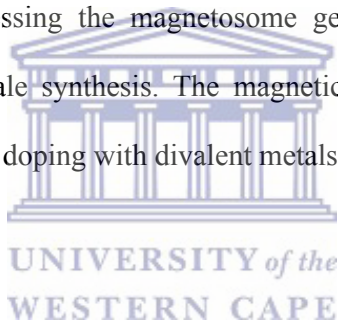
In this study two *E. coli* strains which accumulate high intracellular Ni^{2+} or Co^{2+} were developed to be used as hosts for the MIA in order to produce magnetosomes with altered magnetic properties. These strains were studied for intracellular Ni^{2+} and Co^{2+} accumulation in growth medium metal concentrations known to induce magnetosome doping. The amount of intracellular Ni^{2+} or Co^{2+} accumulated by these strains was found to be higher than the amounts obtained in other published studies. However, these strains were not experimentally studied for the synthesis of chemically altered magnetosomes because they still lack the MIA. This makes it imposible to state conclusively if the amount of Ni^{2+} or Co^{2+} accumulated can result in the alteration of the magnetic properties of the magnetosomes. A conclusive study would have involved co-expressing the MIA and metals uptake gene followed by analyzing magnetic properties of the magnetosome.

Although the techniques and strategies employed in this study were sufficient to develop and screen for strains which accumulate high intracellular Ni^{2+} and Co^{2+}, some improvement could have provided more valuable data. These include Ni^{2+} and Co^{2+} intracellular accumulation experiments conducted under microaerobic conditions. Intracellular Ni^{2+} and Co^{2+} accumulation in this study was conducted under aerobic conditions. This could be a problem because magnetosome formation occurs under microaerobic conditions. The intracellular ratio of free metals and protein bound metals changes under microaerobic conditions. For example, Ni^{2+} is required in *E. coli* mainly for the synthesis of hydrogenase enzymes which are produced during anaerobic and microaerobic metabolism (Rowe *et al.* 2005). This suggests that the metabolic demand of Ni^{2+} increases under microaerobic conditions, which may result in low concentration of free Ni^{2+} ions available for incorporation into the magnetosome.

In addition, measuring the amount of intracellular free metals would have also provided a strong indication of the metals available in the cell for incorporation into the magnetosome. The amounts of free metals in the cell are important in this study because they represent the cellular "quota" of metals available for magnetosome doping. Free metal ions can be determined by using electron paramagnetic resonance spectroscopy (EPS). This study used the ICP-OES technique which determines the total amount of free metals in the cell. This technique could have been combined with the EPS technique to quantify the amount of free Ni^{2+} or Co^{2+} and the total amount of these metals inside the cell.

The total intracellular amount of Ni^{2+} or Co^{2+} in MTB has not yet been studied under any conditions, making it difficult to make rational analysis on the amount of these metals required to induce magnetosome doping. It would be interesting to conduct a study in MTB

to determine the amount of intracellular Ni^{2+} and Co^{2+} and the amount contained in the magnetosome. Using EPS and ICP-OES techniques, the total intracellular amount of Ni^{2+} or Co^{2+} in MTB; the amount of Ni^{2+} or Co^{2+} inside the magnetosome; and the total amount of free Ni^{2+} or Co^{2+} radicals can be quantified.

In general, the synthesis of magnetosomes in recombinant *E. coli* is still at its early research stage. Although *E. coli* metabolic activity has been well studied, most of the information about magnetosome formation is still hypothetical, and there is no experimental evidence that recombinant magnetosomes can be synthesized in hosts such as *E. coli*. However, with more studies on this area, the possibilities of recombinant magnetosome may become more attainable. The use of other organisms which share more metabolic similarities with MTB for magnetosome synthesis, other than using *E. coli* which is clearly different from MTB, might be an alternative. In addition, since magnetosomes are intracellular vesicle structures, using organisms which produce vesicles may also be a good approach.

This study has produced two *E. coli* strains which accumulate high intracellular Ni^{2+} or Co^{2+}. Provided the magnetosome gene island is successfully cloned and expressed in these strains, it is highly likely that the amount of metals accumulated can result in chemically altered magnetosomes which can be used for a variety of applications. Further studies are still required to analyse the amount of free metals in both MTB and *E. coli*. A key study would be to quantify the amount of intracellular free metals ions and the degree to which they change the magnetic coercive force of the magnetosome.

5. REFERENCES

Abdul-Tehrani, H., A. J. Hudson, Y. S Chang, A. R. Timms, C. Hawkins, J. M. Williams, P. M. Harrison, J. R. Guest and S. C. Andrews. 1999. Ferritin mutants of *Escherichia coli* are iron deficient and growth impaired, and *fur* mutants are iron deficient. Journal of Bacteriology **181:** 1415-1428.

Acosta-Avalos, D., E. Wajnberg, P. S. Oliveira, I. I. Leal, M. Farina, and D. M. Esquivel. 1999. Isolation of magnetic nanoparticles from *pachycondyla marginata* ants. Journal of Experimental Biology **202:**2687-2692.

Addy, C., M. Ohara, F. Kawai, A. Kidera, M. Ikeguchi, S. Fuchigami, M. Osawa, I. Shimada, S. Y. Park, J. R. Tame, and J. G. Heddle. 2007. Ni^{2+} binding to NikA: an additional binding site reconciles spectroscopy, calorimetry and crystallography. Acta Crystallographica: Biological Crystallography **63:**221-229.

Agranoff, D. D., and S. Krishna. 1998. Metal ion homeostasis and intracellular parasitism. Molecular Microbiology **28:**403-412.

Amann, R., J. Peplies, and D. Schuler. 2006. Diversity and taxonomy of Magnetotactic bacteria. Applied Microbiology **3:**25-35.

Andrews, S.C., A. K. Robinson, F. Rodriguez-Quinones. 2003. Bacterial iron homeostasis. FEMS Microbiology Reviews **27:** 215-237.

Artus, M., L. B. Tahar, F. Herbst, L. Smiri, F. Villain, Y. Yaacoub, J. M. Gren`eche, S. Ammar, and F. Fievet. 2011. Size-dependent magnetic properties of CoFe2O4 nanoparticles prepared in polyol. Journal of Physics **23:**9-19.

Auer, M., M. J.Kim, M. J. Lemieux, A. Villa, J. Song, X. D. Li, and D. N. Wang. 2001. High-yield expression and functional analysis of *Escherichia coli* Glycerol-3-phosphate transporter. Biochemistry **40:** 6628-6635.

Baek, Y. W., and Y. J. An. 2011. Microbial toxicity of metal oxide nanoparticles (CuO, NiO, ZnO, and Sb2O3) to *Escherichia coli*, *Bacillus subtilis*, and *Streptococcus aureus*. Science of the total Environment **409:**1603-1608.

Baker, G. C., Smith, J. J. and Cowan, D. A. 2003. Review and re-analysis of domain-specific 16S primers. *Journal of Microbiological Methods 55*: 541-555.
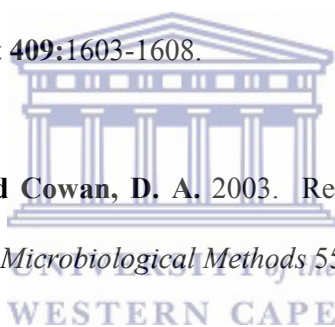
Barton, L.L., F. Goulhen, M. Bruschi, N. A. Woodards, R. M. Plunkett, and F. J. M. Rietmeijer. 2007. The bacterial metallome: composition and stability with specific reference to the anaerobic bacterium *Desulfovibrio desulfuricans*. Biometals **20:** 291-302

Bauerfeind, P., R. M. Garner, and L. T. Mobley. 1996. Allelic exchange mutagenesis of *nix*A in *Helicobacter pylori* results in reduced Ni^{2+} transport and urease activity. Infectious Immunology **64:**2877-2880.

Bazylinski, D. A., A. J. Dean, D. Schuler, E. J. P. Phillips, and D. R. Lovley. 2000. N$_2$-dependent growth and nitrogenase activity in the metal-metabolising bacteria, *Geobacter* and *Magnetospirillum* species. Environmental Microbiology **2:**266-273.

Bazylinski, D. A., A. J. Dean, T. J. Williams, L. Kimble Long, S. L. Middleton, and B. L. Dubbels. 2004. Chemolithoautotrophy in the marine *Magnetotactic bacteria* strains MV-1 and MV-2. Archives in Microbiology **182:**373-387.

Bazylinski, D. A., R. B. Frankel, and H. W. Jannasch. 1988. Anaerobic production of magnetite by marine magnetotactic bacteria. Nature **334:**518-519.

Bazylinski, D. A., and S. Schubbe. 2007. Controlled biomineralisation and application of magnetotactic bacteria. Advanced Applied Microbiology **62:**21-62.
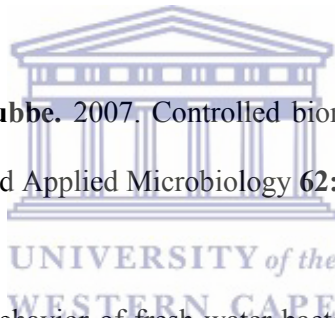
Bellini, S. 1963. On a unique behavior of fresh water bacteria. Institution of Microbiology, University of Pavia.

Berreswill, S., S. Greiner, A. H. M. Van Vliet, B. Waidner, F. Fassibinder, E. Schiltz, and J. G. Kusters. 2000. Regulation of ferritin-mediated cytoplasmic iron storage by the ferric uptake regulator homolog (Fur) of *Helicobacter pylori.* Journal of Bacteriology **182:** 5948-5953.

Berry, C. C., and A. S. G. Curtis. 2003. Functionalisation of magnetic nanoparticles for applications in biomedicine. Journal of Physics **36:**198-206.

Blakemore, R. P. 1975. Magnetotactic bacteria. Science **190:**377-379.

Blakemore, R. P. 1982. Magnetotactic bacteria. Annual Review of Microbiology **36:**217-238.

Bleriot, C., G. Effantin, F. Lagarde, M. Mandrand-Berthelot, and A. Rodrigue. 2011. RcnB Is a Periplasmic Protein Essential for Maintaining Intracellular Ni and Co Concentrations in *Escherichia coli.* Journal of Bacteriology **193:** 3785-3793.

Bosse´, J. T., H. D. Gilmour, and J. I. MacInnes. 2001. Novel genes affecting urease acivity in *Actinobacillus pleuropneumoniae*. Journal of Bacteriology. **183:**1242–1247.

Browne, P., and G. O'Cuinn. 1983. The purification and characterization of a proline dipeptidase from guinea pig brain. Journal of Biology and Chemistry **258:**6147-6154.

Bruno, P. 1991. Theory of the curie temperature of Co^{2+} based ferromagnetic ultrathin films and multilayers. Proceedings of Magneto-Optical Recording lnternational Symposium **91:**15-20.

Buhler, C., S. Yunoki, and A. Moreo. 2000. Magnetic domains and stripes in a spin-fermion model for cuprates. Phycal Review Letters **84:**2690-2693.

Cabrera G., R. Perez, J. M. Gomez, A. Abalos, D. Cantero. 2005. Toxic effects of dissolved heavy metals on *Desulfovibrio vulgaris* and *Desulfovibrio* sp. strains. Journal of Hazardous Materials. **135:** 40-46.

Chaintreuil, C., F. Rigault, L. Moulin, T. Jaffre´, J. Fardoux, E. Giraud, B. Dreyfus, and X. Bailly. 2007. Ni^{2+} resistance determinants in *Bradyrhizobium* strains from nodules of the endemic New Caledonia legume *Serianthes calycina*. Applied Environmental Microbiology**:** 8018-8022.

Chakraverty, S., and M. Bandyopadhyay. 2007. Coercivity of magnetic nanoparticles: a stochastic model. Journal of Applied Physics **19:**16-32.

Chang, S. Y., E. C. McGary, and E. Chang. 1989. Methionine aminopeptidase gene of *Escherichia coli* is essential for cell growth. Journal of Bacteriology **171:**4071–4072.

Chen, Y. Y. M., and R. A. Burne. 2003. Identification and characterization of the Ni^{2+} uptake system for urease biogenesis in *Streptococcus salivarius* 57.I. Journal of Bacteriology. **185:**6773–6779
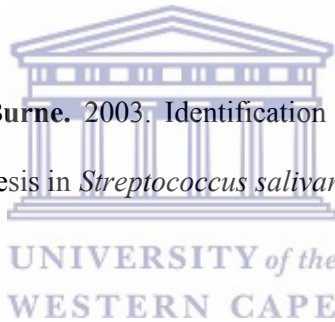
Cheng, J., B. Poduska, R. A. Morton, and T. M. Finan. 2011. An ABC-type Co^{2+} transport system is essential for growth of *Sinorhizobium meliloti* at trace metal concentrations. Journal of Bacteriology. **193:** 4405-4416

Chivers, P. T., and R. T. Sauer. 2002. NikR repressor: High-affinity Ni^{2+} binding to the C-terminal domain regulates binding to operator DNA. Chemistry and Biology **9:**1141-1148.

Cole, S. T., R. Brosch, J. Parkhill, T. Garnier, C. Churcher, D. Harris, S. V. Gordon, K. Eiglmeier, S. Gas, C. E. Barry, F. Tekaia, K. Badcock, D. Basham, *et al.* 1998. Deciphering the biology of *Mycobacterium tuberculosis* from the complete genome sequence. Nature **393:**537-544

Coleman, J. E. 1998. Zinc enzymes. Current Opinion in Chemistry and Biology **2:**222-234.

Cvetkovic, A., A. L. Menon, M. P. Thorgersen, *et al.* 2010. Microbial metalloproteomes are largely uncharacterized. Nature **466:**779-782.

de Medicis, E., J. Paquette, J. J. Gauther, and D. Shapcott. Magnesium and manganese content of hellophilic bacteria. 1986. Applied Environmental Microbiology **52:** 567-573

Deng, X., Q.B. Li, Y.H. Lu, D.H. Sun, Y.L. Huang, X.R. Chen. 2003. Bioaccumulation of Ni^{2+} from aqueous solutions by genetically engineered *Escherichia coli.* Water Research. 37: 2505-2511.

de Pina, K., C. Navarro, L. McWalter, D. H. Boxer, N. C. Price, S. M. Kelly, M. A. Mandrand-Berthelot, and L. F. Wu. 1995. Purification and characterization of the periplasmic Ni^{2+}-binding protein NikA of *Escherichia coli* K12. European Journal of Biochemistry **227:**857-865.

de Souza, K. C., N. D. S. Mohallem, and E. M. B. de Sousa. 2011. Magnetic nanocomposites: Potential for applications in biomedicine. Quimica Nova **34:**1692-1703.

Eitinger, T., and M. A. Mandrand-Berthelot. 2000. Ni^{2+} transport systems in microorganisms. Archives in Microbiology **173:**1-9.

Fantino, J. R., B. Py, M. Fontecave, and F. Barras. 2010. A genetic analysis of the response of *Escherichia coli* to Co^{2+} stress. Environmental microbiology **12:**2846–2857.

Friedberg, R., and D. I. Paul. 1975. New Theory of Coercive Force of Ferromagnetic Materials. Physical Review Letters **34:**1415-1415.

Frimpong, R. A., and J. Z. Hilt. 2010. Magnetic nanoparticles in biomedicine: synthesis, functionalization and applications. Nanomedicine (Lond) **5:**1401-1414.

Fu, C., S. Javedan, F. Moshiri, and R. J. Maiel. 1994. Bacterial genes involved in incorporation of Ni^{2+} into a hydrogenase enzyme. Proceedings of the National Academy of Science of the United States of America **91:**5099-5103.
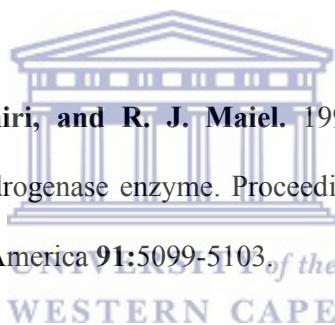
Gelfand, S. M., and D. A. Rodionov. 2008. Comparative genomics and functional annotation of bacterial transporters. Physics of Life Review **5:**22-49.

Gikas, P., S.S. Sengor, T. Ginn, J. Moberly, and B. Peyton. 2009. Effect of heavy metals and temperature on microbial growth and lag phase. Global Nest Journal. **11:** 325-332.

Grass, G., C. Grosse, and D. H. Nies. 2000. Regulation of the *cnr* Co^{2+} and Ni^{2+} resistance determinant from *Ralstonia* sp. strain CH34. Journal of Bacteriology. **182:**1390–1398

Grass, G., S. Franke, N. Taudte, D. H. Nies, L. M. Kucharski, M. E. Maguire, and C. Rensing. 2005. The metal permease ZupT from *Escherichia coli* is a transporter with a broad substrate spectrum. Journal of Bacteriology **187:** 1604-1611

Hansen, M.C., Tolker-Neilson, T., Givskow, M. and Molin, S. 1998. Biased 16S rDNA PCR amplification caused by interference from DNA flanking template region. *FEMS Microbiology Ecology* 26: 141-149.

Hantke, K. 1987. Ferrous iron transport mutants in *Escherichia coli* K-12. FEMS Microbiology Letters **44:**53–57.

Hanzlik, M., C. Heunemann, E. Holtkamp-Rötzler, M. Winklhofer, N. Petersen, and G. Fleissner. 2000. Superparamagnetic magnetite in the upper beak tissue of homing pigeons. Biological Metals **13:**325-331.
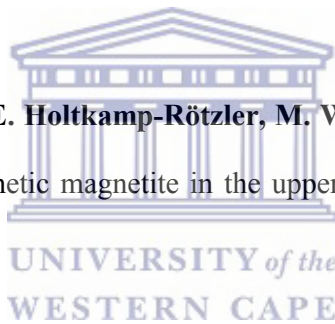
Hendricks, J. K., and H. L. Mobley. 1997. *Helicobacter pylori* ABC transporter: effect of allelic exchange mutagenesis on urease activity. Journal of Bacteriology **179:**5892-5902.

Heyen, U., and D. Schuler. 2003. Growth and magnetosome formation by microaerophilic *Magnetospirillum* strains in an oxygen-controlled fermentor. Applied microbial Biotechnology **61:** 536-544.

Hsu, C. Y., F. Y. Ko, C. W. Li, K. Fann, and J. T. Lue. 2007. Magnetoreception system in honeybees (*Apis mellifera*). Plos One **2:**1-11.

Hyeon, T. 2002. Chemical synthesis of magnetic nanoparticles. The Royal Society of Chemistry **8:** 297-234.

Iwig, J. S., J. L. Rowe, and P. T. Chivers. 2006. Ni^{2+} homeostasis in *Escherichia coli*: The *rcnR-rcnA* efflux pathway and its linkage to NikR function. Molecular Microbiology **61:**252–262.

Jiles, D. C., and D. L. Atherton. 1986. Theory of ferromagnetic hysteresis. Journal of Magnetism and Magnetic Materials **61:**48-60.

Kami, D., S. Takeda, Y. Itakura, S. Gojo, M. Watanabe, and M. Toyoda. 2011. Application of magnetic nanoparticles to gene delivery. International Journal of Molecular Science **12:**3705-3722.
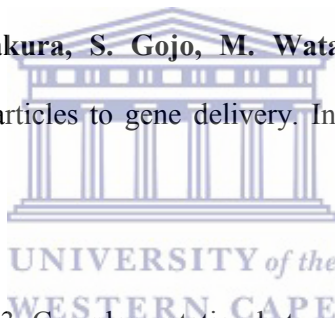
Kaur, P. and B. P. Rosen. 1993. Complementation between nucleotide binding domains in an anion-translocating ATPase. Journal of Bacteriology. **175:** 351-357.

Kirchmayr, H. R. 1996. Permanent magnets and hard magnetic materials. Journal of Physics **29:**2763–2778.

Kirsten, A., M. Herzberg, A. Voigt, J. Seravalli, G. Grass, J. Scherer, and D. H. Nies. 2011. Contributions of five secondary metal uptake systems to metal homeostasis of *Cupriavidus metallidurans* CH34. Journal of Bacteriology **10:**5293-5311.

Khlebnikov, A., K. A. Datsenko, T. Skaug, B. L. Wanner, and J. D. Keasling. 2001. Homogeneous expression of the pBAD promoter in *Escherichia coli* by constitutive expression of the low-affinity high-capacity AraE transporter. Microbiology **147:** 3241-3247.

Koch, D., D. H. Nies, and G. Grass. 2006. The RcnRA (YohLM) system of *Escherichia coli*: A connection between Ni^{2+}, Co^{2+} and iron homeostasis. Biological Metals **20:** 759-771

Komeda, H., M. Kobayashi, and S. Shimizu. 1997. A novel transporter involved in Co^{2+} uptake. Applied Biological Science **94:**36-41.

Krishnaswamy, R., and D. B. Wilson. 2000. Construction and characterisation of an *Escherichia coli* strain genetically engineered for Ni(II) bioaccumulation. Applied and Environmental Microbiology **66:**8383-8386.
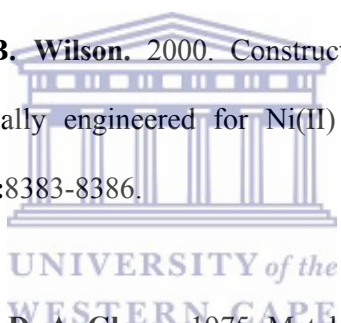
Kung, F. C., J. Roymind, and D. A. Glaser. 1975. Metal iron content of *Escherichia coli* versus cell algae. Journal of Bacteriology **126:** 1089-1095.

Kundu, S., A. A. Kale, A. G. Banpurkar, G. R. Kulkarni, and S. B. Ogale. 2009. On the change in bacterial size and magnetosome features for *Magnetospirillum magnetotacticum* (MS-1) under high concentrations of zinc and Ni^{2+}. Biomaterials **30:** 4211-4218.

Lee Macomber, L., and R. P. Hausinger. 2011. Mechanisms of Ni^{2+} toxicity in microorganisms. Metallomics **3:**1153-1162.

Lefevre, C. T., F. Abreu, M. L. Schmidt, U. Lins, R. B. Frankel, B. P. Hedlund, and D. A. Bazylinski. 2010. Moderately thermophilic magnetotactic bacteria from hot spring in Nevada USA. Applied environmental Microbiology **76:**3740-3743.

Lefevre, C. T., R. B. Frankel, M. Posfai, R. B. Frankel, and D. A. Bandyopadhyay. 2011. Isolation of obligately alkaliphilic magnetostactic bacteria from extremely alikaline environments. Environmental Microbiology **13:** 1462-1468

Li, J.H, Y. X. Pan, Q. S. Liu, H. F. Qin, C. L. Deng, R. C. Che, and X. A. Yang. 2009. A comparative study of magnetic properties between whole cells and isolated magnetosomes of *Magnetospirillum magneticum* AMB-1. Chinese Science Bulletin **55:** 38-44.

Liesegang, H., K. Lemke, R.A. Siddiqui and H. G. Schlegel. 1993. Characterization of the inducible Ni^{2+} and Co^{2+} resistance determinant *cnr* from pMOL28 of *Alcaligenes eutrophus* CH34. Journal of Bacteriology **175:** 767-778.

Linton, K. J., and C. F. Higgins. 2007. Structure and function of ABC transporters: the ATP switch provides flexible control. European Journal of Physiology **453:**555-567.

Lohmann, K. J., N. F. Putman, and C. M. F. Lohmann. 2008. Geomagnetic imprinting: A unifying hypothesis of long-distance natal homing in salmon and sea turtles. Proceedings of National Academy of Science of the United State of America **105:**19096–19101.

Maaz, K., A. Mumtaz, S. K. Hasanain, and M. F. Bertino. 2010. Temperature dependent coercivity and magnetization of Ni^{2+} ferrite nanoparticles. Journal of Magnetism and Magnetic Material **322:**2199-2202.

Maaz, K., A. Mumtaz, S. K. Hasanain, and A. Ceylan. 2007. Synthesis and magnetic properties of Co^{2+} ferrite ($CoFe_2O_4$) nanoparticles prepared by wet chemical route. Journal of Magnetism and Magnetic Material **308:**289-295.

Macomber, L., and R. P. Hausinger. 2011. Mechanisms of Ni^{2+} toxicity in microorganisms. Metallomics **3:**1153-1162.

Mahmoudi, M., S. Sant, B. Wang, S. Laurente, and T. Sen. 2011. Superparamagnetic iron oxide nanoparticles (SPIONs): Development, surface modification and applications in chemotherapy. Advanced Drug Delivary Review **63:**24-46.

Mann, S., R. B. Frankel, and R. P. Blakemore. 1994. Structure, morphology and crystal growth of bacterial magnetite. Nature **405:**405-407.

Matsunaga, T., Y. Okamura, Y. Fukuda, A. T. Wahyudi, Y. Murase, and H. Takeyama. 2005. Complete genome sequence of the facultative anaerobic magnetotactic bacterium magnetospirillum sp. strain AMB-1. DNA Research **12:** 157-166.

McHenry, M. E., and D. E. Laughlin. 2000. Nano scale materials development for future magnetic applications. Acta Matter **48:**223-238.

Mobley, H. L., R. M. Garner, and P. Bauerfeind. 1995. *Helicobacter pylori* Ni^{2+}-transport gene *nixA*: Synthesis of catalytically active urease in *Escherichia coli* independent of growth conditions. Molecular Microbiology **16:**97-109.

Mulrooney, S. B., and R. P. Hausinger. 2003. Ni^{2+} uptake and utilization by microorganisms. FEMS Microbiology Reviews **27:**239-261.

Murat, D., A. Quinlan, H. Vali, and A. Komeili. 2010. Comprehensive genetic dissection of the magnetosome gene island reveales the step wise assembly of a prokaryotic organelle. National Academic of Science, USA **107:**5593-5598.

Nahvi, A., J. E. Barrick, and R. R. Breaker. 2004. Coenzyme B12 riboswitches are widespread genetic control elements in prokaryotes. Nucleic Acids Research **32:**143-150.

Navarro, C., L. F. Wu, and M. A. Mandrand-Berthelot. 1993. The *nik* operon of *Escherichia coli* encodes a periplasmic binding-protein-dependent transport system for Ni^{2+}. Molecular Microbiology **9:**1181-1191.

Nelson, D. L., and E. P. Kennedy. 1971. Magnesium transport in *Escherichia coli.* Inhibition by Co^{2+}ous ion. Journal of Biological Chemistry **246:**3042-3049.

Newcombe, J., J. C. Jeynes, E. Mendoza, J. Hinds, G. L. Marsden, R. A. Stabler, M. Marti, and J. J. McFadden. 2005. Phenotypic and transcriptional characterization of the meningococcal PhoPQ System, a magnesium-sensing two-component regulatory system that
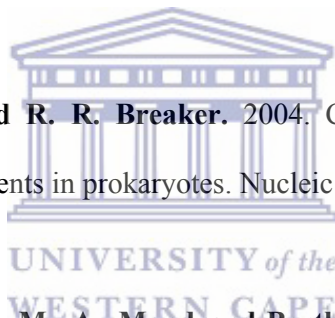
controls genes involved in remodeling the meningococcal cell surface. Journal of Bacteriology **187**: 4797-4975.

Niegowski, D., and S. Eshaghi. 2007. The CorA family: structure and function revisited. Cellular and Molecular Life Sciences **64:**2564-2574.

Nies, D. H., M. Mergeay, B. Friedrich and H.G. Schlegel. 1987. Cloning of plasmid gene coding resistance to cadmium, zinc, and Co^{2+} from *Alcaligenes eutrophus* CH34. Journal of Bacteriology **167:** 4865-4868.

Nies, D. H., L. Chu and S. Silver. 1989. Expression and nucleotide sequence of a plasmid-determined divalent cation efflux system from *Alcaligenes eutrophus*. National Academy of Science USA **86:** 7351-7355.
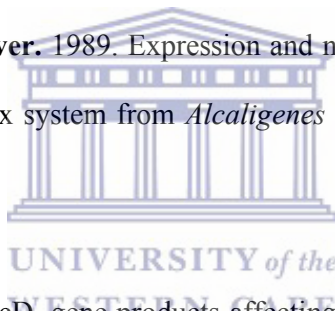
Nies, D. H. 1992. CzcR and CzcD, gene products affecting regulation of resistance to Co^{2+}, zinc, and cadmium (*czc* system) in *Alcaligenes eutrophus*. Journal of Bacteriology **174:**8102-8110.

Nies, D. H. and S. Silver. 1994. Ion efflux systems involved in bacterial metal resistances. Journal of Industrial Microbiology **14:** 186-199.

Nies, D. H. 1995. The Co^{2+}, zinc, and cadmium efflux system CzcABC from *Alcaligenes eutrophus* functions as a cation-proton antiporter in *Escherichia coli*. Journal of Bacteriology **177:**2707–2712.

Nies, D. H. 1999. Microbial heavy-metal resistance. Applied Microbiology and Biotechnology **51:**730-750.

Noinaj, N., M. Guillier, T. J. Barnard, and S. K. Buchanan. 2010. TonB-Dependent Transporters: Regulation, Structure, and Function. Annual Review of Microbiology **64:**43-60.

Odermatt, A., H. Suter, R. Krapf and M. Solioz. 1993. Primary structure of two P-type ATPases involved in copper homeostasis in *Enterococcus hirae.* Journal of Biological Chemistry **268:** 12775-12777.

Outten, C.E., and T.V. O'Halloran. 2001. Femtomolar sensitivity of metalloregulatory proteins controlling zinc homeostasis. Science **292**: 2488-2492
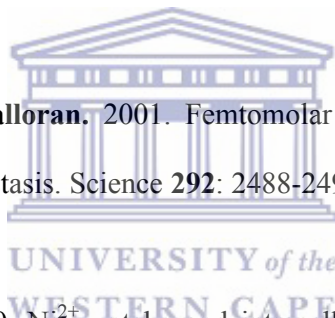
Pal, A., and A. K. Paul. 2010. Ni^{2+} uptake and intracellular localization in *Cupriavidus pauculus* KPS 201, native to ultramafic ecosystem. Advanced Bioscience and Biotechnology **1:** 276-280.

Papp, K. M., and M. E. Maguire. 2004. The CorA Mg^{2+} Transporter Does Not Transport Fe^{2+}. Journal of Bacteriology **186:**7653-7658.

Perez-Gonzalez, T., T. Prozorov, A. Yebra-Rodriguez, D. A. Bazyliski, and C. Jimenez-lopez. 2010. Mn incorporation in magnetosomes: New possibilities for the nanotechnological applications of biomagnetite. Resumen SEM 171-172.

Qi L, J. Li, W. Zhang, J. Liu, C. Rong, *et al.* 2012. Fur in *Magnetospirillum gryphiswaldense* Influences magnetosomes formation and directly regulates the genes involved in iron and oxygen metabolism. PLoS ONE 7(1): e29572. doi:10.1371/journal.pone.0029572

Ragsdale, W. E., and M. Kumar. 1996. Ni^{2+}-containing carbon monoxide dehydrogenase/acetyl-CoA synthase. Chemistry Reviews **96:**2515-2539.

Rolfe, D. M., C. J. Rice, S. Lucchini, C. Pin, A. Thompson, A. D. S. Cameron, M. Alston, M. F. Stringer, R. P. Betts, J. Baranyi, M. W. Peck, and J. C. D. Hinton. 2011. Lag phase is a distinct growth phase that prepares bacteria for exponential growth and involves transient metal accumulation. Journal of Bacteriology **194:** 686-701.

Ranquet, C., S. Ollagnier-de-Choudens, L. Loiseau, F. Barras, and M. Fontecave. 2007. Co^{2+} stress in *Escherichia coli*: The effect on the iron-sulfur proteins. Journal of Biological Chemistry **282:**30442-30451.

Rensing, C., Mitra, B., and P.B. Rosen. 1997. The zntA gene of *Escherichia coli* encodes a Zn(II)-translocating P-type ATPase. Proceedings of the National Academy of Sciences. 94: 14326-14331.

Rodionov, D. A., A. G. Vitreschak, A. A. Mironov, and M. S. Gelfand. 2003. Comparative genomics of the vitamin B12 metabolism and regulation in prokaryotes. Journal of Biological Chemistry **278:**41148-41159.

Rodionov, D. A., P. Hebbeln, M. S. Gelfand, and T. Eitinger. 2006. Comparative and functional genomic analysis of prokaryotic Ni^{2+} and Co^{2+} uptake transporters: Evidence for a Novel Group of ATP-Binding Cassette Transporters. Journal of Bacteriaology **188:**317-327.

Rodrigue, A., G. Effantin, and M. A. Mandrand-Berthelot. 2005. Identification of *rcnA* (yohM), a Ni^{2+} and Co^{2+} resistance gene in *Escherichia coli*. Journal of Bacteriology **187:**2912–2916.

Rowe, J. L., G. L. Starnes, and P. T. Chivers. 2005. Complex transcriptional control links NikABCDE-dependent Ni^{2+} transport with hydrogenase expression in *Escherichia coli*. Journal of Bacteriology **187:**6317-6323.

Rubikas, J., D. Matulis, A. Leipus, and D. Urbaitiene. 1997. Ni^{2+} resistance in *Escherichia coli* V38 is dependent on the concentration used for induction. FEMS Microbiology Letters **155:**193-198.

Schauer, K., B. Gouget, M. Carriere, A. Labigne, and H. de Reuse. 2007. Novel Ni^{2+} transport mechanism across bacterial outer membrane energized by the TonB/ExbB/ExbD machinery. Molecular Biology **64:** 1054-1068.

Schleifer, K. H., D. Schuler, S. Spring, M. Weizenegger, R. Amann, W. Ludwig, and M. Kohler. 1991. The genus *Magnetospirillum*, description of *Magnetospirillum gryphiswaldense* and transfer of *Aquaspirillum magnetotacticum* to *Magnetospirillum magnetotacticum* comb. Applied Microbiology **14:**379-385.

Schmidt, T. and H. G. Schlegel. 1994. Combined Ni^{2+}-Co^{2+}-cadmium resistance encoded by the *ncc* locus of *Alcaligenes xylosoxidans* 31A. Journal of Bacteriology. **176:** 7045-7054.

Sebbane, F., M. Mandrand-Berthelot, M. Simonet. 2002. Genes encoding specific Ni^{2+} transport systems flank the chromosomal urease locus of pathogenic yersiniae. Journal of Bacteriology. **184:** 5706-5713.

Sengor, S. S., S. Barua, P. Gikas, T. R. Ginn, B. Peyton, R. K. Sani, and N. F. Spycher. 2009. Influence of Heavy Metals on Microbial Growth Kinetics Including Lag Time: Mathematical Modeling and Experimental Verification. Environmental Toxicology and Chemistry **28:**2020-2029.

Sensfuss, C. and H. G. Schlegel. 1988. Plasmid pMOL28-encoded resistance to Ni^{2+} is due to specific efflux. FEMS Microbiology Letters. **55:** 295-298.
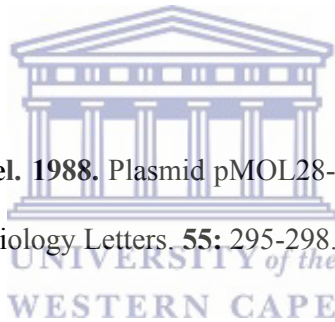
Sermon, J., E. M. Wevers, L. Jansen, P. D. Spiegeleer, K. Vanoirbeek, A. Aertsen, and C. W. Michiels. 2005. CorA affects tolerance of *Escherichia coli* and *Salmonella enterica* Serovar Typhimurium to the lactoperoxidase enzyme system but not to other forms of oxidative stress. Applied Environmental Microbiology **71:**6515-6523.

She, Q., R. K. Singh, F. Confalonieri, Y. Zivanovic, G. Allard, M. J. Awayez, C. C. Y. Chan-Weiher, I. G. Clausen, B. A. Curtis, A. De Moors, G. Erauso, C. Fletcher, P. M. K. Gordon, I. Heikamp-de Jong, A. C. Jeffries, C. J. Kozera, N. Medina, X. Peng, and J. Van der Oost. 2001. The complete genome of the crenarchaeon *Sulfolobus solfataricus* P2.

Proceedings of the National Academy of Science of the United States of America **98:**7835-7840.

Siddiqui, R. A., K. Benthin and H. G. Schlegel. 1989. Cloning of pMOL28-encoded Ni^{2+} resistance genes and expression of the genes in *Alcaligenes eutrophus* and *Pseudomonas* spp. Journal of Bacteriology **171:** 5071-5078.

Silver, S., G. Ji, S. Brer, S. Dey, D. Dou and B. P. Rosen. 1993. Orphan enzyme or patriarch of a new tribe: the arsenic resistance ATPase of bacterial plasmids. Molecular Microbiology. **8:** 637-642.

Silver, S., and T. Phung 2005. A bacterial view of the periodic table: genes and proteins for toxic inorganic ions. Journal of Industrial Microbiology and Biotechnology **32:**587-605.
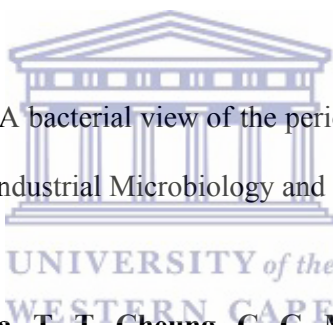
Snavely, D. M., S. A. Gravina, T. T. Cheung, C. G. Miller, and M. Maguire. 1990. Magnesium transport in *Salmonella typhimurium.* Journal of Biological Chemistry **266:** 824-829.

Staniland, S., W. Williams, N. Telling, G. Van Der Laan, A. Harrison, and B. Ward. 2008. Controlled Co^{2+} doping of magnetosomes in vivo. Nature Nanotechnology **3:**158-162.

Tanaka, M., R. Brown, N. Hondow, A. Arakati, T. Matsunaga, and S. Staniland. 2012. Highest levels of Cu, Mn and Co doped into nanomagnetic magnetosomes through optimized biomineralisation. Journal of Materials Chemistry **22:**11919-11921.

Tanaka, M., Y. Okamura, A. Arakati, T. Tanaka, H. Takeyama, and T. Matsunaga. 2006. Origin of magnetosome membranes: Proteomics analysis of magnetosome membrane and comparison with cytoplasmic membrane. Proteomics **6:**5234-5247.

Tibazarwa, C., S. Wuertz, M. Mergeay, L. Wyns, and D. Van der Lilie. 1999. Regulation of the *cnr* Co^{2+} and Ni^{2+} resistance determinant of *Ralstonia eutropha* (*Alcaligenes eutrophus*) CH34. Journal of Bacteriology. **182:** 1399-1409.

Tommi, K. M. and T. Kamehisa. 1998. A comprehensive analysis of ABC transporters in complete microbial genomes. Genome Research **8:** 1045-1059.

Vali, H., O. Forster, G. Amarantidis, and N. Petersen. 1987. Magnetotactic bacteria and their magnetofossils in sediments. Earth Planet Science Letter **86:**389-400.

Van Belle, F., T. J. Hayward, and J. A. C. Blanda. 2007. Coercivity engineering of exchange biased magnetic multilayer samples for digital encoding applications. Journal of Applied Physics **102:**17-27.

Viret, H., O. Pringault, and R. Duran. 2006. Impact of zinc and Ni^{2+} on oxygen consumption of benthic microbial communities assessed with microsensors. Science of the Total Environment **367:**302-311.

Waldron, K. J., J. C. Rutherford, D. Ford, and N. J. Robinson. 2009. Metalloproteins and metal sensing. Nature **460:**823-830.

Wang, D.N., M. Safferling, M. J. Lemieux, H. Griffith, Y. Chen, X.D. Li. 2003. Practical aspects of overexpressing bacterial secondary membrane transporters for structural studies. Biochemisty and Biophysics Acta. **1610:** 23-36.

Watt, R. K., and P. W. Ludden. 1999. Ni($^{2+}$) transport and accumulation in *Rhodospirillum rubrum*. Journal of Bacteriology **181:**4554-4560.

Wolfram, L., F. B. and T. Eitinger. 1995. The *Alcaligenes eutrophus* protein HoxN mediates Ni^{2+} transport in *Escherichia coli*. Journal of Bacteriology **177:**1840-1843.

Wu, L. F., C. Navarro, K. de Pina, M. Quénard, M. Mandrand. 1994. Antagonistic effect of Ni^{2+} on the fermentative growth of *Escherichia coli* K-12 and comparison of Ni^{2+} and Co^{2+} toxicity on the aerobic and anaerobic growth. Environmental Health Perspectives. **102:** 297-300.
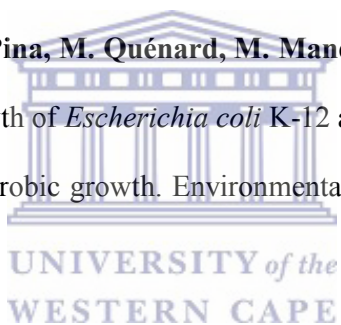
Wu, A., P. Ou, and L. Zeng. 2010. Biomedical application of magnetic nanoparticles. Nanotechnology Review **5:**245-270.

Yamamoto, T., Y. Shimotsuma, M. Sakakura, M. Nishi, K. Miura, and K. Hirao. 2011. Intermetallic magnetic nanoparticle precipitation by femtosecond laser fragmentation in liquid. The ACS Journal of Surfaces and Colloids **27:**8359-8364.

Yan, L., S. Zhang, P. Chen, H. Liu, H. Yin, and H. Li. 2012. Magnetotactic bacteria, magnetosomes and their application. Microbialogy Research**: 167:** 2507-519.

Youn, H. D., E. J. Kim, J. H. Roe, Y. C. Hah, and S. O. Kang. 1996. A novel Ni^{2+}-containing superoxide dismutase from *Streptomyces spp*. Biochemistry Journal **318:**889-896.

6. APPENDICES

APPENDIX 1: Stationary phase intracellular Ni^{2+} accumulation in *E. coli* strains harboring *hoxN*

NiCl$_2$ mM	Cellular Ni mg/g dry weight							
	EPI 300	EPI 300+*hoxN*	*ΔnikA*	*ΔnikA +hoxN*	*ΔcorA*	*ΔcorA +hoxN*	*ΔrcnA*	*ΔrcnA +hoxN*
0	0.000 ± 0.000	0.000 ± 0.000	0.000 ± 0.000	0.000 ± 0.000	0.000 ± 0.000	0.000 ± 0.000	0.000 ± 0.000	0.000 ± 0.000
0.005	0.002 ± 22E-5	0.022 ± 82E-5	0.003± 6E-6	0.031 ± 41E-5			0.003 ± 3E-6	0.063 ± 0.002
0.01							0.005 ± 27E-5	0.089 ± 0.002
0.02							0.019 ± 0.009	0.091 ± 0.001
0.05	0.028 ± 21E-7	0.126 ± 0.007						
0.1	0.154 ± 0.035	0.394 ± 0.031	0.135 ± 0.084	0.366 ± 0.034	0.064 ± 0.002	0.265 ± 0.026		
0.5			1.087 ± 0.240	1.289 ± 0.278	0.132 ± 0.016	0.500 ± 0.034		
1					0.673 ± 0.093	1.109 ± 0.107		

Cellular Ni^{2+} was measure in cells grown in M9-cam medium. The culture was grown until OD_{600} reached 0.8-1, followed by addition of up to 0.2% L-arabinose and $NiCl_2$ and harvested at the end of stationary phase. The results shown here represent the mean ± standard deviation of ICP-OES analysis of three independent experiments.

APPENDIX 2: Stationary phase intracellular Fe in *E. coli* strains harboring *hoxN* in the presence of Ni^{2+}

	Cellular Fe mg/g dry weight							
NiCl$_2$ mM	EPI 300	*hoxN*	*ΔnikA*	*ΔnikA + hoxN*	*ΔcorA*	*ΔcorA + hoxN*	*ΔrcnA*	*ΔrcnA + hoxN*
No metal	0.307 ± 0.071	0.329 ± 0.036	0.330 ± 0.013	0.369 ± 0.088	0.054 ± 0.004	0.084 ± 0.006	0.335 ± 0.072	0.340 ± 0.037
0.005	0.360 ± 0.050	0.373 ± 0.006	0.389 ± 0.059	0.336 ± 0.015			0.315 ± 0.063	0.351 ± 0.093
0.01							0.358 ± 0.068	0.300 ± 0.089
0.02							0.378 ± 0.015	0.282 ± 0.083
0.05	0.350 ± 0.014	0.372 ± 0.001						
0.1	0.298 ± 0.041	0.320 ± 0.090	0.344 ± 0.038	0.332 ± 0.002	0.043 ± 0.002	0.074 ± 0.008		
0.5			0.092 ±0.002	0.082 ± 0.002	0.028 ± 0.001	0.055 ± 0.003		
1					0.016 ± 0.006	0.033 ± 0.008		

Cellular Iron was measure in cells grown in M9-cam broth until OD$_{600}$ reached 0.8-1. L-arabinose and NiCl$_2$ were added and cells were harvested at late stationary phase. The results shown here represent the mean ± standard deviation of ICP- OES analysis of three independent experiments.

APPENDIX 3: Stationary phase intracellular Mg in *E. coli* strains harboring *hoxN* in the presence of Ni^{2+}

	Cellular Mg mg/g dry weight							
NiCl$_2$ mM	EPI 300	*hoxN*	*ΔnikA*	*ΔnikA + hoxN*	*ΔcorA*	*ΔcorA + hoxN*	*ΔrcnA*	*ΔrcnA + hoxN*
0	3.050 ± 0.079	3.126 ± 0.341	2.880 ± 0.013	2.988 ± 0.158	0.615 ± 0.117	0.594 ± 0.008	3.048 ± 0.144	2.982 ± 0.093
0.005	3.012 ± 0.055	3.049 ± 0.183	2.951 ± 0.170	2.900 ± 0.172			2.945 ± 0.039	2.946 ± 0.129
0.01							2.802 ± 0.114	2.855 ± 0.245
0.02							2.875 ± 0.284	2.814 ± 0.110
0.05	2.933 ± 0.089	2.945 ± 0.003						
0.1	2.835 ± 0.338	2.919 ± 0.043	2.950 ± 0.232	2.906 ± 0.138	0.572 ± 0.019	0.582 ± 0.088		
0.5			2.915 ± 0.060	2.953 ± 0.108	0.571 ± 0.067	0.551 ± 0.009		
1					0.423 ± 0.046	0.541 ± 0.046		

Cellular magnesium was measured in cells grown in M9-cam broth until OD$_{600}$ reached 0.8-1. L-arabinose and NiCl$_2$ were added and cells were harvested at late stationary phase. The results shown here represent the mean ± standard deviation of ICP-OES analysis of three independent experiments.

APPENDIX 4: Stationary phase intracellular Co^{2+} accumulation in *E. coli* strains harboring *cbiKMQO*

CoCl mM	Cellular Co mg/g dry weight							
	EPI 300	EPI 300+ *cbi*	*ΔnikA*	*ΔnikA + cbi*	*ΔcorA*	*ΔcorA + cbi*	*ΔrcnA*	*ΔrcnA + cbiKMQO*
0	0.000 ± 0.000	0.000 ± 0.000	0.000 ± 0.000	0.000 ± 0.000	0.000 ± 0.000	0.000 ± 0.000	0.000 ± 0.000	0.000 ± 0.000
0.005	0.007 ± 5E-5	0.049 ± 0.001	0.004± 8E-4	0.038 ± 0.001			0.004 ± 22E-5	0.088 ± 0.001
0.01							0.006 ± 91E-5	0.107 ± 0.004
0.02							0.013 ± 0.001	0.206 ± 0.002
0.05	0.038 ± 0.007	0.216 ± 0.006						
0.1	0.127 ± 0.005	0.673 ± 0.011	0.161± 0.053	0.693 ± 0.093	0.053 ± 17E-5	0.294 ± 0.012		
0.5			1.372 ± 0.256	1.492 ± 0.185	0.332 ± 0.047	0.866 ± 0.126		
1					0.667 ± 0.021	1.527 ± 0.086		

Cellular Co^{2+} was measure in cells grown in M9-cam medium. The cells were grown until OD_{600} reached 0.8-1, followed by addition of up to 0.2% L-arabinose and $CoCl_2$ and harvested at the end of stationary phase. The results shown here represent the mean ± standard deviation of ICP-OES analysis of three independent experiments.

APPENDIX 5: Stationary phase intracellular Co^{2+} accumulation in *E. coli* strains harboring *nhlF*

	Cellular Co mg/g dry weight							
CoCl$_2$mM	EPI 300	EPI 300 + *nhlF*	*ΔnikA*	*ΔnikA + nhlF*	*ΔcorA*	*ΔcorA + nhlF*	*ΔrcnA*	*ΔrcnA + nhlF*
0	0.000 ± 0.000	0.000 ± 0.000	0.000 ± 0.000	0.000 ± 0.000	0.000 ± 0.000	0.000 ± 0.000	0.000 ± 0.000	0.000 ± 0.000
0.005	0.007 ± 2E-5	0.022 ± 31E-4	0.004± 21E-5	0.020 ± 1E-4			0.004 ± 33E-5	0.052± 46E-4
0.01							0.006 ± 2E-5	0.081 ± 3E-4
0.02							0.013 ± 0.001	0.133 ± 0.002
0.05	0.038 ± 0.007	0.187 ± 0.003						
0.1	0.127 ± 0.005	0.425 ± 0.013	0.161± 0.053	0.477 ± 0.024	0.053 ± 13E-4	0.191 ± 0.017		
0.5			1.372 ± 0.256	1.450 ± 0.185	0.332 ± 0.047	0.730 ± 0.138		
1					0.667 ± 0.021	1.197 ± 0.077		

Cellular Co^{2+} was measure in cells grown in M9-cam medium. The cells were grown until OD_{600} reached 0.8-1, followed by addition of up to 0.2% L-arabinose and CoCl$_2$ and harvested at the end of stationary phase. The results shown here represent the mean ± standard deviation of ICP-OES analysis of three independent experiments.

APPENDIX 6: Stationary phase intracellular iron in *E. coli* strains harboring *cbiKMQO* in the present of Co^{2+}

	Cellular Fe mg/g dry weight							
CoCl$_2$ mM	EPI 300	EPI 300+ *cbi*	*ΔnikA*	*ΔnikA + cbi*	*ΔcorA*	*ΔcorA + cbi*	*ΔrcnA*	*ΔrcnA + cbi*
0	0.307 ± 0.071	0.326 ± 0.069	0.330 ± 0.013	0.307 ± 0.022	0.054 ± 0.014	0.051 ± 0.003	0.335 ± 0.003	0.343 ± 0.010
0.005	0.341 ± 0.024	0.395 ± 0.035	0.380 ± 0.061	0.381 ± 0.009			0.361 ± 0.092	0.386± 0.094
0.01							0.321 ± 0.059	0.369 ± 0.046
0.02							0.318 ± 0.029	0.333 ± 0.041
0.05	0.368 ± 0.018	0.318 ± 0.064						
0.1	0.369 ± 0.069	0.388 ± 0.042	0.325 ± 0.697	0.349 ± 0.067	0.061 ± 0.005	0.058 ± 0.004		
0.5			0.058 ± 0.003	0.068 ± 0.002	0.053 ± 0.002	0.055 ± 0.008		
1					0.055 ± 0.008	0.050 ± 0.002		

Cellular Iron was measure in cells grown in M9-cam broth until OD$_{600}$ reached 0.8-1. L-arabinose and CoCl$_2$ were added and cells were harvested at late stationary phase.

The results shown here represent the mean ± standard deviation of ICP OES analysis of three independent experiments

APPENDIX 7: Stationary phase intracellular iron in *E. coli* strains harboring *nhlF* in the present of Co^{2+}

	Cellular Fe mg/g dry weight							
CoCl$_2$ mM	EPI 300	EPI 300+ *nhl*F	*ΔnikA*	*ΔnikA + nhlF*	*ΔcorA*	*ΔcorA + nhlF*	*ΔrcnA*	*ΔrcnA + nhlF*
0	0.307 ± 0.071	0.322 ± 0.045	0.330 ± 0.013	0.323 ± 0.005	0.051 ± 0.004	0.056 ± 0.004	0.335 ± 0.003	0.372 ± 0.075
0.005	0.341 ± 0.004	0.300 ± 0.011	0.380 ± 0.061	0.379 ± 0.080			0.361 ± 0.092	0.361 ± 0.012
0.01							0.321 ± 0.059	0.363 ± 0.059
0.02							0.318 ± 0.029	0.331 ± 0.060
0.05	0.368 ± 0.018	0.360 ± 0.054						
0.1	0.369 ± 0.069	0.395 ± 0.022	0.325 ± 0.097	0.320 ± 0.009	0.036 ± 0.005	0.052 ± 0.004		
0.5			0.088 ± 0.003	0.080 ± 0.003	0.020 ± 0.002	0.031 ± 0.001		
1					0.019 ± 0.008	0.022 ± 0.008		

Cellular Iron was measure in cells grown in M9-cam broth until OD$_{600}$ reached 0.8-1. L-arabinose and CoCl$_2$ were added and cells were harvested at late stationary phase.

The *nhl*F gene shows no effect on cellular iron. The results shown here represent the mean ± standard deviation of ICP-OES analysis of three independent experiments

APPENDIX 8: Stationary phase intracellular magnesium in *E. coli* strains harboring *cbiKMQO* in the presence of Co^{2+}

CoCl$_2$ mM	Cellular Mg mg/g dry weight							
	EPI 300	EPI 300+ *cbi*	*ΔnikA*	*ΔnikA + cbi*	*ΔcorA*	*ΔcorA + cbi*	*ΔrcnA*	*ΔrcnA + cbi*
0	2.906 ± 0.050	3.355 ± 0.545	2.880 ± 0.013	3.198 ± 0.207	0.615 ± 0.117	0.589 ± 0.019	3.048 ± 0.144	3.030 ± 0.193
0.005	2.963 ± 0.313	2.966 ± 0.249	2.939 ± 0.090	2.975 ± 0.109			2.925 ± 0.048	3.047 ± 0.110
0.01							2.950 ± 0.150	2.902 ± 0.118
0.02							2.959 ± 0.089	2.943 ± 0.228
0.05	2.956 ± 0.038	2.930 ± 0.198						
0.1	2.905 ± 0.103	2.918 ± 0.113	2.981 ± 0.071	2.939 ± 0.195	0.414 ± 0.177	0.639 ± 0.043		
0.5			2.888 ± 0.025	2.913 ± 0.137	0.303 ± 0.018	0.679 ± 0.141		
1					0.287 ±0.036	0.471 ± 0.103		

Cellular Magnesium was measure in cells grown in M9-cam broth until OD600 reached 0.8-1. L-arabinose and CoCl$_2$ were added and cells were harvested at late stationary phase. The results shown here represent the mean ± standard deviation of ICP-OES analysis of three independent experiments

.

APPENDIX 9: Stationary phase intracellular magnesium in *E. coli* strains harboring *nhlF* in the presence of Co^{2+}

	Cellular Mg mg/g dry weight							
CoCl₂ mM	EPI 300	EPI 300+ *nhlF*	*ΔnikA*	*ΔnikA + nhlF*	*ΔcorA*	*ΔcorA + nhlF*	*ΔrcnA*	*ΔrcnA + nhlF*
0	2.906 ± 0.050	3.140 ± 0.063	2.880 ± 0.013	3.265 ± 0.125	0.615 ± 0.117	0.614 ± 0.069	3.048 ± 0.144	3.211 ± 0.089
0.005	2.963 ± 0.313	2.864 ± 0.008	2.939 ± 0.090	3.251 ± 0.265			2.925 ± 0.048	3.386 ± 0.554
0.01							2.950 ± 0.150	3.019 ± 0.475
0.02							2.959 ± 0.089	3019 ± 0.475
0.05	2.956 ± 0.038	3.180 ± 0.156						
0.1	2.905 ± 0.103	3.302 ± 0.417	2.981 ± 0.071	2.975 ± 0.170	0.414 ± 0.177	0.623 ± 0.137		
0.5			2.888 ± 0.025	2.941 ± 0.246	0.303 ± 0.018	0.352 ± 0.067		
1					0.287 ±0.036	0.461± 0.206		

Cellular Magnesium was measure in cells grown in M9-cam broth until OD_{600} reached 0.8-1. L-arabinose and CoCl₂ were added and cells were harvested at late stationary phase. The results shown here represent the mean ± standard deviation of ICP-OES analysis of three independent experiments.

APPENDIX 10: Log phase intracellular Co^{2+}, iron and magnesium in *E. coli* EPI 300 in the presence of iron and Co^{2+}

Metals	Cellular Co (mg/g dry weight)		Cellular Fe (mg/g dry weight)		Cellular Mg (mg/g dry weight)	
	EPI 300	EPI 300 + *cbiKMQO*	EPI 300	EPI 300 + *cbiKMQQ*	EPI 300	EPI 300 + *cbiKMQ*
No metal	0.000±0.000	0.000 ± 0.000	0.420 ± 0.001	0.411 ± 0.023	3.790 ± 0.235	3.656 ± 0.321
0.1 mM Co	0.043 ± 13E-6	0.239 ± 0.004	0.420 ± 0.076	0.406 ± 0.008	3.656 ± 0.215	3.642 ± 0.061
0.1 mM Co+ 0.361 mM Fe	0.057 ± 0.001	0.368 ± 0.039	0.585 ± 0.088	0.517 ± 0.022	3.631 ± 0.299	3.697 ± 0.100

Cellular Co^{2+}, iron and magnesium were determined in cells grown until early log phase in M9-can medium followed be addition of Co^{2+} or Co^{2+} and iron. Results shown here represent the mean ± standard deviation of ICP-OES analysis of three independent experiments.

UNIVERSITY *of the*
WESTERN CAPE